

**DEVELOPMENT OF THE TECHNOLOGY
FOR THE FABRICATION OF
RELIABLE LAMINAR FLOW CONTROL PANELS**

D. D. Weiss and D. V. Lindh

February 1977

CASE FILE
COPY

Distribution of this report is provided in the interest of information exchange.
Responsibility for the contents resides in the author or organization that
prepared it.

Prepared under contract NAS1-14407 by

Boeing Commercial Airplane Company
P.O. Box 3707
Seattle, Washington 98124

for



National Aeronautics and
Space Administration

1. Report No. NASA CR-145124	2. Government Accession No.	3. Recipient's Catalog No.	
4. Title and Subtitle DEVELOPMENT OF THE TECHNOLOGY FOR THE FABRICATION OF RELIABLE LAMINAR FLOW CONTROL PANELS		5. Report Date February 1977	6. Performing Organization Code
7. Author(s) D. D. Weiss and D. V. Lindh		8. Performing Organization Report No. D6-44184	10. Work Unit No.
9. Performing Organization Name and Address Boeing Commercial Airplane Company P. O. Box 3707 Seattle, Washington 98124		11. Contract or Grant No. NAS1-14407	13. Type of Report and Period Covered Final Report
12. Sponsoring Agency Name and Address National Aeronautics and Space Administration Washington, D. C. 20546		14. Sponsoring Agency Code	
15. Supplementary Notes			
16. Abstract <p>The results of a 5 months test program to evaluate LFC surface materials are reported. Requirements for LFC surface smoothness and flow were compiled from existing data. Various configurations of porous, perforated and slotted materials were flow tested to determine if they would meet these requirements.</p> <p>The candidate materials were then tested for susceptibility to clogging and for resistance to corrosion. Of the materials tested, perforated titanium, porous polyimide, and slotted assemblies demonstrated a much greater resistance to clogging than other porous materials.</p> <p>Three concepts for installing LFC materials were studied.</p>			
17. Key Words (Suggested by Author(s)) Laminar Flow Control (LFC)		18. Distribution Statement Unclassified -- Unlimited	
19. Security Classif. (of this report) Unclassified	20. Security Classif. (of this page) Unclassified	21. No. of Pages 119	22. Price*

*For sale by the National Technical Information Service, Springfield, Virginia 22151

CONTENTS

	Page
FOREWORD	
FIGURES	v
TABLES	vi
1.0 SUMMARY.....	1
2.0 INTRODUCTION.....	3
3.0 SYMBOLS AND ABBREVIATIONS.....	4
4.0 TASK I LAMINAR FLOW CONTROL.....	6
4.1 Suction Requirements and Flow Rates Normal to the Surface	7
4.2 Design Concepts and Materials Selected for Testing	7
4.3 Test Set-up and Procedures.....	9
4.3.1 Flow Test	9
4.3.2 Clogging Test.....	10
4.3.3 Corrosion Test.....	10
4.3.4 Water Ingress Test	10
4.4 Test Results and Discussion.....	10
4.4.1 Tests Conducted	10
4.4.2 Flow and Clogging Test Results.....	10
4.4.2.1 Flow Test Correlation and Prediction Methods.....	12
4.4.2.2 Gore-Tex.....	13
4.4.2.3 Brunscoustic	14
4.4.2.4 Aircraft Porous Media.....	14
4.4.2.5 Michigan Dynamics.....	14
4.4.2.6 Polyimide	14
4.4.2.7 Perforated Titanium	16
4.4.2.8 Slot Assembly	17
4.4.2.9 Strip Assembly	17
4.4.2.10 Aluminum Core Panel Assembly	17
4.4.3 Corrosion Test Results	17
4.4.4 Water Ingress Test Results.....	18
4.5 Compliance with Aerodynamic Smoothness and Waviness Requirements	18

CONTENTS (Concluded)

	Page
5.0 TASK 2 MECHANICAL PROPERTIES MATERIAL	20
6.0 TASK 3 PARTICIPATION IN SYMPOSIUM	21
7.0 CONCLUSIONS AND RECOMMENDATIONS.....	22
7.1 Conclusions.....	22
7.2 Recommendations.....	23
APPENDIX A--DESCRIPTION OF TEST COUPONS.....	25
APPENDIX B--FLOW AND CLOGGING TEST RESULTS	45
APPENDIX C--AERODYNAMIC REQUIREMENTS	68
APPENDIX D--SPECIMEN PRESSURE LOSS CORRELATION	74
REFERENCES	80

FIGURES

No.		Page
1	Suction Requirements for LFC Wing	81
2	Continuously Porous or Perforated Skin Concept	82
3	Porous or Perforated Strip Concept	83
4	Slot-Strip Metal Overlay Strip Concept	84
5	Photograph of Flow Test Set-up	85
6	Schematic of Flow Test Set-up	86
7	Photograph of Rayl Test Machine	87
8	Schematic of Rayl Test Set-up	88
9	Photograph of Clogging Test Set-up and Location.	89
10	Flow Test Results, Test Coupon No. 1, Gore-Tex	90
11	Flow Test Results, Test Coupon No. 3, Brunscoustic #1, as Received.	91
12	Flow Test Results, Test Coupon No. 3, Brunscoustic #1, 48 Hour Clogging	92
13	Flow Test Results, Test Coupon No. 3, Brunscoustic #1, Reverse Flow	93
14	Flow Test Results, Test Coupon No. 4, Brunscoustic #2, as Received.	94
15	Flow Test Results, Test Coupon No. 5, Aircraft Porous Media	95
16	Flow Test Results, Test Coupon No. 6, Michigan Dynamics, as Received	96
17	Flow Test Results, Test Coupon No. 6, Michigan Dynamics, 48 Hour Clogging	97
18	Flow Test Results, Test Coupon No. 7, Polyimide (16 Ply), as Received.	98
19	Flow Test Results, Test Coupon No. 8, Polyimide (7 Ply), as Received.	99
20	Flow Test Results, Test Coupon No. 9, Perforated Titanium, .003 Hole, as Received	100
21	Flow Test Results, Test Coupon No. 9, Perforated Titanium, .003 Hole, 48 and 72 Hour Clogging.	101
22	Flow Test Results, Test Coupon No. 9, Perforated Titanium, .003 Hole, Surface Washed	102
23	Flow Test Results, Test Coupon No. 10, Perforated Titanium, .005 Hole	102
24	Flow Test Results, Test Coupon No. 11, Perforated Titanium, .008 Hole	104
25	Flow Test Results, Test Coupon No. 12, .0073 Slot Assembly, as Received, and 48 Hour Clogging	105
26	Flow Test Results, Test Coupon No. 12, .0075 Slot Assembly, Surface Washed	106
27	Flow Test Results, Test Coupon No. 13, Perforated Titanium Strip Assembly	107
28	Flow Test Results, Test Coupon No. 14, Brunscoustic Strip Assembly	108
29	Flow Test Results, Test Coupon No. 15, Brunscoustic on Aluminum Core Panel Assembly	109
30	Flow Test Results, Test Coupon No. 16, Perforated Titanium, .005 Holes, on Aluminum Core Panel Assembly	110
31	Flow Test Results, Test Coupon No. 17, Polyimide (7-Ply), as Received, 48 and 144 Hour Clogging.	111
32	Flow Test Results, Test Coupon No. 17, Polyimide (7-Ply), Water Soak Test	112
33	Comparison of Flow Test Results, Test Coupons No. 3 and No. 4, Brunscoustic, as Received	113
34	Comparison of Flow Test Results, Test Coupons No. 9, 10 and 11, Perforated Titanium	114

TABLES

No.		Page
1	Material Evaluations	2
2	Test Matrix	11
3	Results of Corrosion Test	18

1.0 SUMMARY

This program has developed new techniques required for the fabrication of reliable laminar flow control panels that will be suitable for application on subsonic aircraft wings. Twenty two (22) variations of materials and design concepts were fabricated, tested, and evaluated. The results were compared with those predicted by aerodynamic analytical methods which were used to compute suction requirements and flow rates normal to the surface.

A set of requirements for LFC surface smoothness and flow have been compiled from data which exist in current literature. Various configurations of porous, perforated, and slotted materials were flow-tested to determine if they would meet these requirements. Perforated titanium, porous (loose weave) polyimide/fiberglass, and slotted configurations exhibited favorable results in the initial screening tests and are considered potential candidates for LFC surface materials. A summary of the material evaluations is shown in Table 1.

The flow tests were conducted in a vacuum chamber in order to evaluate the affect of altitude on flow performance. The candidate materials were then tested for susceptibility to clogging. These tests were conducted in an industrial environment and were used for relative comparisons of materials. Selected materials were also tested for resistance to corrosion by subjecting the panels to a 5% salt spray environment.

Current Boeing aircraft wing surfaces were inspected and found to be within the LFC smoothness requirements except at joints. Therefore, the waviness and smoothness requirements are not expected to cause any significant problems for manufacturing of LFC wings.

Load-bearing LFC surface installations are preferred over nonloaded (gloved) coverings because of the lower weight, simplicity, inherent ruggedness, and inspectability of the primary structure.

The criteria for flow and smoothness were adequate for this preliminary screening of materials, however, they should be further validated before the final determination of LFC designs is made. Following this program, the materials and design concepts should be further investigated to determine the fatigue life, damage susceptibility, cleaning requirements, and repair methods.

Table 1.—Summary of LFC Material Tests and Evaluations

Material evaluated	Potential candidate for LFC surface	Remarks
Perforated titanium	Yes	Suitable for strip and continuous skin configurations. Perforations showed less of a tendency to clog (25% increase in pressure) than those in porous metals and can be cleaned more easily to restore flow. Additional work is required to determine fatigue properties and cleaning techniques.
Polyimide	Yes	Suitable for strip configurations. Showed least tendency of all materials to clog (10% increase in pressure). Requires painting for ultraviolet protection. Not suitable for leading edge because of erosion. Additional work is required to determine cleaning technique.
Slotted configurations	Yes	Showed less of a tendency to clog (20% increase in pressure) than perforations but more than polyimide. Slots may be cleaned to restore flow. Aluminum slots must be adequately protected to prevent corrosion in the slot. This is difficult to do with narrow slots, so titanium slots should be considered. Slots are difficult to produce economically and will require additional manufacturing development.
Aircraft porous media material	No	This material had a 225% increase in pressure due to clogging and would be difficult to clean.
Brunscoustic	No	This material had a 250% increase in pressure due to clogging and would be difficult to clean.
Gore-Tex	No	This material had a 175% increase in pressure due to clogging and would be difficult to clean. Thickness of material would have to be greater than the 0.127 mm (0.005 in.) tested which would increase the flow resistance.
Michigan Dynamics Company material	No	The material had a 100% increase in pressure due to clogging and would be difficult to clean.

2.0 INTRODUCTION

Over the past two (2) decades many studies and several flight programs (including the Northrop X-21) have shown that drag reduction by laminar flow control (LFC) can substantially reduce the fuel consumption of large subsonic transports. However, some critical elements of technology and practical design approaches needed for successful application of LFC have been lacking. Among these are the development of satisfactory permeable aerodynamic surfaces and suction systems required to maintain the appropriate flow distribution through these surfaces.

The objective of the program was to develop the technology required for the fabrication of reliable laminar flow control panels suitable for application to subsonic aircraft wing skins. The approach used was: screen suitable materials for LFC surfaces; test candidate design concepts; and evaluate the results against established requirements and predicted values.

The program consisted of three tasks. Task 1 included screening of candidate materials and concepts, fabrication and flow testing of selected materials, and establishing flow requirements. Task 2 consisted of furnishing (to NASA) the selected specimens and materials used in Task 1 for mechanical properties tests. Task 3 was participation in a symposium, October 28, 1976, to summarize the total contract effort.

The program was accomplished during the time period April, 1976, to September, 1976, and was monitored by W. Edward Howell of the Composites Section, Materials Application Branch, Materials Division, NASA Langley Research Center.

The individuals who made technical contributions to the program and their areas of activity were:

B. L. Reynolds	Program Manager
D. D. Weiss	Principal Investigator
D. V. Lindh	Materials and Processes, Testing
R. C. Gunness	Aerodynamics
R. M. Kulfan	Aerodynamics
F. J. Traeger	Mechanical Systems, Flow Predictions
W. L. Cotton	Testing

3.0 SYMBOLS AND ABBREVIATIONS

C	Local Chord Length, m (inch)
cfm	Cubic Feet per Minute
cms	Cubic Meters per Second
D, L	Characteristic Dimensions m (in)
EB	Electron Beam
h	Wave Amplitude, m (inch)
Hr	Hour
K	Loss Factors
LFC	Laminar Flow Control
M	Mach Number
P	Pressure, Pa (psi)
P _O	Pressure of Standard Atmosphere at Sea Level Pa (psia)
P _T	Local Surface Pressure, Pa (psia)
psi	lb/in ²
psia	lb/in ² absolute
Re	Reynolds Number, $\rho \frac{VD}{\mu}$
Rec	Chord Reynolds Number
SEM	Scanning Electron Microscope
T _O	Temperature of Standard Atmosphere at Sea Level, °K (°R)
T _T	Local Temperature, °K (°R)
UV	Ultraviolet
V	Velocity m/sec (ft/sec)
w	Airflow Kg/sec·m ² (lbs/sec·ft ²)

3.0 SYMBOLS AND ABBREVIATIONS (Concluded)

Δ	Increment
Λ_s	Sweep of Structural Axis
λ	Wavelength, m (inch)
μ	Dynamic Viscosity Pa·sec (psi·sec)
ρ	Mass Density Kg·sec ² /m ⁴ (lbs·sec ² /in ⁴)
ρ_o	Mass Density at Standard Conditions Kg·sec ² /m ⁴ (lb·sec ² /in ⁴)
σ	Density Ratio, 35.3 $\frac{P_T}{T_T}$

4.0 TASK 1 LAMINAR FLOW CONTROL

Candidate surface materials, surface concepts, and fabrication and maintenance procedures were screened for suitable laminar flow control aircraft skins. Based on the most promising materials, three design concepts were selected, fabricated, tested, and evaluated for laminar flow control panels. The design conditions were those associated with application to a 200-passenger commercial transport with a 5500 nautical mile range at a cruise Mach number of 0.8. Aerodynamic analytical prediction methods were used to compute suction requirements and flow rates normal to the panel surface. Test panels were fabricated with material thickness and porosity that varied over a realistic range. Flow resistance tests were performed on the panels to determine the loss coefficient. The test results were compared with the predicted values to assess concept feasibility.

Aerodynamic analytical prediction methods described in Appendix C were used to compute suction requirements and flow rates normal to the panel surface. The aerodynamic requirements were established by searching the existing literature on LFC surfaces and applying it to the specified commercial transport.

Using these flow rates as a basis, porous candidate materials were evaluated to see if they could meet the functional and environmental requirements of a commercial transport. The selection of candidate materials for an LFC surface was based on their predicted flow rates, surface smoothness, structural compatibility with the primary wing structure and the materials' ability to meet environmental requirements, such as erosion, corrosion, hail damage, etc.

All of the porous and perforated materials were flow tested to determine their flow resistance. These measured flow rates were compared with the flow requirements given in Section 4.1. Materials which met the suction requirements were run through the clogging test to determine their susceptibility to clogging. A detailed description of the flow and clogging tests is given in Section 4.3.

Perforated titanium and Brunscoustic were selected from the flow tests and fabricated into strip assemblies and sandwich panels. These assemblies and panels were flow tested to verify the predicted flow resistance and to assess concept feasibility. See Section 4.4.2.1.2 for predicted flow resistance.

Slotted-aluminum panel assemblies were fabricated and flow tested. Two specimens were tested in a 5% salt spray exposure to determine susceptibility to corrosion. Another specimen was run through the clogging test. A graphite-composite panel with titanium-slotted cover was fabricated and tested in a 5% salt spray exposure.

4.1 SUCTION REQUIREMENTS AND FLOW RATES

The recommended surface porosity characteristics are representative of NASA specified airplane mission objectives (range = 10,186 km (5500 nautical miles), 200-passenger commercial transport, $M = 0.8$).

The pressure loss associated with the porosity of a material, must provide a compromise between conflicting demands. Minimizing the pressure loss across an LFC surface reduces the suction system design power requirements. However, the inflow distribution of a low-resistance surface is quite sensitive to changes in the external pressure distribution that occurs when the angle of attack is altered. Excessive variations could lead to outflow through the surface or surging of the flow into the internal ducts.

The porosity of a material for an LFC suction surface should be selected to provide balanced flow control with low suction system power requirements and also avoid local flow disturbances that could feed back into the boundary layer causing transition. This minimum pressure loss must also take into account installation considerations. For example, the use of strips with higher local inflow would permit the use of a porous material that is not suitable for a completely porous surface installation.

The surface flow rate tests of candidate LFC materials were generally limited to those representative of the design mission requirements. Figure 1 shows the flow rate envelope for a typical LFC airplane with a slotted surface. This envelope corresponds to a cruise Mach number = 0.8, cruise altitude from 7,620 m to 11,582 m (25,000 ft to 38,000 ft), and a local chord of 7.62 m (25 feet). The losses through the slots and through the bleed holes to the tributary ducts are included in the ΔP . The wing chord locations used to develop this envelope include 10%, 50% and 95% of chord for the upper and lower surfaces. The boundaries shown on Figure 1 provide a general operating envelope rather than definite limits. Material flow characteristics falling outside the envelope will result in a performance penalty which must either be accepted or compensated for in the airplane design. In general, the reasons for the limits are explained on the figure.

This envelope was determined using the calculation procedures established by Norair (Reference 1).

4.2 DESIGN CONCEPTS AND MATERIALS SELECTED FOR TESTING

The LFC suction surface may be either a glove concept which is not part of the primary load-carrying material or the suction surface may be made as an integral part of the load-carrying skin panel. Due to the difficulties of supporting a glove concept, lack of inspectability of the primary structure, increased maintenance requirements and increased weight of the glove concept, it was decided to investigate only integral structural concepts. The following concepts and materials were selected for testing:

A. Concepts

- Porous or perforated materials on backing of adhesive bonded honeycomb (see Figure 2)
- Porous or perforated material inserted into narrow strips built into the wing panel (see Figure 3). Manifolding would be inside the main wing skin. Bleed holes through the skin would be cold expanded to maintain fatigue resistance
- Narrow slots installed on the panel similar to the porous or perforated strips (see Figure 4).

B. Materials

- *Porous materials.* Brunscoustic, Aircraft Porous Media, Michigan Dynamics porous metal, porous teflon, and porous polyimide
- *Perforated.* Titanium sheet 0.076 mm (0.003 inch), 0.127 mm (0.005 inch), and 0.203 mm (0.008 inch) diameter holes
- *Slotted concepts.* Aluminum, titanium, and graphite composite.

The concepts and materials tested are fully described in Appendix A. In selecting the above materials only off-the-shelf materials were considered to minimize construction and testing time.

The characteristics desired in LFC materials are not significantly different from structural materials presently in use. Resistance to damage during assembly, structural and aerodynamic compatibility, electrical compatibility for some structural concepts, resistance to the environment in which the aircraft must operate, and repairability must be taken into consideration just as they are for existing subsonic aircraft materials.

Some unique characteristics must be considered in screening materials for LFC structure. They are:

- Resistance to flow
- Resistance to clogging
- Corrosion effects on flow
- Resistance to water ingress
- Aerodynamic smoothness

The materials listed were initially selected with critical requirements taken into consideration. Some of the materials were intended for use as-is, while others such as Gore-Tex were intended to be fabricated into a composite material possessing many of the desirable characteristics of each of the individual constituents.

4.3 TEST SET-UP AND PROCEDURES

4.3.1 FLOW TEST

The flow resistance of the materials and structural configurations were measured in a vacuum chamber which was evacuated to the air density corresponding to the selected altitude. Analysis showed that the flow loss characteristics of a porous or slotted surface can be expected to correlate in terms of $\sigma\Delta P$ (σ = air density ratio) and airflow per unit area. This relationship was verified by testing at values of σ corresponding to representative operational altitudes. For this purpose, chamber pressures were selected to provide appropriate values of σ with chamber temperature held constant.

The test chamber is shown in Figure 5 and the complete set-up illustrated in Figure 6. The test sample was placed in the aluminum specimen holder, where it was sandwiched between a backing frame and silicone rubber gasket to produce a seal and force the flow through the specimen. A manometer was used to monitor the pressure differential across the specimen required to maintain flow. Because of the low pressure, the fluid in the manometer is Dow Corning 200 fluid which has a specific gravity of 0.96. The flow was measured using either of two flow meters depending on rate. For flow below 0.00057 cms (1.2 cfm), a National Instrument Lab VOL-O-FLO Venturi Meter was used in conjunction with a water manometer. For flow above 0.00057 cms (1.2 cfm) a Rotometer was used. The flow meter not in use was isolated from the system by blocking its atmospheric inlet port.

The chamber pressure was read from a vacuum gage calibrated to an accuracy of 0.5%. However, the chamber pressure varied by ± 0.25 inch of mercury during a test run. Since the chamber did not have automatic control, pumps were stopped during a test. At the high flow rates the chamber pressure would slowly change. To overcome this, the test was started above the desired pressure and completed slightly below it. Tests were run starting at the low flow rates and at the high flow rates in each test run and the results averaged to minimize the effect of pressure fluctuation. The chamber pressure variation has a small effect on the test results.

The accuracy of the recorded data was controlled by the calibration accuracy of the test instruments. The flow rate was measured to an accuracy of 2% of the reported value. The pressure differential across the test sample was read to an accuracy of ± 0.05 inch of fluid. This resulted in an inability to distinguish changes occurring in very low-flow resistant materials such as polyimide material.

For additional accuracy at low flow rates, testing on polyimide (7-ply) materials was conducted at standard pressures on the Rayl test machine. The Rayl test machine is shown in Figure 7 and the complete set-up illustrated in Figure 8. The manometer can be read to 0.001 inch of water with a repeatability of ± 0.01 inch of water.

Test sample size was 0.0635 m x 0.229 m (2.5 x 9.0 inches) for material evaluation and for structural concepts with the entire surface of porous or perforated material. Strip or slotted structural configurations were tested over a 0.229 m (9.0 inch) long single strip or slot.

4.3.2 CLOGGING TEST

The clogging test consisted of passing a large volume of air through the test sample for a given period of time, usually 48 hours, except where noted otherwise. The sample was then retested for flow to determine any change in flow resistance. The flow-test fixture accommodates a 0.178 m x 0.229 m (7.0 x 9.0 in.) specimen for basic material tests. Assemblies 0.076 m x 0.305 m (3.0 x 12.0 inches) were tested by placing them diagonally on the samples and blocking out the remaining area. The unobstructed flow rate was 0.041 cms (86.5 cfm). The approximate rate with test samples was a function of flow resistance and is shown in the flow test data for each material. Figure 9 shows the large-volume sampler with a basic material specimen in test on the roof of the Boeing Renton plant. The test was protected from rain by a small roof, which is shown in the near left of the photograph (Figure 9).

4.3.3 CORROSION TEST

The corrosion susceptibility of selected assemblies was evaluated by subjecting 0.076 m x 0.305 m (3.0 x 12.0 inches) details to a 5% NaCl salt spray environment for 336 hours per ASTM B117. The samples had the long axis elevated 1.31 rad (75°) from the horizontal.

4.3.4 WATER INGRESS TEST

A water ingress test was conducted on the scottfelt material. The test consisted of placing a drop of water on the surface of the sample and noting the time for its complete absorption. A visual examination of the sample was then conducted. The 7-ply polyimide material was tested by immersing the test specimen in water and immediately running a flow test to determine the amount of blockage. The flow test was continued for 25 minutes and flow rates recorded.

4.4 TEST RESULTS AND DISCUSSION

4.4.1 TESTS CONDUCTED

Table 2 identifies each specimen and assembly evaluated in this program and identifies the testing to which it was subjected. Each part tested was given a coupon number and is described in Appendix A. The results of the flow and clogging tests are shown in Appendix B and discussed in Section 4.4.2. The results of the corrosion and water ingress tests are shown and discussed in Sections 4.4.3 and 4.4.4.

4.4.2 FLOW AND CLOGGING TEST RESULTS

The flow tests were conducted at several different chamber pressures to simulate the different cruise altitudes that materials are subjected to in commercial transport usage. Correlation between the tests at different altitudes was made by using $\sigma\Delta P$ parameter. The testing demonstrated that for preliminary screening of LFC candidate materials flow tests could be run at sea level, but for selected LFC materials they should be run at simulated altitude conditions. This would allow prediction of loss characteristics at the operational cruise altitude of an LFC airplane. The flow tests were conducted on test coupons No. 1 through 17. Results of these tests are presented in detail in Figures 10 through 34. Raw test data and reduced data are contained in Appendix B. A discussion of the results of the flow and clogging tests by coupon number follows.

Table 2.—Test Matrix

Test coupon no.	Description	Flow tests					Clogging tests				Other tests
		Chamber pressure (in.Hg)					48 hr	72 hr	144 hr	Wash clean	
		30.0	22.6	8.9	6.1	3.4					
1	Gore-Tex L10814			X	X		X				
2	Gore-Tex L10813					X					
3	Brunscoustic (#1)		X	X	X	X	X			X	
4	Brunscoustic (#2)		X	X	X						
5	Aircraft porous media			X	X	X	X				
6	Michigan Dynamics		X	X	X	X	X				
7	Polyimide (16 ply)		X	X	X	X	X	X	X		
8	Polyimide (7 ply)		X	X	X						
9	Perforated Titanium 0.003 hole		X	X	X		X	X		X	
10	Perforated Titanium 0.005 hole			X	X		X				
11	Perforated Titanium 0.008 hole		X	X	X		X				
12	0.0073 slot assy.		X	X			X			X	
13	0.005 perforated titanium strip assy		X	X							
14	Brunscoustic strip assy			X	X						
15	Brunscoustic on aluminum core panel assy				X						
16	Perforated titanium on aluminum core		X	X							
17	Polyimide (7 ply)	X					X		X		Water soaked
18	Slotted panel assy 0.004 slot										Corrosion
19	Slotted panel assy (painted)										Corrosion

Table 2.—(Concluded)

Test coupon no.	Description	Flow tests					Clogging tests					Other tests
		Chamber pressure (in.Hg)					48 hr	72 hr	144 hr	Wash clean	Reverse flow	
		30.0	22.6	8.9	6.1	3.4						
20	Slotted panel assy											Corrosion
21	Slotted panel assy (painted)											Corrosion
22	Scottfelt											Water ingress

The data scatter observed in the flow test results was due primarily to the manometer used with the vacuum chamber test set-up (Figures 5 and 6). This manometer could only indicate pressure differentials to ± 0.05 inch of fluid. For flows and pressures in the suction requirements envelope, this represents a variance in pressure readings of 2% to 5%. At very low Δ pressures the variance could be as much as 50%.

For additional accuracy at low Δ pressures testing on polyimide (7-ply) materials was conducted at atmospheric pressure on the Rayl test machine (Figures 7 and 8). The manometer can be read to 0.001 inch of water.

The clogging tests provided a relative rating of the susceptibility of the materials to contaminants in the air. Since the criteria for contamination that the LFC materials will see in commercial service has not been established, these tests were not intended to be necessarily representative of service conditions, but an indication of the materials susceptibility to clogging. The volume of air passing through the specimen in the clogging test is approximately 0.024 cms (50 cfm). This is approximately 50 times the volume of air per unit area passing through the specimen in the service environment. Therefore, 48 hours in the clogging test would be equivalent to 2400 service hours or approximately one year of service. The amount of contaminants would not necessarily be the same as for one year of service as these criteria have not been defined.

4.4.2.1 Flow Test Correlation and Prediction Methods

4.4.2.1.1 Surface Airflow and Pressure Loss Characteristics.—The flow through the suction surface should be primarily viscous to prevent passage irregularities from causing premature separation through feedback of disruptions in flow. In addition, pressure losses should be sufficient to assure positive inflow under all normal operation conditions. The friction loss characteristics in the viscous laminar flow regime can be readily defined as the loss is directly proportional to flow velocity. However, the expansion or turbulent flow losses associated with inlet, exit and flow passage sizes and shapes must also be evaluated. For irregular shapes the loss characteristics must be determined by test.

The relationships of parameters that must be considered in the evaluation of the surface pressure losses are shown in the following derivation.

Symbols used include:

SYMBOL	DEFINITION	UNITS
D, L	Characteristic dimensions	m
Re	Reynolds Number, $\rho \frac{VD}{\mu}$	
μ	Dynamic Viscosity	Pa·s
ρ	Mass Density	Kg·sec ² /m ⁴
V	Velocity	m/sec
w	Airflow	Kg/sec·m ²
P	Pressure	Pa
σ	Density ratio to standard, $\frac{\rho}{\rho_0}$	
K	Loss factor	
ρ_0	Mass Density at Standard Conditions	Kg·sec ² /m ⁴

Total pressure loss is made up of friction and expansion losses.

$$\Delta P = \Delta P_{frict} + \Delta P_{exp}$$

For laminar flow in a tubular-like passage

$$\Delta P_{frict} = K \left(\frac{L}{D} \right) \left(\frac{1}{Re} \right) \left(\frac{PV^2}{2} \right)$$

Where L generally corresponds to the length and D, the diameter of the passage. The expansion losses are generally proportional to dynamic pressure and are expressable as:

$$\Delta P_{exp} = K_{exp} \left(\frac{PV^2}{2} \right)$$

However, for present purposes it is more convenient to express the losses in terms of air flow. This is easily done in the above expressions to yield the following equation for the total loss.

$$\sigma \Delta P = K_{frict} (w) + K_{exp} (w)^2$$

Where w = weight flow per square meter of flow area.

This relationship can also be used in the same form when airflow is defined in terms of any reference area such as projected porous surface area.

There would be considerable difficulty in evaluating the K factors associated with different surfaces. However, for the purposes of comparing test panels and predicting off-design performance, the parametric plot of airflow versus corrected pressure loss used for the test information represents a choice of parameters that would allow direct evaluation of test sample characteristics. This method was preferred because all tests were conducted at laboratory ambient temperature that was essentially constant (approximately 70°F). Therefore, a viscosity correction was not required and both pressure loss and airflow were determined directly.

The testing of the perforated and slotted samples was conducted at flow velocities through the surfaces such that the characteristic Reynolds numbers were generally less than 200 and considerably below critical Reynolds number for transition (approximately 2000).

The losses measured for the slotted specimens show direct correlation with those determined by analysis from procedures developed by Norair for slots and holes between plenums (Reference (1); see Figure 25). Detailed calculations are shown in Appendix D.

The results for the holes in perforated plate do not correlate directly with Norair data (Reference 1). This is because the Norair data was for straight holes and the perforated titanium had irregular hole shapes, sizes and tapers. These influence effective inlet area and velocity profile development, thus resulting in loss variations that differ from those of a uniform passage. However, the pressure losses would still be expected to vary in the manner generally predicted by the pressure loss equation above.

In addition, reference open areas for the holes in porous surface specimens cannot be established by direct measurement because of the random inlet hole sizes, irregular passage shapes, and nonuniform passage areas.

4.4.2.1.2 Prediction Methods for Strip Assemblies.—The data obtained from the sheet materials (coupons No. 3 and 10) can be used to predict the flow resistance of the strip assemblies. To predict the flow resistance of the assemblies, the increased local flow is corrected due to the reduced surface area. Then the $\sigma\Delta P$ is read from the curve developed for the sheet material. To this value is added the pressure drop due to the supporting structure, such as bleed holes, the result is the predicted $\sigma\Delta P$ for the strip assembly. Sample calculations for the strip assemblies (coupons No. 13 and 14) are shown in Appendix D.

4.4.2.2 Gore-Tex

The Gore-Tex material test coupon No. 1 had a relatively high but acceptable initial flow resistance and exhibited an increased pressure of approximately 175% after a 48 hour clogging test. The data is presented in Figure 10. Test coupon No. 2, which was a less permeable material, exhibited a high initial flow which exceeded the capability of the test set-up. Testing of the material was discontinued.

4.4.2.3 Brunscoustic

The Brunscoustic material test coupons No. 3 and No. 4 were flow tested and the results for the as-received condition are compared on Figure 33. An average difference in $\sigma\Delta P$ for these two samples was 15% higher for coupon No. 4. The flow resistance for the as-received material was lower than the projected envelope, but is acceptable when added to the pressure losses of the supporting structure. The pressure required to maintain the same flow was increased approximately 250% after a 48 hour clogging test. An attempt to clean this material by reversing the flow was unsuccessful. The flow test data for these coupons is presented in Figures 11, 12, 13, and 14.

4.4.2.4 Aircraft Porous Media

The Aircraft Porous Media material test coupon No. 5 had an as-received flow resistance similar to the Brunscoustic material. The pressure required to maintain the same flow was increased approximately 225% after a 48 hour clogging test. The data is presented in Figure 15.

4.4.2.5 Michigan Dynamics

The Michigan Dynamics material test coupon No. 6 had an as-received flow resistance similar to the Brunscoustic material. The pressure required to maintain the same flow was increased approximately 100% after a 48 hour clogging test. The data is presented in Figures 16 and 17.

4.4.2.6 Polyimide

The polyimide material (16-ply and 7-ply) test coupons No. 7 and 8 had the least flow resistance of all the materials tested. When the material was tested for clogging susceptibility it showed a decrease in flow resistance after a 48 hour clogging test. This indicated an error in the conducting of the test, such as an undetected leak. Because of this inconsistency, plus the fact that the test was at the minimum pressure measuring capability of the test set-up, it was decided to run additional flow and clogging tests. These flow tests were run on the Rayl test machine (see Figure 7), which has a more accurate manometer and the capability for higher flow rates. The data scatter which was exhibited in the tests of coupons 7 and 8 (Figures 18 & 19) was due to the low ΔP which had to be measured. The manometer used was not sensitive enough to read these low pressures accurately. This data scatter and inconsistency on the clogging test was eliminated by testing on the Rayl test machine.

The polyimide material (7-ply) test coupon No. 7 was flow tested on the Rayl test machine and the flow rate was much higher than required for an LFC surface material at the required $\sigma\Delta P$. Therefore, the material would be suitable only if used in a concept which will give higher local flows, such as a strip concept. The pressure required to maintain the same flow was increased approximately 10% after a 48 hour clogging test and 40% after a 144 hour clogging test. The data is presented in Figure 31. An additional test was run on the polyimide material to determine the effect of blockage due to moisture. Coupon No. 17 was

soaked in a water bath and then tested on the Rayl test machine to determine the amount of blockage and the time required to return to normal flow. The initial blockage was severe. The pressure increased from 124 to 1138 Pa (0.018 to 0.165 psi). There was a rapid recovery in the first 2 minutes to 265 Pa (0.0385 psi) with a slower recovery to normal pressures after 14 minutes (see Figure 32). This test is more severe than would be encountered in service, since the coupon was completely immersed in water, but does not account for additional water being added such as in rain or freezing conditions. These conditions are beyond the scope of this contract and should be considered in follow-on programs.

Based on previous manufacturing experience, the flow resistance of porous polyimide materials can be controlled to within 10% of the desired values.

4.4.2.7 Perforated Titanium

Perforated titanium sheets with three different hole sizes were tested. The hole diameters were 0.076, 0.127, and 0.203 mm (0.003, 0.005 and 0.008 in.) which correspond to test coupons No. 9, 10 and 11. The open area was 0.37% for coupon No. 9 (0.003 in. holes), 0.24% for coupon No. 10 (0.005 in. holes), and 0.55% for coupon No. 11 (0.008 in. holes). The material was tested in the as-received condition and the results are compared on Figure 34.

The control of hole-inlet shape and size was such that the actual open flow area per square foot of coupons No. 9, 10 and 11 was not equal. The hole passages had irregular tapers and the exit areas varied considerably. Therefore, the test results did not correlate directly with predicted values from Norair data (Reference 1). The test results are shown in Figure 34. The open area was largest for coupon No. 11 (0.008 in. holes) followed by coupon No. 9 (0.003 in. holes) and coupon No. 10 (0.005 in. holes) with the least open area. At the higher flow rates coupon No. 10 had the highest flow resistance followed by coupon No. 9 and coupon No. 11 with the lowest flow resistance. This is as expected because of the relative open area. The slope of the curves at the higher flow rates is approximately proportional to velocity squared. This indicates that the pressure losses due to expansion are predominate. As the flow rate is decreased the slopes of the curves tend to change due to the increasing effect of friction losses which tend to be proportional to velocity. The slope of the curve for coupon No. 9 (0.003 in. holes) changes more rapidly than coupon No. 10 and coupon No. 11. This is expected because the smaller diameter holes which have the lower Reynolds numbers are affected the most by pressure losses due to friction. This is why test data from coupon No. 9 (0.003 in. holes) crosses the data from coupon No. 10 (0.005 in. holes). Additional discussion and analysis of the data are presented in Section 4.4.2.1 and Appendix D.

Electron beam perforations of titanium resulted in holes which were consistent within ± 0.00025 in. However, the diameters varied as much as 0.0007 in. from the desired diameter. The spacings were within 0.001 in. It is anticipated that these tolerances could be improved. Therefore, the flow resistance should be able to be controlled to less than 10%.

The pressure required to maintain the same flow was increased approximately 25% after a 48 hour clogging test. The flow test data is presented in Figures 20, 21, 23 and 24. Test coupon No. 9 was run an additional 24 hours in the clogging test. The pressure required increased an additional 40%. The specimen was then washed with water, wiped with a cloth, and flow tested. The pressure required decreased by 40%, which was approximately the same as for the 48 hour test (Figures 21 and 22).

4.4.2.8 Slot Assembly

A slotted aluminum assembly test coupon No. 12 was fabricated with an average slot width of 0.185 mm (0.0073 in.). The flow resistance of the as-received coupon fell within the specified envelope (Figure 25), which was as predicted in establishing the suction requirements (Section 4.1). For a discussion of the data see Section 4.4.2.1.1 and Appendix D.

The pressure required to maintain the same flow was increased approximately 20% after a 48 hour clogging test. The coupon was then washed with water, wiped with a cloth, and flow tested. The pressure required decreased only slightly from that of the 48 hour test (Figures 25 and 26).

4.4.2.9 Strip Assembly

The 0.127 mm (0.005 in.) perforated titanium sheet and the Brunscoustic materials were fabricated into strip panel assemblies and flow tested (coupons No. 13 and 14). The perforated titanium strip flow resistance was too high (Figure 27). For this concept to be acceptable a perforated titanium with more open area would have to be used to reduce the flow resistance. The Brunscoustic strip assembly flow resistance was within the suction rate envelope (Figure 28). The data obtained from the sheet materials coupons No. 3 and 10 can be used to predict the flow resistance of the strip assemblies. See Section 4.4.2.1.2 and Appendix D for predictions on these assemblies.

4.4.2.10 Aluminum Core Panel Assembly

The Brunscoustic material and the 0.127 mm (0.005 in.) perforated titanium sheet were fabricated into aluminum core panel assemblies and flow tested (test coupons 15 and 16). The flow resistance of coupon No. 15 (Brunscoustic) was less than indicated by the suction rate requirements (see Figure 29). The flow resistance of coupon No. 16 (perforated titanium) was within that indicated by the suction rate requirements (see Figure 30). Predictions of the panel assembly flow resistance were not made because of the difficulty of determining the pressure loss through the supporting structure.

4.4.3 CORROSION TEST RESULTS

Four slotted assemblies were tested in a 5% NaCl salt spray environment for 336 hours per ASTM B117. This test was conducted to provide a guide as to the susceptibility of the slotted assemblies to corrosion and is a standard test to check airplane components. The results of the tests are presented in Table 3.

Table 3.—Results of Corrosion Test

Test coupon no.	Sample	Visual description
18	Aluminum slot (7075) phosphoric anodized (not painted)	Slot completely filled with aluminum oxide Al_2O_3 . Oxide could be removed easily with thin knife blade.
19	Aluminum slot (7075) phosphoric anodize + primed (BMS 10-11) painted corogard	No clogging or corrosion products detected by visual inspection.
20	Titanium slot bare (graphite base)	No clogging or corrosion products detected by visual inspection.
21	Aluminum slot (5052) phosphoric anodized (not painted)	Small amount of corrosion products but no clogging detected by visual inspection.

4.4.4 WATER INGRESS TEST RESULTS

A water ingress test was conducted on the Scottfelt material test coupon No. 22. The material behaved as a sponge. A drop of water placed on the surface was completely absorbed in 15 minutes. The Scottfelt material was considered as a backing support for LFC material, therefore it was important that it not absorb water. Water absorbed into the material would be difficult to remove and would affect the suction characteristics of the LFC surface. No additional testing was conducted on this material.

Polyimide (7-ply) test coupon No. 17 was soaked in a water bath and then flow tested. The test results are discussed in Section 4.4.2.5 and presented in Figure 32.

4.5 COMPLIANCE WITH AERODYNAMIC SMOOTHNESS AND WAVINESS REQUIREMENTS

The requirements for aerodynamic surface smoothness and waviness are presented in Appendix C and derived primarily from Norair data and work by Dr. Pfenninger (References 1 through 4). However, precise aerodynamic smoothness criteria are not available for the types of arrangements evaluated under this contract. Furthermore, these criteria are, in many cases, not applicable since they can not be related to that portion of the surface where inflow actually occurs such as a porous area. Although each sample tested was examined for general compliance with the requirements, no final conclusions were drawn about the suitability of any material or concept from the standpoint of smoothness in areas of inflow.

In many cases, therefore, promising materials and concepts would have to be tested in the wind tunnel or in flight to establish suitability for application on an LFC airplane.

Except in the areas noted (i.e. inflow areas), the surfaces of the arrangements tested generally meet the aerodynamic smoothness requirements. Porous materials, while fairly smooth to the touch, were probably rougher than allowable and should be used in a configuration which permits some smoothing technique (e.g. paint or filler), except in the actual inflow area. Alternately, improved tooling combined with a finer weave or fiber content could provide a smoother surface and one closely approaching the required porosity.

From the standpoint of waviness, the examination of a small coupon is inconclusive. However, an examination of production wings of the 737 and 747 airplanes was conducted and the results compared with the requirements. Although the LFC waviness requirements are more stringent than the existing specifications, the current wings meet the LFC waviness standards. Fastener smoothness requirements were within the LFC standards. It is doubtful that an LFC wing with large numbers of fasteners would be acceptable in practice. Gaps and mismatches did not meet the LFC requirements, but should not be difficult to achieve with different design and tooling.

The existence of "flats" on the wing surface may trigger turbulence. These "flats" may occur when the surface material is slotted in a contoured area of the wing. This condition was not evaluated under this contract. The "flats" could be minimized or eliminated by having the material to be slotted preformed to contour prior to installation. This condition should not exist on a perforated or porous strip concept.

5.0 TASK 2 MECHANICAL PROPERTIES MATERIAL

The following materials and panel assemblies with accompanying data sheets were sent to NASA Langley Research Center, Hampton, Virginia, October 5, 1976, for materials properties tests. For detail specimen description, see Appendix A.

Sheet material (5 total) test coupons No. 7, 8, 9, 10 & 11

Polyimide 7-ply and 16-ply

Perforated titanium sheet 0.076 mm (0.003 in.),
0.127 mm (0.005 in.) and 0.203 mm (0.008 in.)
diameter holes

Strip panel assemblies (2 total) test coupons No. 13 & 14

Brunscoustic

Perforated titanium 0.127 mm (.005 in.)
diameter holes

Continuously porous or perforated panel assembly (2 total) test coupons No. 15 & 16

Brunscoustic

Perforated titanium 0.127 mm (0.005 in.)
diameter holes

Slotted panel assemblies (3 total) test coupon No. 18, 12 & 19

Aluminum slot with slot widths of 0.102 mm (.004 in.),
0.185 mm (0.0073 in.) and 0.229 mm (.009 in.)

6.0 TASK 3 PARTICIPATION IN SYMPOSIUM

On October 28, 1976, the symposium was held at the National Aeronautics and Space Administration, Langley Research Center, Hampton, Virginia. The Boeing Commercial Airplane Company made an oral presentation summarizing the total contract effort.

7.0 CONCLUSIONS AND RECOMMENDATIONS

7.1 CONCLUSIONS

The screening of candidate materials for Laminar Flow Control was based on their flow rates and resistance to clogging and corrosion. Although no firm criteria has been established relative to clogging, it is an important consideration because of the potentially high maintenance and replacement costs.

Of the materials tested, perforated titanium, porous polyimide, and slotted assemblies demonstrated a much greater resistance to clogging than other porous materials. Corrosion tests on slotted assemblies indicated that a titanium surface is preferred to aluminum because of the comparative corrosion resistance of the two materials and the difficulty of applying adequate corrosion protection to the edges of the slots. However, combining titanium with aluminum base structure requires the consideration of other factors such as galvanic corrosion and differential thermal expansion characteristics.

Three concepts for installing LFC materials were studied and are listed below in order of preference.

1. Strip concept (Figure 3)
2. Slot metal overlay strip concept (Figure 4)
3. Continuous skin concept (Figure 2).

These are all load-bearing LFC surface concepts which are preferred over nonloaded (glove) concepts because of the lower weight, inspectability of primary structure, improved damage resistance, and reduced maintenance. However, certain combinations of materials may present fatigue problems that must be considered in design.

For slotted specimens, the pressure losses showed good correlation between test results and analytical prediction methods. For perforated titanium, the pressure losses did not show direct correlation with Norair data (Reference 1) because of the irregular hole shapes.

LFC surface smoothness and waviness requirements are similar to those required of current commercial aircraft, except at joints and gaps. Therefore, it was concluded that future design and manufacturing of LFC wings will require improvements in joints and gaps. Also there is considerable doubt that present aerodynamic smoothness requirements for LFC wings are adequate particularly when different types and large numbers of roughness elements are present. Current manufacturing methods may not be adequate for LFC wings.

7.2 RECOMMENDATIONS

The program supported the feasibility of producing reliable Laminar Flow Control materials and therefore it is recommended that future work be performed. Listed below are additional specific recommendations:

1. Materials recommended for further evaluations are perforated titanium, porous polyimide, and corrosion resistant slotted assemblies.
2. Continue searching for surface materials which are naturally corrosion resistant rather than trying to protect the walls of the flow path (slot edges, holes, tortuous path, etc.).
3. Strip concepts, shown in Figure 3, have a lot of potential advantages in repair and maintenance and should be studied further.
4. Slot metal overlay strip concept, shown in Figure 4, and continuously porous or perforated skin concept, shown in Figure 2, are recommended for further study.
5. Verify aerodynamic requirements by wind tunnel and flight testing.
6. Continue clogging evaluation considering other possible contaminants, such as, fuel, skydrol, etc. Requirements should be verified by in-service testing.
7. Develop cleaning techniques for each of the recommended concepts.
8. Conduct fatigue tests to verify durability of each of the recommended concepts.
9. Develop repair and replacement procedures.
10. Define maintenance requirements for each of the recommended concepts.

APPENDIX A

DESCRIPTION OF TEST COUPONS

Table A-1.—Index to Description of Test Coupons

Test coupon no.	Specimen	For coupon dimensions see figure	For coupon photograph see figure	For detail material description see page
1	Gore-Tex L10814	A-1	---	42
2	Gore-Tex L10813	A-1	---	42
3	Brunscoustic #1	A-3	A-4	42
4	Brunscoustic #2	A-3	---	42
5	Aircraft porous media material	A-3	A-5	43
6	Michigan Dynamics porous metal	A-3	A-6	43
7	Polyimide (16-ply)	A-1	A-2	43
8	Polyimide (7-ply)	A-1	---	43
9	Perforated titanium 0.003 in. holes	A-7	A-8 & A-9	44
10	Perforated titanium 0.005 in. holes	A-7	A-8 & A-10	44
11	Perforated titanium 0.008 in. holes	A-7	A-8 & A-11	44
12	Aluminum slotted assembly (0.0073 in.)	A-12	---	44
13	Perforated titanium strip assembly	A-13	---	---
14	Brunscoustic strip assembly	A-13	---	---
15	Brunscoustic on aluminum core panel assembly	A-14	---	---
16	Perforated titanium on aluminum core panel assembly	A-14	---	---
17	Polyimide (7-ply)	A-15	---	43
18	Aluminum slotted assembly	A-12	---	44
19	Aluminum slotted assembly	A-12	---	44
20	Slotted assembly graphite base titanium cover	A-16	---	44
21	Aluminum slotted assembly	A-12	---	44
22	Scottfelt	A-17	---	44

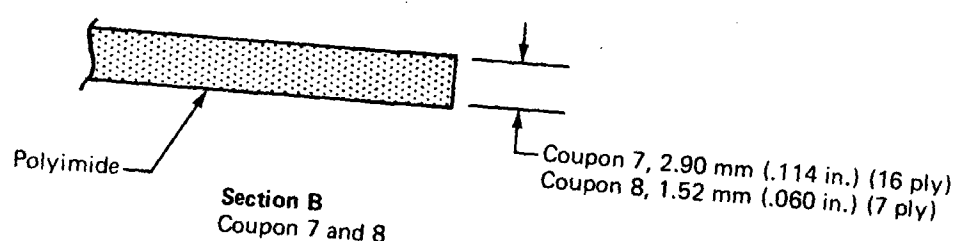
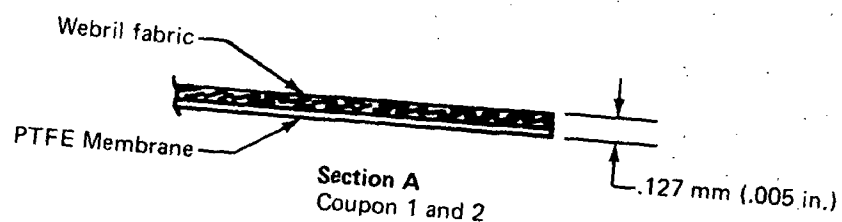
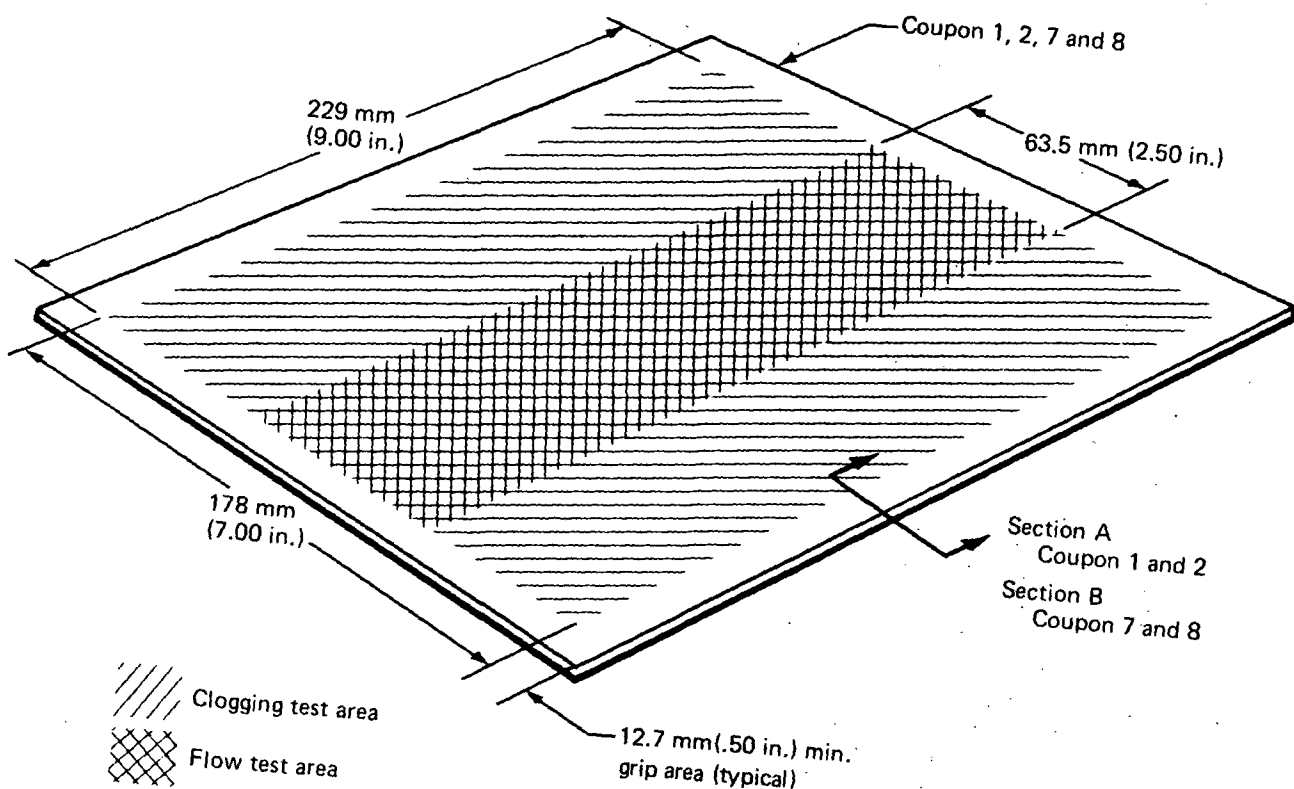
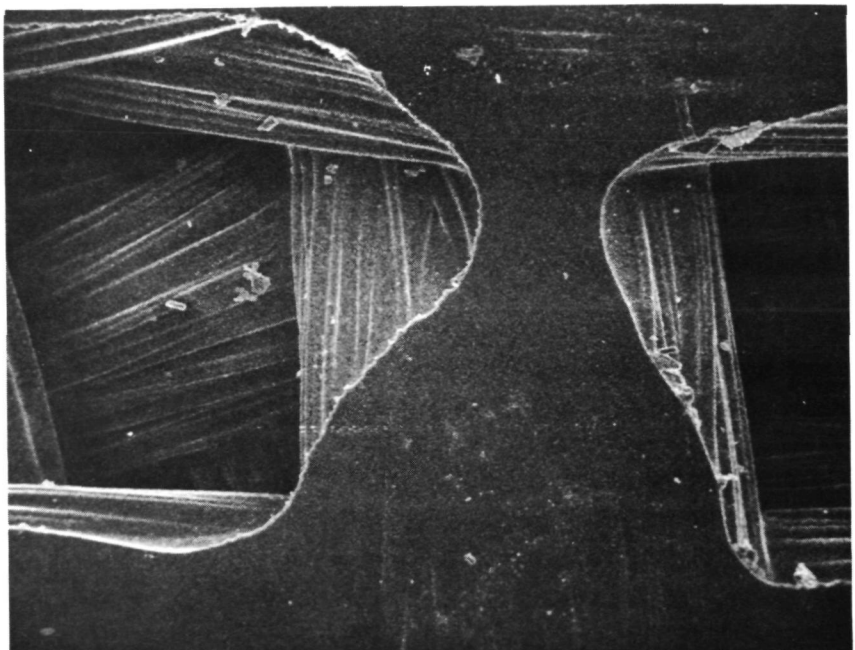
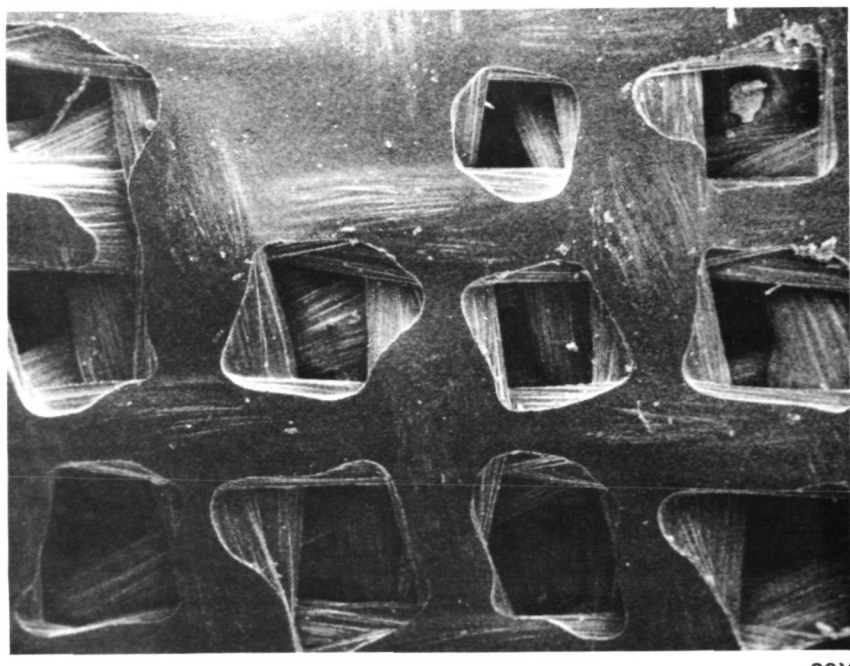


Figure A-1.—Description of Test Coupons 1, 2, 7 and 8



100X

Enlargement of Local Area



30X

Figure A-2.—SEM Photograph of Polyimide Material Surface

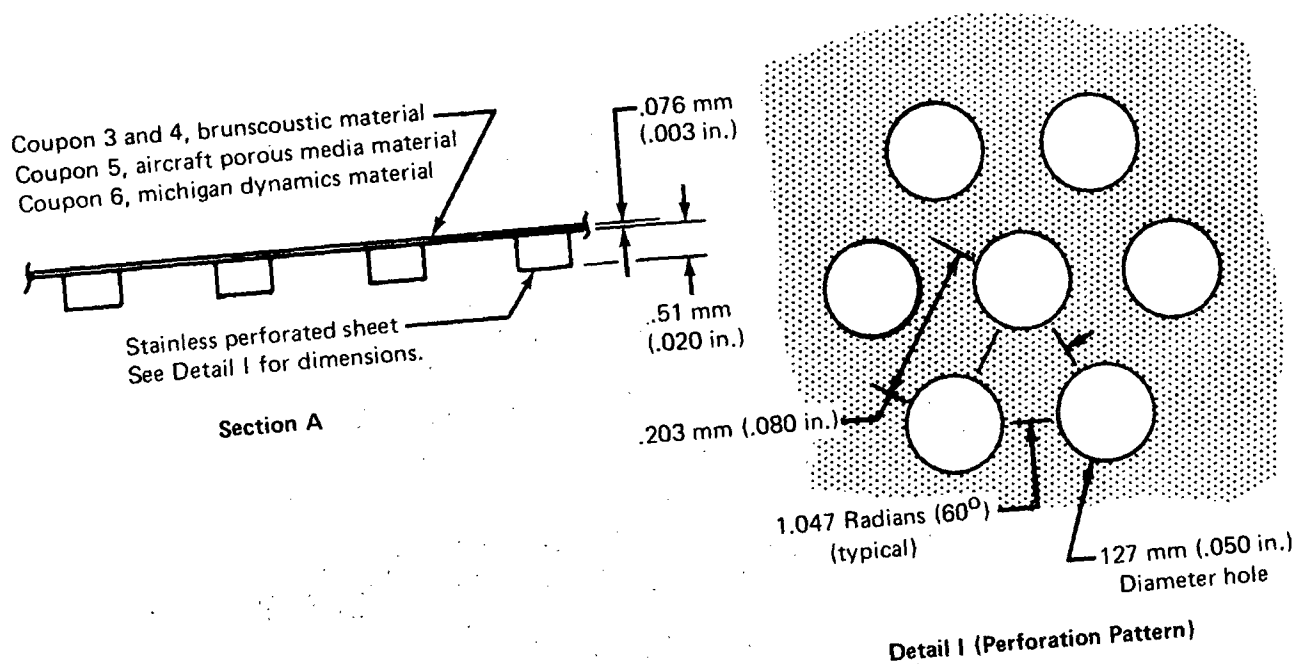
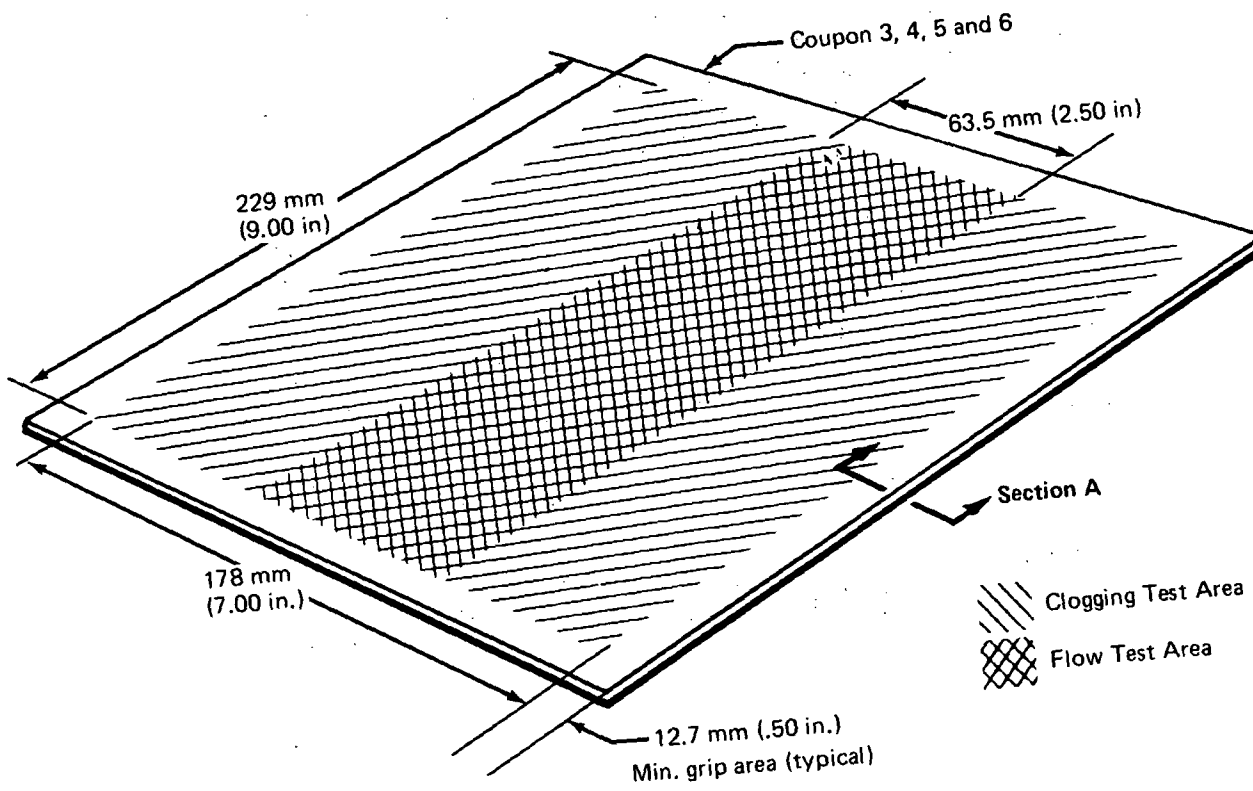
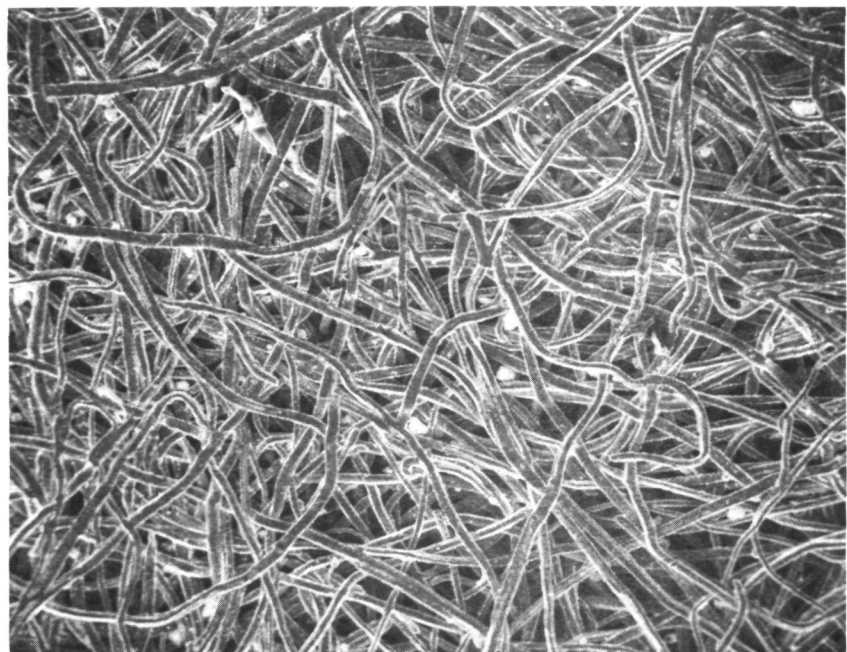
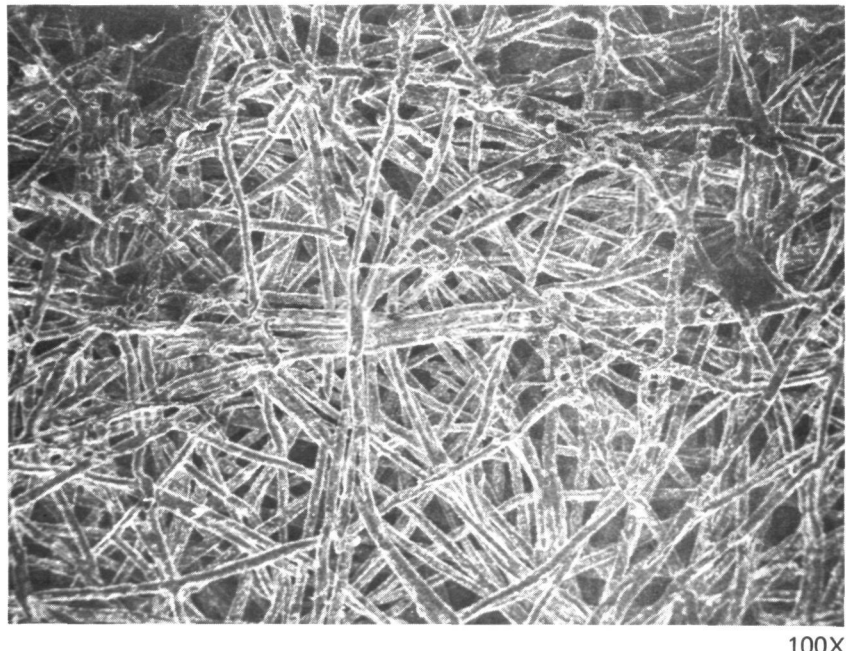


Figure A-3.—Description of Test Coupon 3, 4, 5 and 6



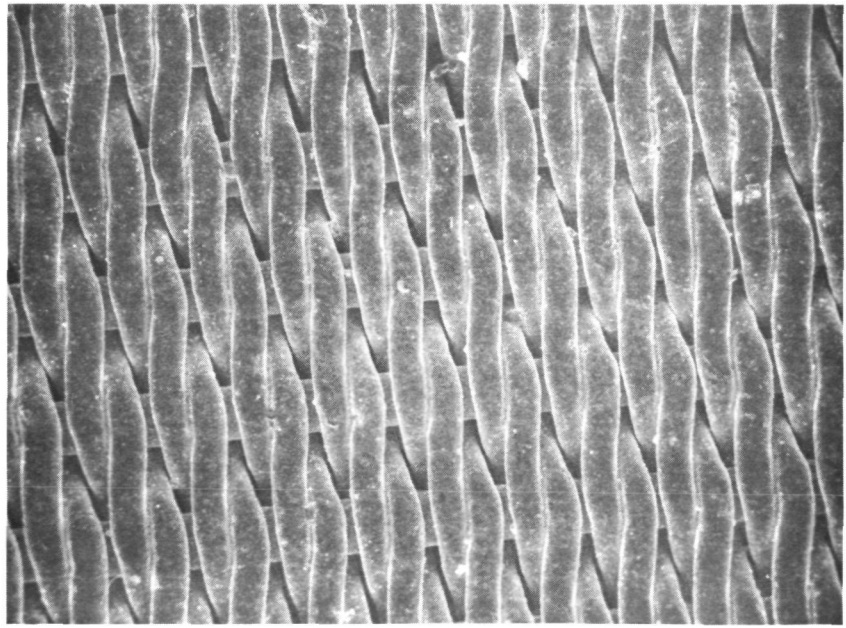
100X

Figure A-4.—Scanning Electron Microscope (SEM) Photograph of Brunscoustic Fiber Mat



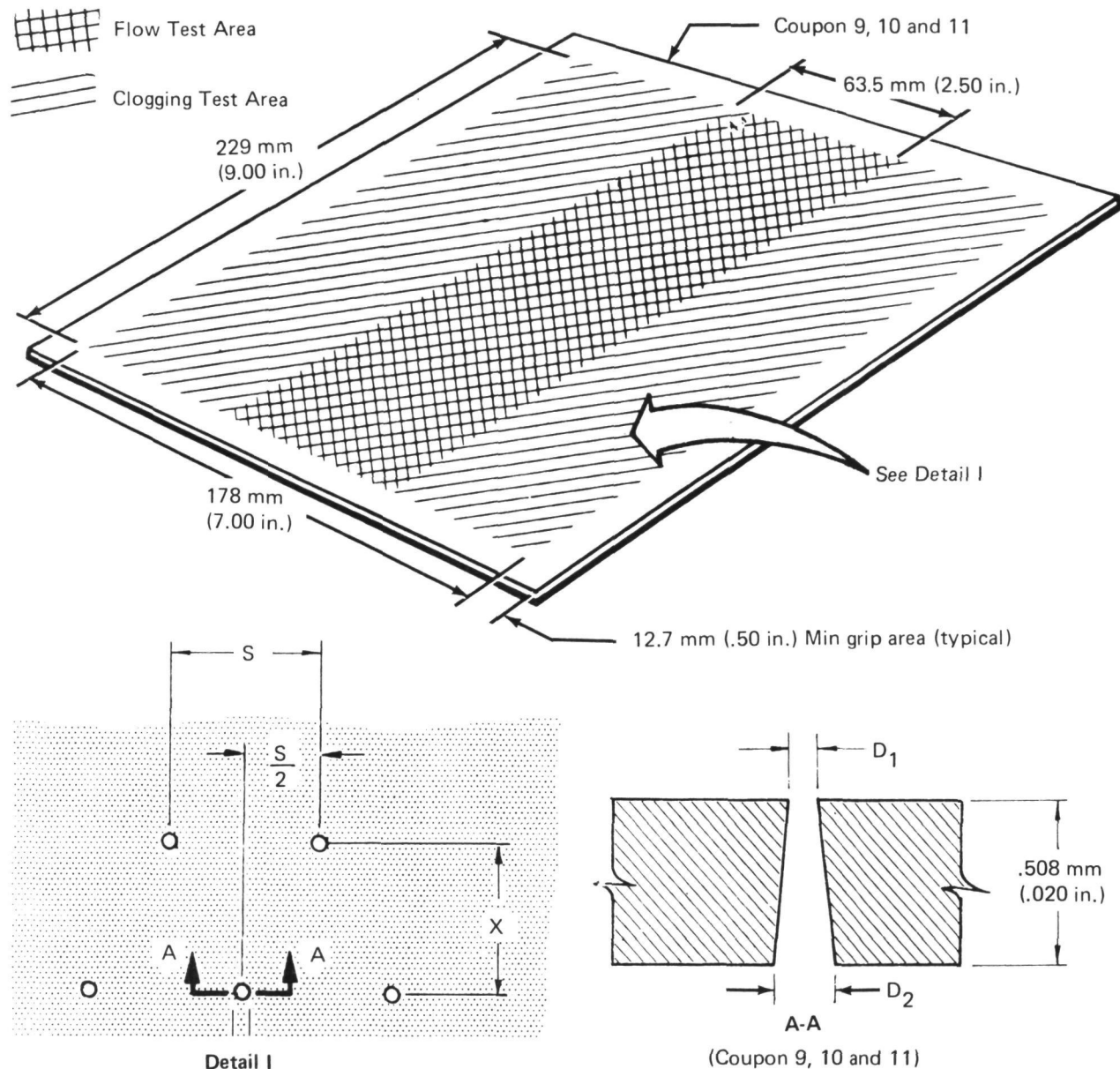
100X

Figure A-5.—SEM Photograph of Michigan Dynamics Material



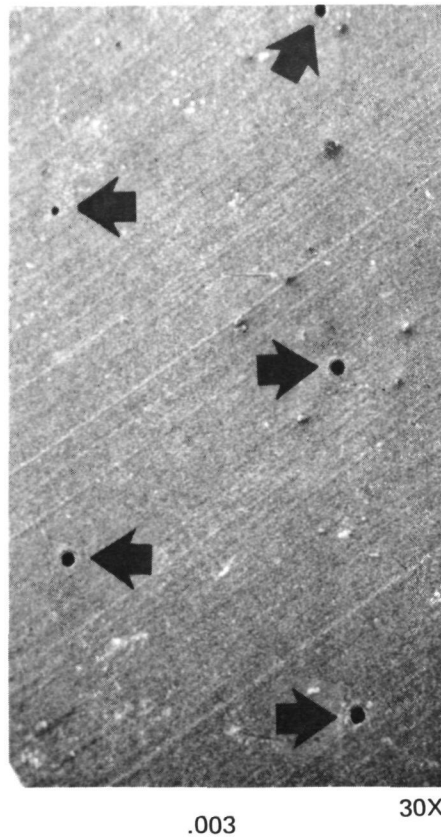
100X

Figure A-6.—SEM Photograph of Aircraft Porous Media Woven Fiber Mat



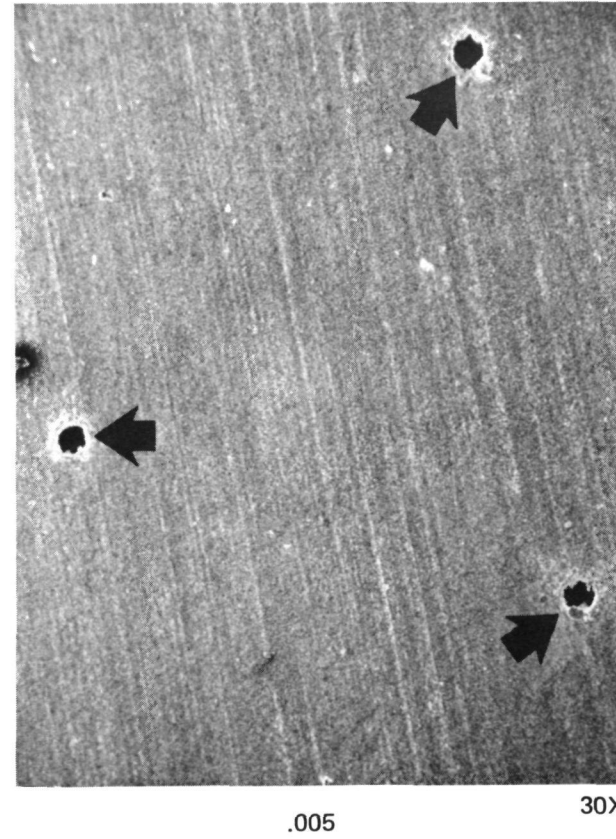
Average Optically Measured Dimensions					
Coupon Number	D ₁	D ₂	S	X	Percent Open Area
9	.081 mm (.0032 in.)	.229 mm (.009 in.)	1.27 mm (.050 in.)	1.09 mm (.043 in.)	.37
10	.109 mm (.0043 in.)	.229 mm (.009 in.)	2.11 mm (.083 in.)	1.83 mm (.072 in.)	.24
11	.185 mm (.0073 in.)	.356 mm (.014 in.)	3.38 mm (.133 in.)	1.45 mm (.057 in.)	.55

Figure A-7.—Description of Test Coupon 9, 10 and 11



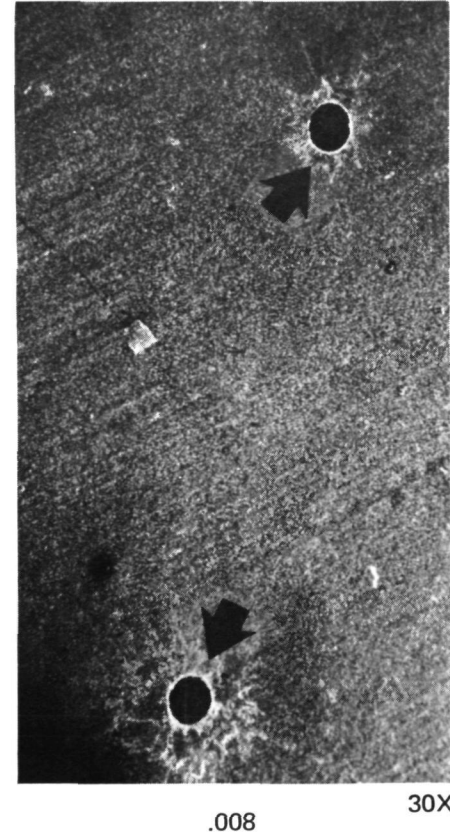
.003

30X



.005

30X

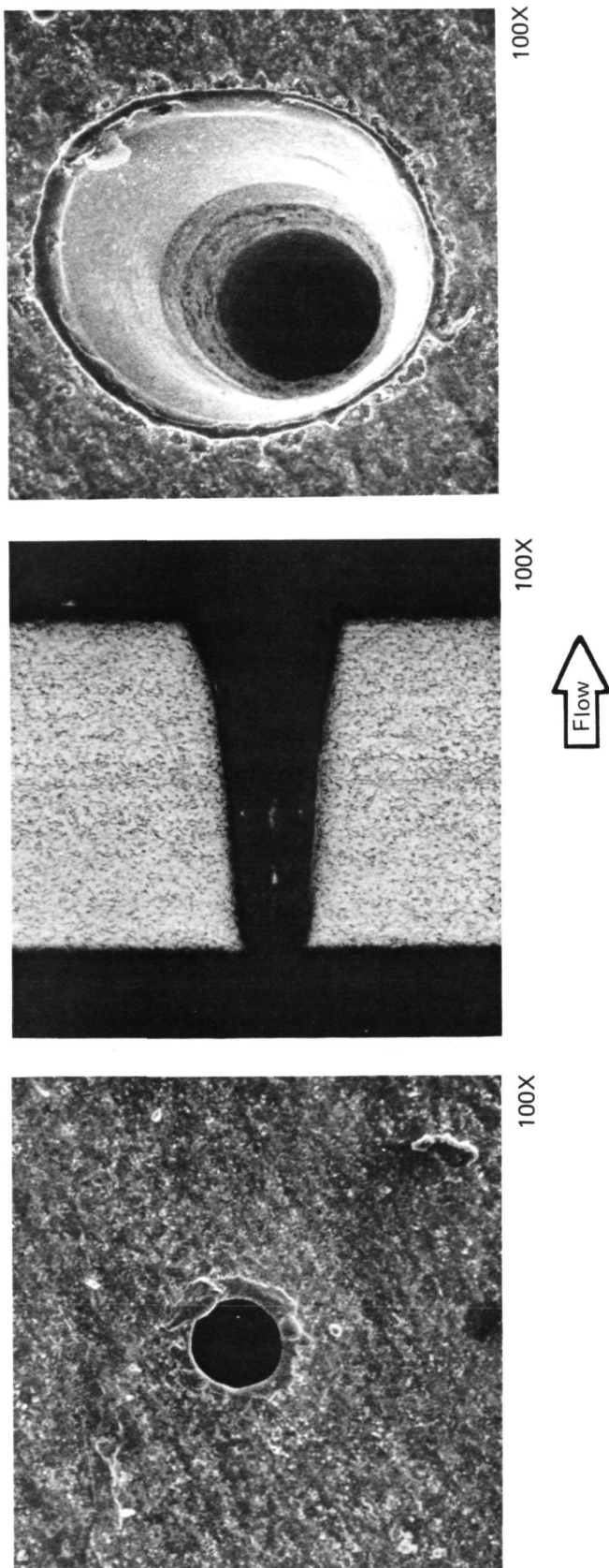


.008

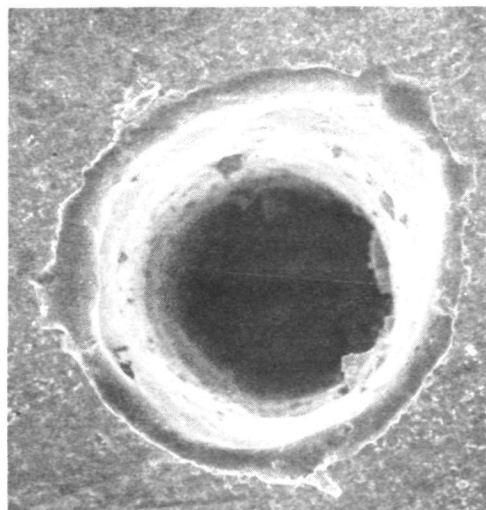
30X

Figure A-8.—SEM Photograph Showing Hole Spacing of Perforated Titanium

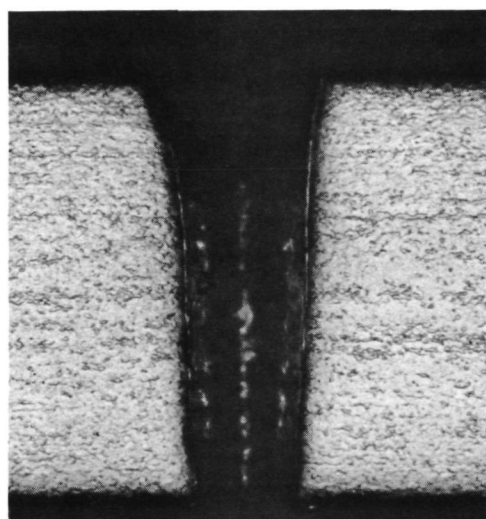
Figure A-9.—Photograph .003 Perforated Titanium



100X



100X



100X

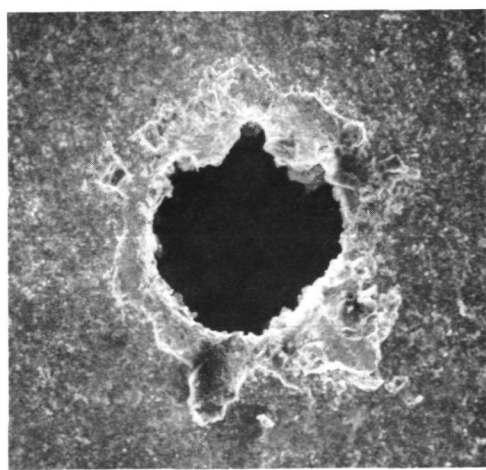
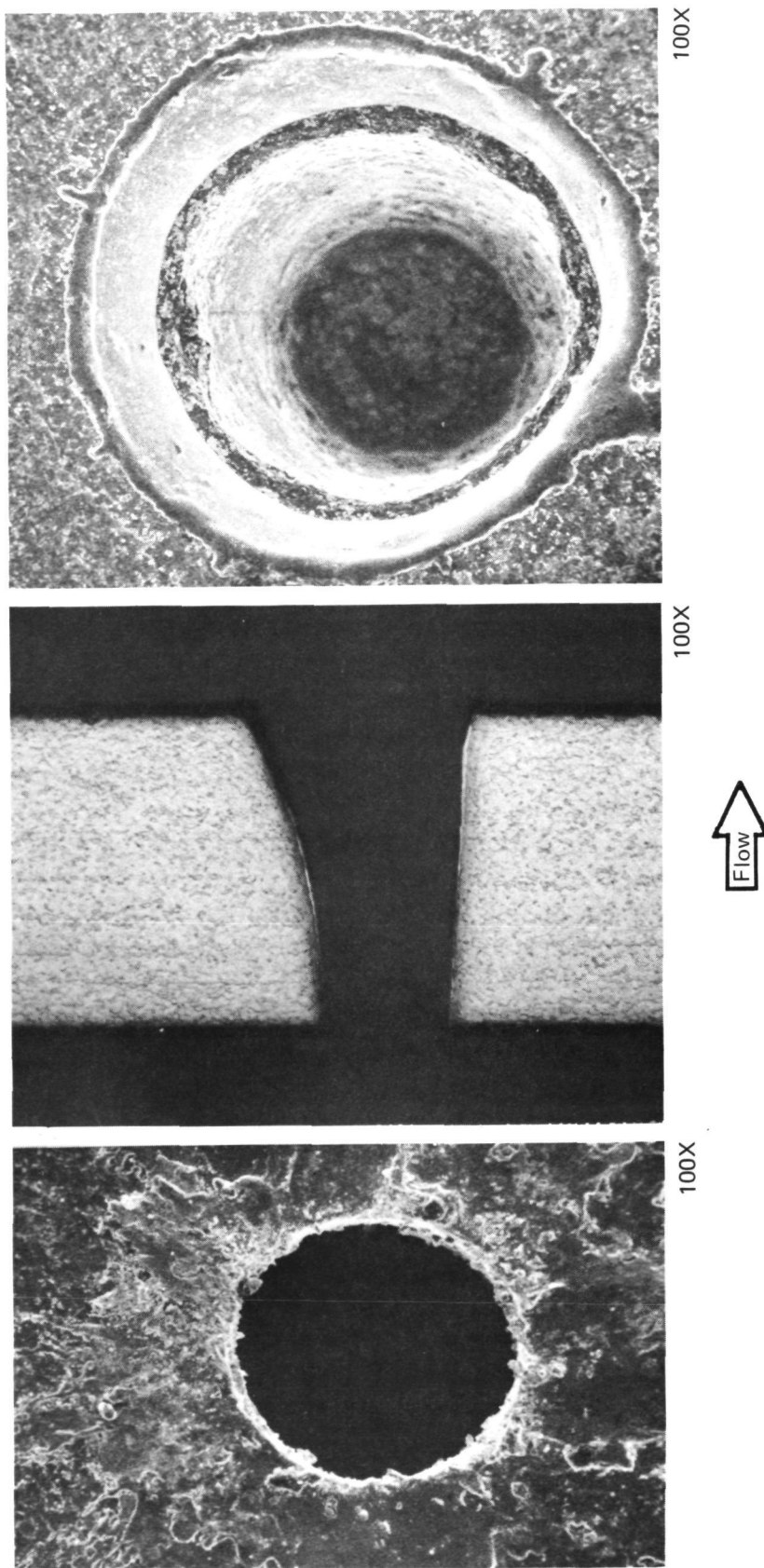


Figure A-10.—Photograph .005 Perforated Titanium

Figure A-11.—Photograph of .008 Perforated Titanium



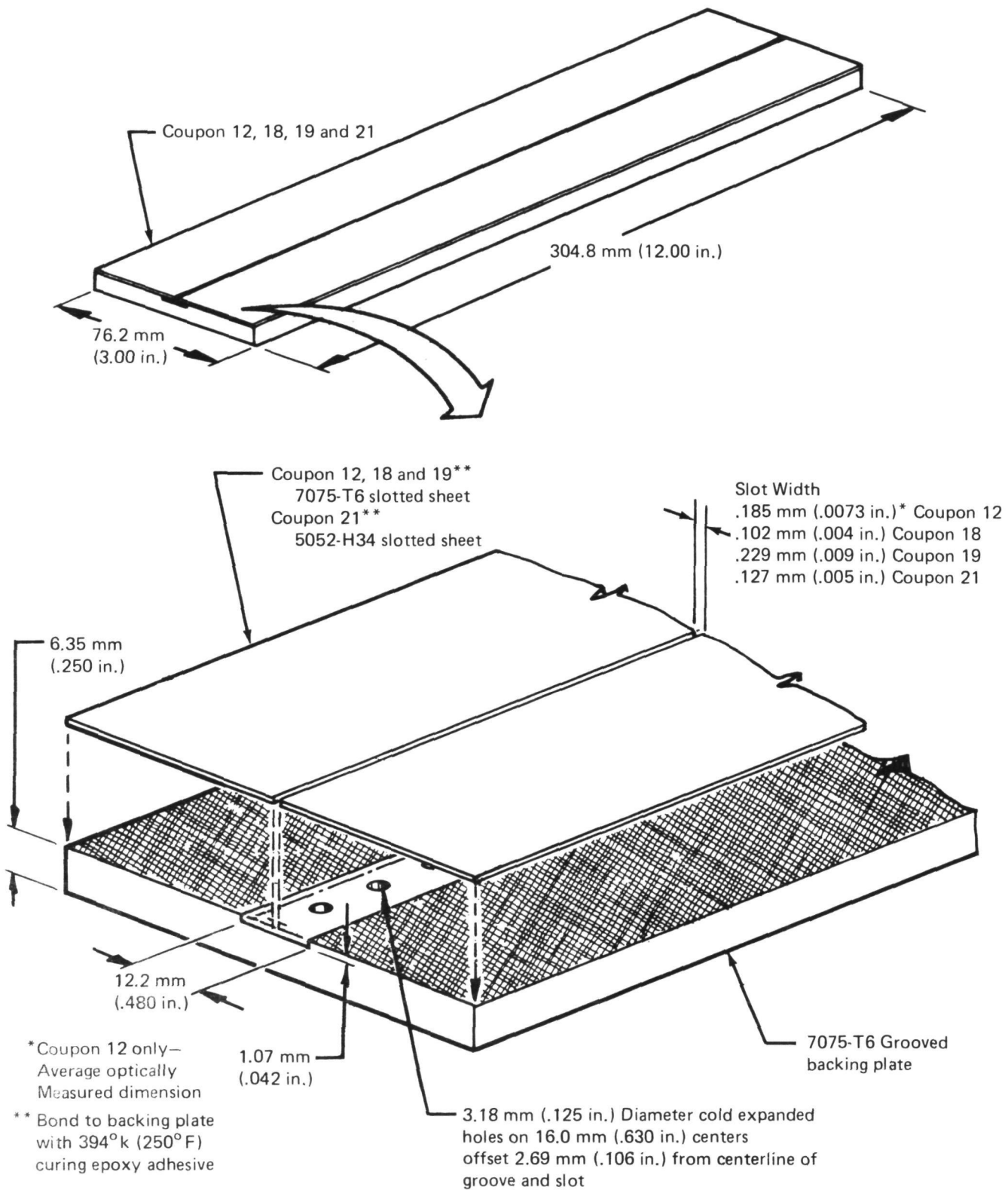


Figure A-12.—Description of Test Coupons 12, 18, 19 and 21

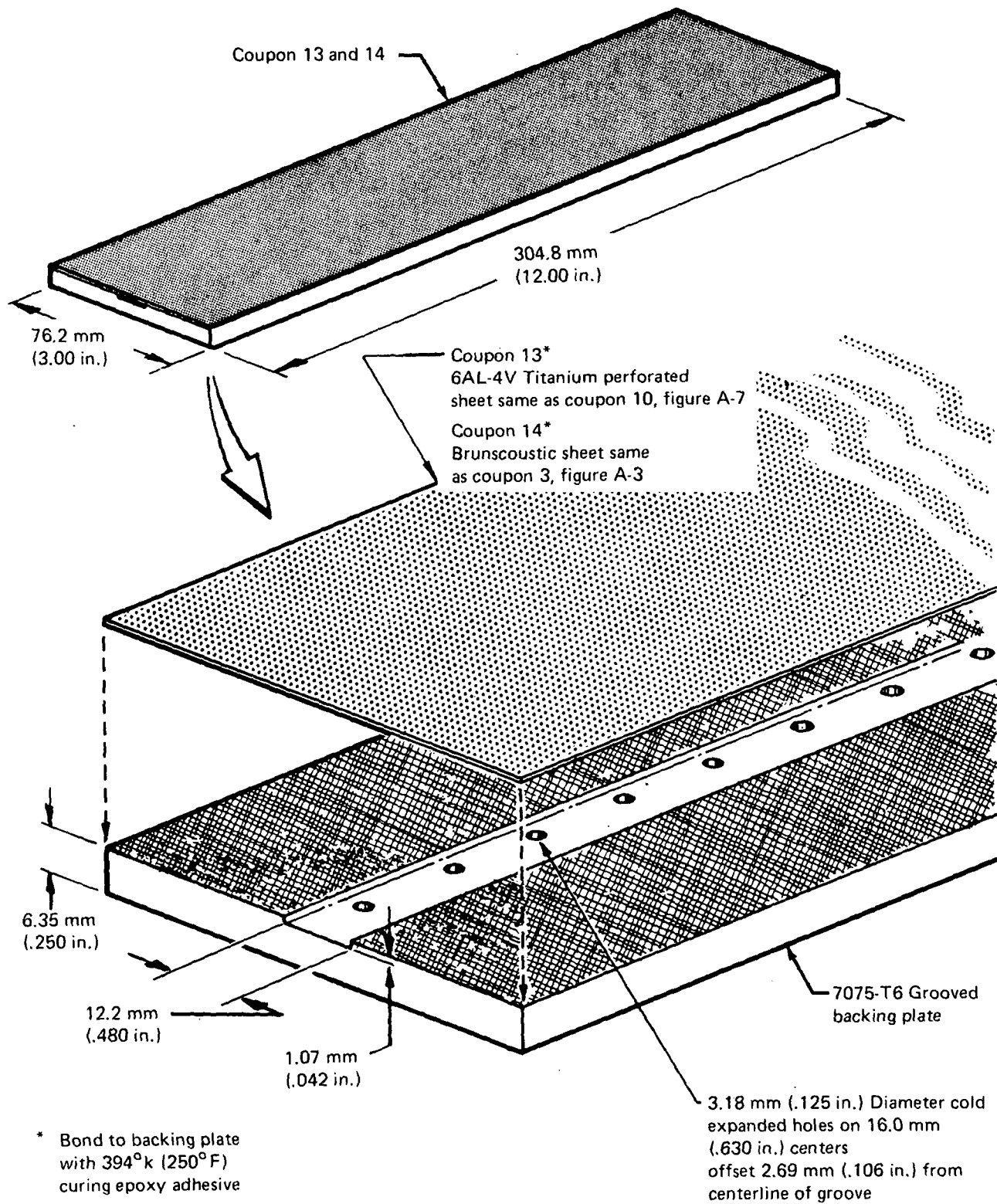


Figure A-13.—Description of Test Coupons 13 and 14

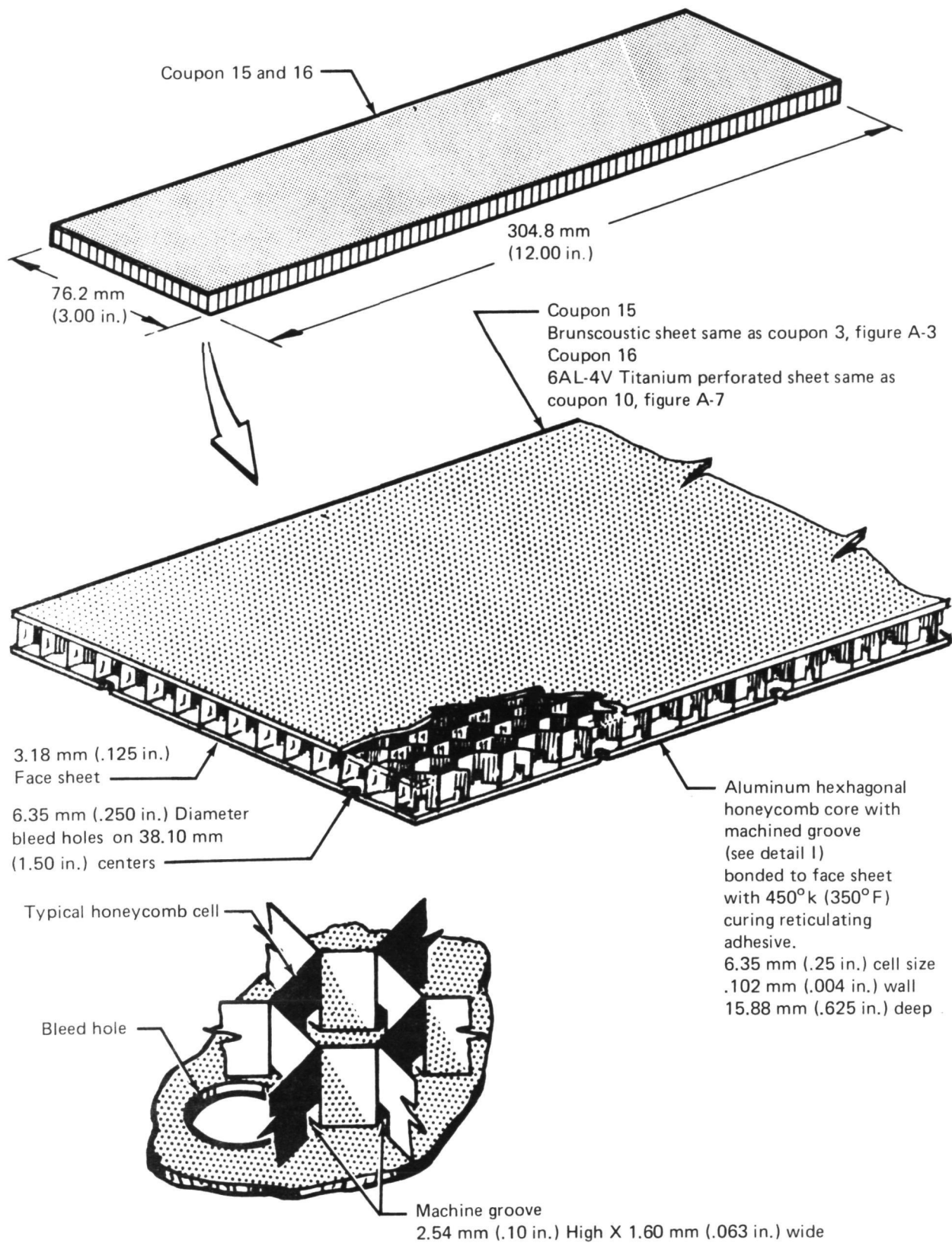
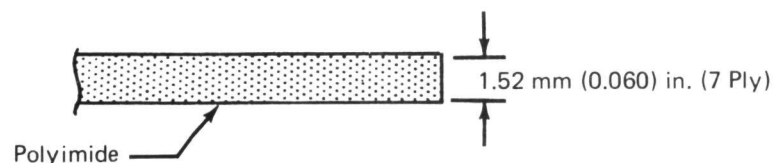
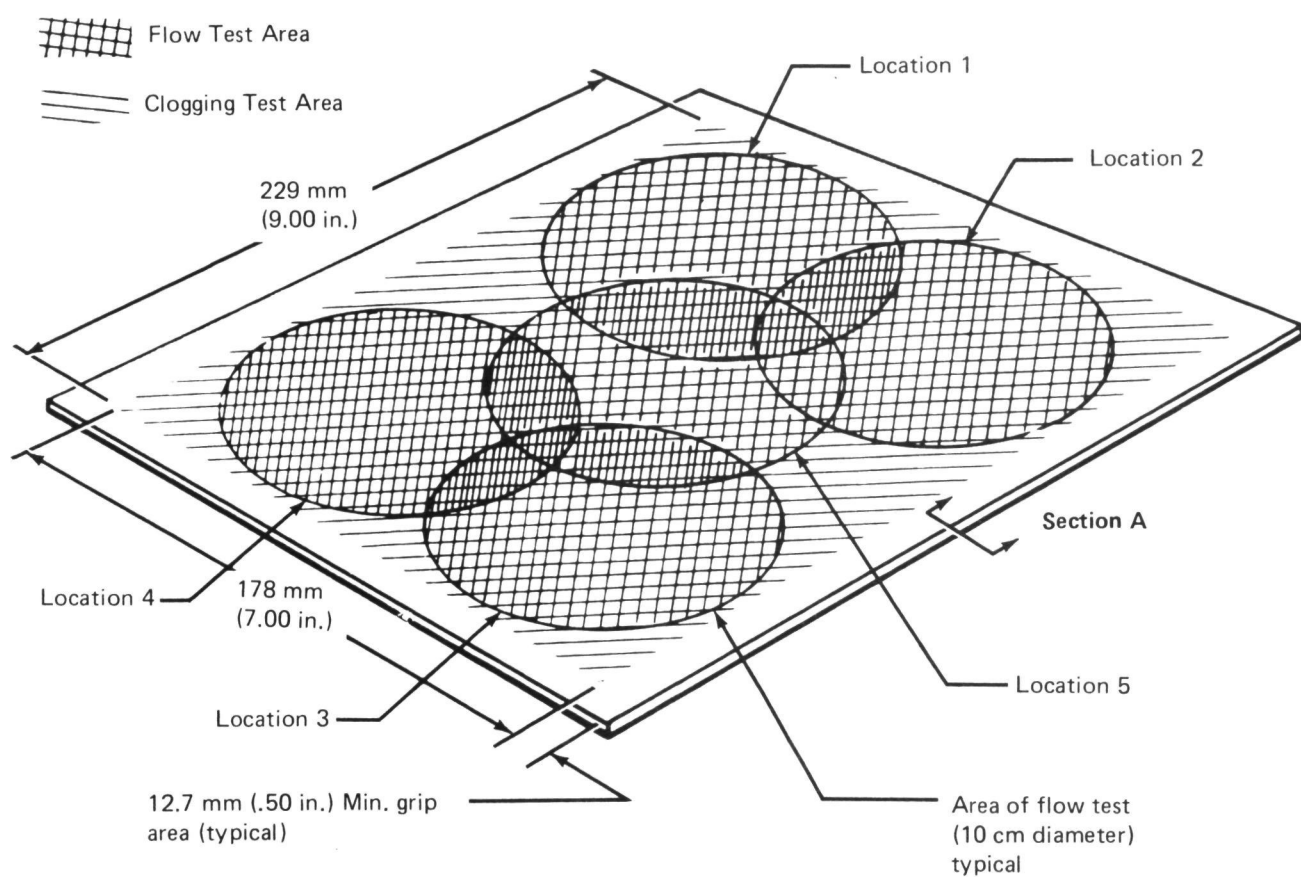


Figure A-14.—Description of Test Coupon 15 and 16



Section A

Figure A-15.—Description of Test Coupon 17

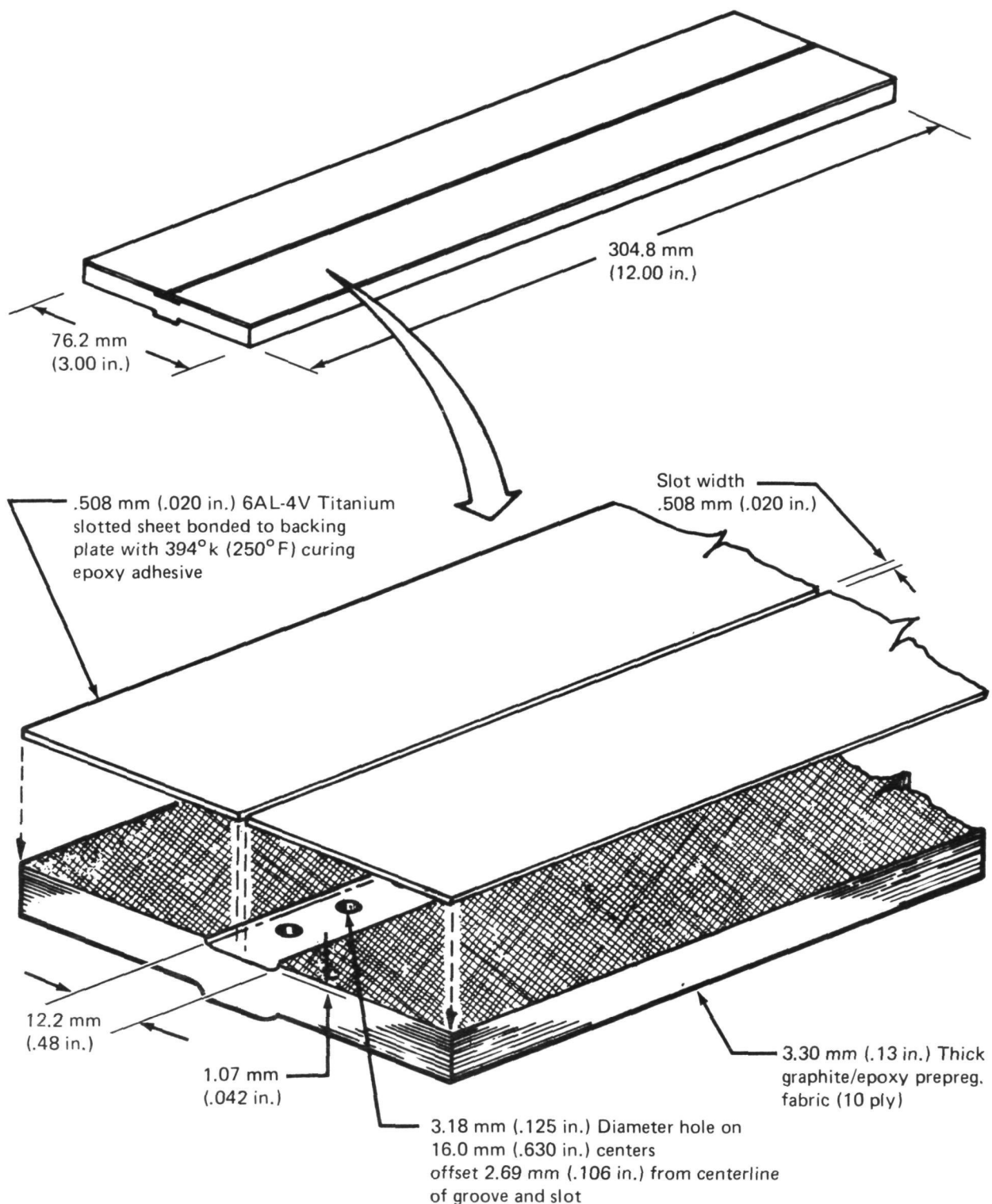
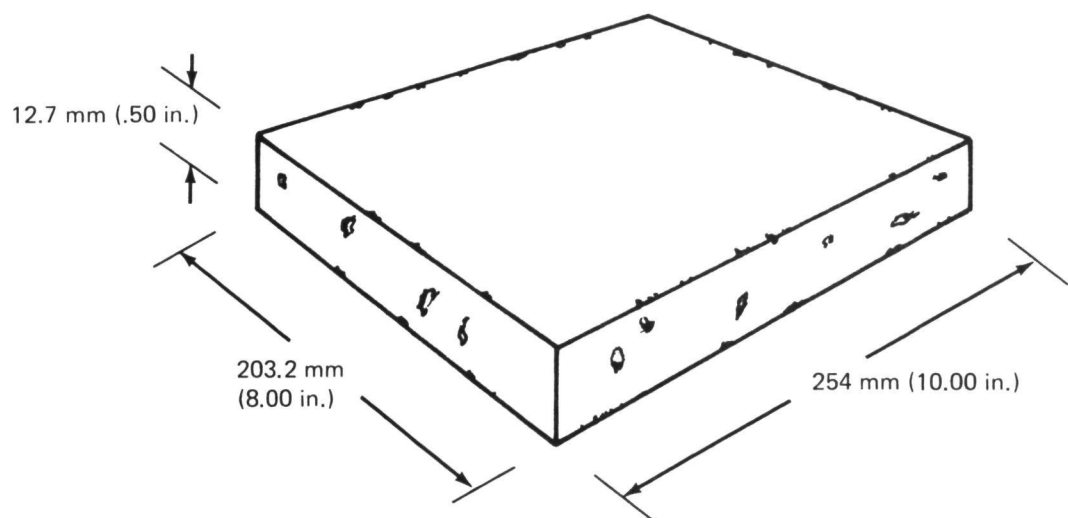


Figure A-16.—Description of Test Coupon 20



SCOTTFELT

Figure A-17.—Description of Test Coupon 21

MATERIALS DESCRIPTION

I Porous Materials

Six porous materials were selected for testing and described as follows:

- (1) Material: Gore-Tex
Supplier: W. L. Gore and Associates, Inc.
Route 213 North
Elkton, Md. 21921
- Coupon 1 & 2 Gore-Tex is a microporous PTFE (Teflon) product having pore sizes of 3 to 15 microns. It consists of a 100% PTFE membrane 0.0127 mm (0.0005 in.) bonded to webril, a nonwoven polypropylene fabric, for added strength. The total product thickness is about 0.127 mm (0.005 in.).
- Two porosity levels were selected;
- L10813 – 3 microns size and 13,800 Pa (2 psi) resistance to water ingress (coupon 2).
 - L10814 – 10-15 microns size with some resistance to water ingress (coupon 1)
- (2) Material: Brunscoustic
Supplier: Brunswick Corporation
One Brunswick Plaza
Skokie, Ill. 60076
- Coupon 3 & 4 The Brunscoustic material consisted of a 347 stainless perforated sheet 0.51 mm (0.020 in.) thick to which was diffusion bonded a 347 stainless fiber mat (Figures A-3 and A-4) to enhance flow resistance and make a smoother surface. Coupons 3 and 4 were made from the same sheet of material. The mat was diffusion bonded at about 30% of the contact points with the perforated sheet. The porous mat had a density of 0.43 kg/m² (0.088 lb/ft²) after assembly. The material had a reported yield strength of 103×10^6 Pa (15 ksi) and a reported ultimate strength of 228×10^6 Pa (33 ksi). It had a Rayl value of 90 at a flow rate of 60 cm/sec and 101,000 Pa (14.7 psia). The fiber mat (after bonding to the perforated sheet) was resistant to erosion by high velocity air.

- (3) Material: Aircraft Porous Media Material
 Supplier: Aircraft Porous Media, Inc.
 32 Sea Cliff Avenue
 Glen Cove, N.Y. 11542
- Coupon 5 The Aircraft Porous Media Material was of similar construction to Brunscoustic, except that the mat was woven screen (Figure A-3 and A-5). The perforated 347 stainless sheet was identical to that previously described. The diffusion bond between the mat and perforated sheet was complete less than 15% of the time. The density of the woven mat was 0.644 kg/m^2 (0.132 lb/ft^2) after diffusion bonding. The reported yield strength was $96.5 \times 10^6 \text{ Pa}$ (ksi) and the ultimate strength was $221 \times 10^6 \text{ Pa}$ (32 ksi). The woven mat (after bonding to the perforated sheet) was resistant to erosion by high velocity air.
- (4) Material: Michigan Dynamics Porous Metal
 Supplier: Michigan Dynamics
 32400 Ford Road
 Garden City, Mich. 48135
- Coupon 6 The Michigan Dynamics material was similar to Brunscoustic in construction. The perforated 347 stainless sheet was identical in configuration. The fiber mat (Figures A-3 and A-6) had a density of 0.547 kg/m^2 (0.112 lb/ft^2) after diffusion bonding. The material's reported yield strength was $82.7 \times 10^6 \text{ Pa}$ (12 ksi) and ultimate strength was $207 \times 10^6 \text{ Pa}$ (30 ksi). The Rayl value was 107 at a flow rate of 60 cm/sec and 101,000 Pa (14.7 psia). The fiber mat after bonding to the perforated sheet was resistant to erosion by high velocity air.
- (5) Material: Polyimide
 Supplier: Boeing Commercial Airplane Co.
 P.O. Box 3707
 Seattle, Wash. 98124
- Coupon 7, 8 & 17 The Polyimide panels were fabricated from multiple layers oriented at 0 rad , $\pm 0.26 \text{ rad}$ (0° , $\pm 15^\circ$) of 31×31 weave (clark-schwevel 16-456/38-3) fiberglass cloth finished with A1100 and impregnated with polyimide resin (Figures A-1, A-6, and A-15). The resin content and number of layers controlled the flow resistance. Specifically the panels included in the test program were of 7-ply (coupons 8 and 17) and 16-ply (coupon 7) acoustic laminates fabricated per BAC 5532 (Reference 9) using Type A polyimide prepreg. The 7-ply panels were spray coated with a black polyurethane paint of the type used to provide UV protection of production commercial aircraft.

- (6) Material: Scottfelt
 Supplier: Scott Foam Division
 Scott Paper Company
 1500 E. Second Street
 Chester, Penna.
- Coupon 22 The Scottfelt was a high-permeability felted polyester polyurethane open cell foam. The felting compressed the initial thickness by a factor of 8.0 and produced a pore density of 60 per lineal inch. The reported tensile strength of the material was 827,400 Pa (120 psi).

II Perforated Material

- Material: 0.508 mm (0.020 in.) perforated titanium sheet
 Supplier: Farrel Company
 Division USM Corporation
 Ansonia, Connecticut
- Coupon 9, 10 & 11 Perforated Ti-6AL-4V, per Mil-T-9046 (Annealed), was fabricated by Farrel Company using electron beam equipment. Material having three hole sizes, 0.076, 0.127, and 0.203 mm (0.003, 0.005, and 0.008 in.) (coupons 9, 10 and 11) and two different percent open areas (Figure A-7) was selected for the test program. The holes were intentionally tapered (Figures A-9 through A-11) to produce a hole which would be less likely to become clogged when exposed to flow from the small diameter. The EB process produced a thin as-cast layer in the hole.

III Slotted

- Coupon 12, 18, 19 and 21 The aluminum slotted assemblies (Figure A-12) were bonded using 394⁰K (250⁰F) epoxy adhesive to bond the sheets to grooved (7075-T6) backing plate. The slots were made by spacing the two cover sheets during bonding. The backing plates had holes which were cold expanded to improve fatigue quality. Coupons 12, 18 and 19 had 7075-T6 slotted sheets, while coupon 21 had 5052-H34 slotted sheets. Coupons 12, 18 and 21 had a phosphoric acid anodize while coupon 19 was primed (BMS 10-11) and painted (corogard) in addition to the phosphoric acid anodize.
- Coupon 20 This coupon (Figure A-16) had a titanium cover plate bonded to a graphite epoxy base. The cover and base were bonded with the same adhesive as the aluminum assemblies.

APPENDIX B

FLOW AND CLOGGING TEST RESULTS

Table B-1.—Raw Data (Vacuum Flow Test)

Pressure Drop (ΔP) Across Test Coupon in Inches of Fluid Specific Gravity 0.96

Table B-1.—(Continued)

Coupon number	Material configuration, or condition	Chamber pressure in. Hg ±0.5	Airflow rate, cfm (at 70°F and 14.7 psia)										
			0.1	0.2	0.625	1.2	1.4	1.6	1.8	2.0	2.2	2.4	2.6
5	Aircraft porous media as received	8.9	—	—	—	0.45	0.55	0.60	0.70	0.75	0.80	0.90	1.00
		6.1	—	—	—	0.70	0.80	0.90	1.00	1.10	1.20	1.30	1.35
		3.4	—	—	—	1.10	1.25	1.30	1.50	1.80	1.90	2.00	2.10
5	Aircraft porous media 48 hour clogging test	8.9	—	—	—	1.50	1.70	2.00	2.20	2.40	2.70	3.00	3.20
		6.1	—	—	—	2.10	2.60	2.90	3.20	3.50	3.70	4.00	4.30
6	Michigan Dynamics as received	22.6	—	—	—	0.25	0.30	0.35	0.40	0.45	0.50	—	—
		8.9	—	—	—	0.50	0.60	0.70	0.80	0.90	1.00	1.05	1.10
		6.1	—	—	—	0.70	0.80	0.95	1.05	1.10	1.30	1.40	1.50
6	Michigan Dynamics 48 hour clogging test	3.4	—	—	—	1.25	1.40	1.60	1.70	1.80	1.90	2.20	2.30
		22.6	—	—	—	0.40	0.50	0.55	0.60	0.70	0.80	0.85	—
		8.9	—	—	—	1.00	1.20	1.30	1.50	1.70	1.90	2.00	2.10
6	Polyimide (16-Plys) as received	6.1	—	—	—	1.50	1.70	2.00	2.20	2.30	2.70	2.80	2.90
		22.6	—	—	—	0.10	0.13	0.15	0.20	—	—	—	—
		8.9	—	—	—	0.25	0.30	0.35	0.40	0.40	0.45	0.50	0.50
7	Polyimide (16-Plys) 48 hour clogging test	6.1	—	—	—	0.30	0.40	0.45	0.50	0.60	0.65	0.70	0.80
		3.4	—	—	—	0.80	0.95	1.00	1.20	1.40	—	—	—
		22.6	—	—	—	0.10	0.10	0.10	0.10	0.15	0.15	—	—
7	Polyimide (16-Plys) 72 hour clogging test	8.9	0.10	—	0.10	0.15	—	0.20	0.25	0.30	0.35	0.40	0.45
		6.1	—	—	—	0.30	0.40	0.50	0.50	0.55	0.60	0.70	0.80
		3.4	—	—	—	0.70	0.80	0.90	0.90	1.10	1.10	1.20	1.30
7	Polyimide (16-Plys) 72 hour clogging test	22.6	—	—	—	0.15	0.20	0.20	0.20	0.20	0.30	—	—
		8.9	0.10	0.15	0.20	0.30	0.35	0.40	0.40	0.50	0.55	0.60	0.60
		6.1	0.15	0.20	0.30	0.50	0.50	0.55	0.60	0.70	0.70	0.80	0.85
7	Polyimide (16-Plys) 72 hour clogging test	3.4	—	—	—	0.80	0.90	1.00	1.10	1.20	1.20	1.30	1.40

Table B-1.—(Continued)

Coupon number	Material configuration, or condition	Chamber pressure in. Hg +0.5	Airflow rate, cfm (at 70°F and 14.7 psia)								
			0.1	0.2	0.625	1.2	1.4	1.6	1.8	2.0	2.2
7	Polyimide (16-Plys) 144 hour clogging test	22.6	—	—	0.10	0.15	0.15	0.20	0.20	—	—
		8.9	<0.1	0.10	0.15	0.30	0.40	0.40	0.45	0.50	0.50
		6.1	<0.1	0.10	0.20	0.40	0.50	0.60	0.60	0.70	0.75
8	Polyimide (7-Plys) as received polyurethane paint	22.6	—	—	0.05	0.05	0.05	0.05	0.05	0.10	—
		8.9	—	—	0.10	0.10	0.15	0.20	0.20	—	—
		6.1	—	—	0.20	0.20	0.20	0.25	0.25	0.25	0.25
9	Perforated T1-6AL-4V 0.003 hole as received	22.6	—	—	1.10	1.40	1.70	2.00	2.20	2.50	—
		8.9	0.30	0.50	1.40	2.90	3.30	3.90	4.80	5.50	7.00
		6.1	—	—	4.00	5.00	6.00	7.00	—	—	—
9	Perforated T1-6AL-4V 48 hour clogging test 0.003 hole	22.6	0.10	0.30	0.70	1.50	1.80	2.20	2.50	2.90	3.15
		8.9	0.30	0.60	1.70	3.50	4.20	4.90	6.00	6.80	—
		6.1	0.40	0.90	2.50	5.10	6.10	7.40	—	—	—
9	Perforated T1-6AL-4V 72 hour clogging test 0.003 hole	22.6	0.10	0.20	0.80	1.80	2.40	2.90	3.60	4.00	4.60
		8.9	0.40	0.70	2.20	4.90	6.20	7.40	—	—	—
		6.1	0.50	1.00	3.30	7.60	—	—	—	—	—
9	Perforated T1-6AL-4V surfaced washed 0.003 hole	22.6	0.10	0.20	0.65	1.30	1.70	2.10	2.40	2.70	3.10
		8.9	0.20	0.50	1.60	3.40	4.30	5.00	5.80	6.40	8.00
		6.1	0.40	0.80	2.40	5.10	—	—	—	—	—
10	Perforated T1-6AL-4V 0.005 hole as received	8.9	0.15	0.40	1.40	3.10	4.00	4.90	5.60	6.40	7.20
		6.1	0.30	0.60	2.10	4.70	5.90	—	—	—	—

Table B-1.—(Continued)

Coupon number	Material configuration, or condition	Chamber pressure in. Hg ± 0.5	Airflow rate, cfm (at 70°F and 14.7 psia)								
			0.1	0.2	0.625	1.2	1.4	1.6	1.8	2.0	2.2
10	Perforated T1-6AL-4V 48 hour clogging test 0.005 hole	22.6 8.9 6.1	0.10 0.30 0.30	0.25 0.60 0.80	0.80 1.80 2.60	1.60 3.90 5.80	2.10 5.00 7.40	2.40 6.00	2.90 7.20	3.30 —	3.90 —
11	Perforated T1-6AL-4V 0.008 hole as received	8.9 6.1	0.10 0.12	0.15 0.25	0.60 0.80	1.40 1.90	1.60 2.40	2.10 2.90	2.60 3.60	3.10 4.20	3.60 5.60
11	Perforated T1-6AL-4V 48 hour clogging test 0.008 hole	22.6 8.9 6.1	0.05 0.10 0.15	0.10 0.20 0.20	0.20 0.60 0.75	0.70 1.70 2.10	0.90 2.30 2.90	1.10 2.80 3.50	1.50 4.20 4.20	2.10 5.30 5.80	— 6.00 —
12	0.0073 slot assy as received	22.6 8.9	— 0.10	— 0.30	— 1.30	— 3.70	1.40 4.90	1.90 6.20	2.50 7.60	3.10 7.60	3.60 —
12	0.0073 slot assy 48 hour clogging test	22.6 8.9	0.08 0.10	0.15 0.30	0.70 1.50	1.80 4.60	2.50 6.10	3.00 7.80	3.80 —	4.40 —	5.20 —
12	0.0073 slot assy 48 hour clogging test surfaced washed	22.6 8.9	— 0.10	— 0.30	— 1.45	— 4.40	1.80 6.00	2.30 7.60	2.90 —	3.55 —	4.20 —
13	0.005 perforated T1 strip assy as received	22.6 8.9	0.50 1.50	1.40 3.70	8.00 —	— —	— —	— —	— —	— —	— —

Table B-1.—(Concluded)

Coupon number	Material configuration, or condition	Chamber pressure in. Hg ±0.5	Airflow rate, cfm (at 70°F and 14.7 psia)										
			0.1	0.2	0.625	1.2	1.4	1.6	1.8	2.0	2.2	2.4	2.6
14	Brunsound strip assy as received	8.9 6.1	0.30 0.40	0.55 0.80	1.70 2.30	3.30 4.60	4.00 5.60	4.60 6.50	5.20 7.40	5.80 —	6.40 —	7.00 —	— —
15	Brunsound on aluminum core panel assy	8.9	0.10	0.20	0.50	0.90	1.10	1.30	1.40	1.60	1.80	1.90	2.10
16	Perforated Ti-6AL-4V 0.005 hole on aluminum core panel assy	22.6 8.9	0.15 0.40	0.40 0.80	1.50 3.60	4.20 >8.0	5.50 —	7.40 —	— —	— —	— —	— —	

*Table B-2.—Raw Data (Rayl Test Machine)
Pressure Drop (ΔP) Across Test Coupon in Inches of Water*

Coupon number	Material configuration, or condition	Chamber pressure in. Hg 30.27	Airflow rate, cfm (at 70°F and 14.7 psia)				
			LOC 1	LOC 2	LOC 3	LOC 4	LOC 5
17	Polyimide (7-Ply) as received	4.99	8.32	11.85	16.64	24.96	
		0.379	0.916	1.654	3.044	6.371	
		0.412	1.025	1.885	3.456	6.700	
		0.400	0.975	1.772	3.228	6.838	
		0.408	1.002	1.806	3.297	6.877	
		0.375	0.912	1.647	3.020	6.336	
17	Polyimide (7-Ply) 48 hour clogging test	0.406	0.991	1.784	3.186	6.713	
		0.455	1.113	1.993	3.648	7.666	
		0.432	1.027	1.870	3.389	7.181	
		0.438	1.057	1.908	3.481	7.198	
		0.406	0.981	1.748	3.187	6.683	
17	Polyimide (7-Ply) 144 hour clogging test	0.526	1.245	2.235	4.030	8.385	
		0.587	1.382	2.505	4.539	9.472	
		0.548	1.280	2.536	4.256	8.891	
		0.564	1.313	2.370	4.310	8.931	
		0.512	1.217	2.191	3.971	8.168	

Table B-3.—Raw Data (Water Soak) Polyimide (7-ply) Coupon 17

Temperature 25° C, Airflow Rate 4.99 cfm (at 14.7 psia)

Time in in minutes	ΔP in. H ₂ O
0	5.00
0.25	4.65
0.83	4.05
1.08	3.00
1.33	2.25
1.58	1.80
1.83	1.37
2.08	1.17
2.33	1.05
2.83	0.990
3.33	0.923
3.83	0.900
4.33	0.851
5.00	0.825
5.50	0.810
6.00	0.785
7.00	0.751
8.00	0.711
9.00	0.671
10.00	0.646
12.00	0.581
14.00	0.545
16.00	0.523
20.00	0.475
25.00	0.446

SAMPLE CALCULATION RAW DATA TO REDUCED DATA

EXAMPLE (Gor-Tex L10814 as Rec'd)

Given

Air flow 1.6 cfm (70°F , 14.7 psia)

Pressure drop 2.30 ΔP (in inches of fluid)

Specific gravity of fluid (0.96)

Chamber pressure 8.9 in. Hg

Reduced Data

$$1. \quad \text{Airflow Conversion} \quad (\text{cfm}) (K) = \text{lbs/s} \cdot \text{ft}^2$$

Specific wt air = 0.076474 lb/ft³ @S.T.P. 59° , 14.7 psi

Specimen area = 2.5 in. x 9.0 in. = 22.5 in.²

$$K = \frac{\text{specific wt air}}{60} \left(\frac{T_o}{T_t} \right) \left(\frac{144}{\text{specimen area in.}^2} \right)$$

$$K = \frac{0.076474}{60} \left(\frac{518.69}{529.69} \right) \left(\frac{144}{22.5} \right) = .007988$$

(Raw Data) (K) = Reduced Data

$$(1.6 \text{ cfm}) (.007988) = 0.01278 \text{ lbs/s} \cdot \text{ft}^2$$

2. *Altitude Conversion*

Pressure at seal level = 29.92 in. Hg

$$\text{Constant} = \frac{1}{29.92} \left(\frac{T_o}{T_t} \right)$$

$$= \frac{1}{29.92} \left(\frac{518.69}{529.69} \right)$$

$$= 0.03273$$

$$\frac{P}{P_o} = (\text{in. Hg}) (0.3273)$$

In. Hg	$\frac{P}{P_o}$	Equiv Alt. (U.S. Standard Atmosphere)	Use
8.9	0.2913	36,555	36,500

3. Pressure Drop Conversion $(\Delta P) (K) = \sigma \Delta P$

ΔP at chamber pressure and 70°F specific gravity of manometer fluid 0.96

one inch of water = 0.03613 psi

$$\text{in. Hg to psi constant} = \frac{14.7}{29.92} = 0.4913$$

Constant at 8.9 in Hg

$$K = 0.03613 (0.96) (35.3) \frac{P_T}{T_t}$$

$$= 0.03613 (0.96) (35.3) \left(\frac{4.372}{529.69} \right)$$

$$= 0.0101$$

$$2.30 (0.0101) = \sigma \Delta P$$

$$= 0.02323 \text{ lbs/sec} \cdot \text{ft}^2$$

Table B-4.—Reduced Data (Vacuum Flow Test)
 $\sigma \Delta P$ (PSIA) $\times 10^{-4}$

Coupon number	Material configuration, or condition	Equivalent altitude ft.	Airflow (lbs/sec. ft. ²) $\times 10^{-4}$								
			8	16	50	96	112	128	144	160	176
1	Gore-Tex L10814 as received	36,500	—	—	—	172	202	232	252	283	313
		44,500	—	—	—	132	160	180	201	222	242
1	Gore-Tex L10814 48 hour clogging test	36,500	—	—	—	475	535	586	626	—	—
		56,500	—	—	—	200	—	—	—	—	—
2	Gore-Tex L10813 as received	56,500	—	—	—	—	—	—	—	—	—
		36,500	—	—	—	30	40	51	51	61	66
3	Brunscoustic (#1) as received	44,500	—	—	—	35	42	42	49	59	59
		56,500	—	—	—	31	37	42	46	50	54
3	Brunscoustic (#1) 48 hour clogging test	10,000	—	—	—	103	129	154	180	206	218
		36,500	—	—	—	101	121	131	152	162	182
3	Brunscoustic (#1) 48 hour clogging test reversed flow	44,500	—	—	—	104	118	132	146	159	173
		56,500	—	—	—	100	116	131	139	150	170
4	Brunscoustic (#2) as received	36,500	15	25	51	91	111	131	141	162	172
		10,000	—	—	—	—	—	—	—	—	—
4	Brunscoustic (#2) as received	36,500	10	—	20	40	51	51	64	77	—
		44,500	—	—	—	42	49	55	62	69	76

Table B-4.—(Continued)

Coupon number	Material configuration, or condition	Equivalent altitude ft.	Airflow (lbs/sec. ft. ²) × 10 ⁻⁴								
			8	16	50	96	122	128	144	160	
5	Aircraft porous media as received	36,500	—	—	—	45	56	61	71	76	81
		44,500	—	—	—	49	55	62	69	76	83
		56,500	—	—	—	42	48	50	58	69	73
5	Aircraft porous media 48 hour clogging test	36,500	—	—	—	152	172	202	222	242	273
		44,500	—	—	—	146	180	201	222	242	256
		—	—	—	—	—	—	—	—	277	298
6	Michigan Dynamics as received	10,000	—	—	—	64	77	90	90	103	116
		36,500	—	—	—	51	61	71	81	91	101
		44,500	—	—	—	49	55	66	73	76	90
6	Michigan Dynamics 48 hour clogging test	56,500	—	—	—	48	54	62	66	69	73
		10,000	—	—	—	103	128	141	154	180	200
		36,500	—	—	—	101	121	131	152	172	192
7	Polyimide (16-Ply) as received	44,500	—	—	—	104	118	139	152	159	187
		44,500	—	—	—	—	—	—	—	—	—
		56,500	—	—	—	—	—	—	—	—	—
7	Polyimide (16-Ply) 48 hour clogging test	10,000	—	—	—	26	33	38	51	—	—
		36,500	—	—	—	25	30	35	40	40	45
		44,500	—	—	—	21	28	31	35	42	45
7	Polyimide (16-Ply) 72 hour clogging test	56,500	—	—	—	31	37	39	46	54	—
		<10	—	—	10	15	—	20	25	30	35
		44,500	—	—	—	21	28	34	34	38	41
7	Polyimide (16-Ply) 72 hour clogging test	56,500	—	—	—	27	31	35	42	42	46
		10,000	—	—	—	38	51	51	51	77	—
		36,500	10	15	20	30	35	40	40	51	56
		44,500	10	14	21	34	34	38	41	48	55
		56,500	—	—	—	31	35	38	42	46	50

Table B-4.—(Continued)

Coupon number	Material configuration, or condition	Equivalent altitude ft.	Airflow (lbs/sec. ft. ²) × 10 ⁻⁴										
			8	16	50	96	122	128	144	160	176	192	208
7	Polyimide (16-Ply) 144 hour clogging test	10,000	—	—	26	38	51	51	—	—	—	—	—
		36,500	10	10	15	30	40	45	51	51	51	56	56
		44,500	7	7	14	28	34	41	41	48	48	52	52
8	Polyimide (7-Ply) as received polyurethane paint	10,000	—	—	—	13	13	13	13	26	—	—	—
		36,500	—	—	—	10	10	15	15	20	20	—	—
		44,500	—	—	—	14	14	14	14	17	17	17	17
9	Perforated Ti-6AL-4V 0.003 hole as received	10,000	—	—	—	283	360	437	514	565	643	—	—
		36,500	30	51	141	293	333	394	485	556	636	707	—
		44,500	—	—	—	277	347	416	485	—	—	—	—
9	Perforated Ti-6AL-4V 48 hour clogging test 0.003 hole	10,000	26	77	180	386	463	565	643	745	810	—	—
		36,500	30	61	172	354	424	495	606	688	—	—	—
		44,500	28	62	173	353	423	513	—	—	—	—	—
9	Perforated Ti-6AL-4V 72 hour clogging test 0.003 hole	10,000	26	51	201	463	617	745	925	1028	1182	—	—
		36,500	40	71	222	495	626	747	—	—	—	—	—
		44,500	35	69	229	527	—	—	—	—	—	—	—
9	Perforated Ti-6AL-4V surfaced washed 0.003 hole	10,000	26	51	167	334	437	540	617	694	797	—	—
		36,500	20	51	162	343	434	505	586	646	808	—	—
		44,500	28	55	166	353	—	—	—	—	—	—	—
10	Perforated Ti-6AL-4V 0.005 hole as received	36,500	15	40	141	313	404	495	566	646	727	—	—
		44,500	21	42	146	326	409	—	—	—	—	—	—

Table B-4.—(Continued)

Table B-4.—(Concluded)

Table B-5.—Reduced Data (Rayl Test)

Coupon number	Material configuration, or condition	Equivalent altitude ft.	Airflow (lbs/sec. ft. ²) x 10 ⁻⁴					
			745	1240	1770	2480	3730	570
17	Polyimide (7-Ply) as received	0	130	320				
17	48 hour clogging test	0	140	340	610	1110	2330	
17	144 hour clogging test	0	180	400	720	1380	2670	

Table B-6.—Reduced Data (Water Soak) Polyimide (7-ply) Coupon 17

Temperature 25° C, Airflow 0.0745 pounds/sec ft² 0.3637 kg/sec m²

Time in minutes	$\sigma\Delta P$ (psi)	$\sigma\Delta P$ Pa
0	0.165	1137
0.25	0.153	1054
0.83	0.133	917
1.08	0.0988	681
1.33	0.0741	511
1.58	0.0593	409
1.83	0.0451	310
2.08	0.0385	265
2.33	0.0346	239
2.83	0.0326	225
3.33	0.0304	210
3.83	0.0296	204
4.33	0.0280	193
5.00	0.0272	188
5.50	0.0267	184
6.00	0.0258	178
7.00	0.0247	170
8.00	0.0234	161
9.00	0.0221	152
10.00	0.0213	147
12.00	0.0191	132
14.00	0.0179	123
16.00	0.0172	119
20.00	0.0156	108
25.00	0.0147	101

Table B-7.—Reduced Data (Vacuum Flow Test) (SI Units)

$\sigma\Delta P$ (Pa)

Coupon number	Material configuration, or condition	Equivalent altitude meters	Airflow (kg/s m ²) × 10 ⁻⁴								1016
			39	78	244	469	547	625	703	781	
1	Gore-Tex L10814 as received	11,125	—	—	—	118.6	139.3	160.0	173.7	195.1	215.8
		13,564	—	—	—	91.0	110.3	124.1	138.6	153.1	166.9
1	Gore-Tex L10814 48 hour clogging test	11,125	—	—	—	327.5	368.9	404.6	431.6	—	—
		17,221	—	—	—	>137.9	—	—	—	—	—
2	Gore-Tex L10813 as received	11,125	—	—	—	20.68	27.58	34.47	41.37	44.81	48.26
		13,564	—	—	—	23.44	28.26	33.09	39.99	39.99	44.81
3	Brunseoustic (#1) as received	11,125	—	—	—	23.7	25.51	28.95	31.71	34.47	37.23
		13,564	—	—	—	—	—	—	—	—	—
3	Brunseoustic (#1) 48 hour clogging test	11,125	—	—	—	68.95	89.63	103.4	110.3	110.3	117.2
		13,564	—	—	—	68.95	82.74	89.63	96.53	96.53	103.4
3	Brunseoustic (#1) 48 hour clogging test reversed flow	11,125	10.34	17.23	34.47	62.05	75.84	89.63	96.53	110.3	117.2
		17,221	—	—	—	68.95	82.74	89.63	96.53	103.4	117.2
4	Brunseoustic (#2) as received	3,048	—	—	—	68.95	89.63	103.4	124.1	137.9	151.6
		11,125	—	—	—	68.95	82.74	89.63	103.4	110.3	124.1
3	Brunseoustic (#2) 48 hour clogging test reversed flow	13,564	—	—	—	68.95	82.74	89.63	96.53	96.53	103.4
		17,221	—	—	—	68.95	82.74	89.63	96.53	103.4	117.2
4	Brunseoustic (#2) as received	3,048	—	—	—	17.72	26.20	35.16	44.12	53.09	—
		11,125	6.895	—	—	13.79	27.58	34.47	41.37	44.81	51.71
3	Brunseoustic (#2) 48 hour clogging test reversed flow	13,564	—	—	—	28.26	33.09	37.92	42.74	47.57	52.40
		17,221	—	—	—	—	—	—	—	—	—

Table B-7.—(Continued)

Coupon number	Material configuration, or condition	Equivalent altitude meters	Airflow (kg/s m^2) $\times 10^{-4}$										
			39	78	244	469	547	625	703	781	859	937	1016
5	Aircraft porous media as received	3,048	—	—	—	31.02	37.92	42.05	48.95	52.40	55.84	62.74	68.95
		11,125	—	—	—	33.09	37.92	42.74	47.57	52.40	57.22	62.05	62.05
		13,564	—	—	—	28.95	33.09	34.47	34.47	47.57	50.33	53.09	55.16
5	Aircraft porous media 48 hour clogging test	11,125	—	—	—	104.8	118.6	139.3	153.1	166.9	188.2	208.9	222.7
		13,564	—	—	—	100.7	124.1	138.6	153.1	166.9	176.5	191.0	205.5
		—	—	—	—	—	—	—	—	—	—	—	—
6	Michigan Dynamics as received	3,048	—	—	—	44.12	53.09	62.05	68.95	82.74	89.63	—	—
		11,125	—	—	—	34.47	42.05	48.26	55.16	62.05	68.95	75.84	75.84
		13,564	—	—	—	33.09	47.92	44.81	49.64	52.40	62.05	66.88	68.95
6	Michigan Dynamics 48 hour clogging test	17,221	—	—	—	33.09	37.23	42.74	44.81	47.57	50.33	58.60	60.67
		3,048	—	—	—	68.95	89.63	96.53	103.4	124.1	137.9	151.6	—
		11,125	—	—	—	68.95	82.74	89.63	103.4	117.2	131.0	137.9	144.7
7	Polyimide (16-Ply) as received	13,564	—	—	—	68.95	82.74	96.53	103.4	110.3	131.0	131.0	137.9
		—	—	—	—	—	—	—	—	—	—	—	—
		—	—	—	—	17.92	22.75	26.20	35.16	35.16	35.16	35.16	—
7	Polyimide (16-Ply) 48 hour clogging test	11,125	>6.9	—	6.9	10.3	—	17.9	17.9	20.7	24.13	34.47	34.47
		13,564	—	—	—	14.48	19.31	23.4	23.4	26.2	28.3	33.1	37.92
		17,221	—	—	—	18.6	21.4	24.1	24.1	29.0	29.0	31.7	37.23
7	Polyimide (16-Ply) 72 hour clogging test	3,048	—	—	—	26.2	35.2	35.2	35.2	53.1	—	—	—
		11,125	6.9	10.3	13.8	20.7	24.1	27.6	34.5	34.5	38.6	42.0	42.0
		13,564	6.9	9.7	14.5	23.4	23.4	26.2	33.1	33.1	37.9	40.7	40.7
		17,221	—	—	—	21.4	24.1	26.2	29.0	29.0	31.7	34.5	37.2

Table B-7.—(Continued)

Coupon number	Material configuration, or condition	Equivalent altitude meters	Airflow ($\text{kg/s m}^2 \times 10^{-4}$)								
			39	78	244	469	547	625	703	781	859
7	Polyimide (16-Ply) 144 hour clogging test	3,048	—	—	17.9	26.2	35.2	35.2	—	—	—
		11,125	6.9	10.3	20.7	27.6	31.0	35.2	35.2	35.2	38.6
		13,564	4.8	9.7	19.3	23.4	28.3	28.3	33.1	33.1	35.9
8	Polyimide (7-Ply) as received polyurethane paint	3,048	—	—	9.0	9.0	9.0	9.0	17.9	—	—
		11,125	—	—	6.93	6.98	10.3	13.8	13.8	13.8	13.8
		13,564	—	—	9.7	9.7	9.7	11.7	11.7	11.7	11.7
9	Perforated TI-6AL-4V 0.003 hole as received	3,048	—	—	193.0	248.2	303.3	351.6	386.1	441.2	—
		11,125	20.68	34.47	96.53	193.0	227.5	268.9	330.9	379.2	441.2
		13,564	—	—	193.0	234.4	282.6	330.9	—	489.5	—
9	Perforated TI-6AL-4V 48 hour clogging test 0.003 hole	3,048	17.92	53.09	124.1	262.0	317.1	386.1	441.2	510.2	558.4
		11,125	20.68	42.05	117.2	241.3	289.5	337.8	420.5	475.7	—
		13,564	18.61	42.74	117.2	241.3	289.5	351.6	—	—	—
9	Perforated TI-6AL-4V 72 hour clogging test 0.003 hole	3,048	17.92	35.16	137.9	317.1	420.5	510.2	634.3	703.2	813.6
		11,125	27.58	48.95	151.6	337.8	427.4	517.1	—	—	—
		13,564	23.44	47.57	158.5	358.5	—	—	—	—	—
9	Perforated TI-6AL-4V surfaced surfaced washed 0.003 hole	3,048	17.92	35.16	117.2	227.5	303.3	372.3	420.5	475.7	544.7
		11,125	13.79	34.47	110.3	234.4	296.4	344.7	406.8	448.1	558.4
		13,564	19.30	37.92	114.4	241.3	—	—	—	—	—
10	Perforated TI-6AL-4V 0.005 holes as received	11,125	10.34	27.58	96.53	213.7	275.8	337.8	386.1	441.2	496.4
		13,564	14.47	28.26	96.53	220.6	282.6	—	—	—	—

Table B-7.—(Continued)

Coupon number	Material configuration, or condition	Equivalent altitude meters	Airflow (kg/s m^2) $\times 10^{-4}$								
			39	78	244	469	547	625	703	781	
10	Perforated TI-6AL-4V 48 hour clogging test 0.005 hole	3,048	17.92	44.12	137.9	282.6	372.3	427.4	510.2	579.1	689.5
		11,125	20.68	41.37	124.1	268.9	344.7	413.7	496.4	—	—
		13,564	14.47	37.92	124.1	275.8	351.6	—	—	—	—
11	Perforated TI-6AL-4V 0.008 holes as received	11,125	6.89	10.3	42.1	97.2	111.7	146.2	181.3	215.8	251.0
		13,564	5.5	11.7	37.9	91.0	114.4	138.6	171.7	200.6	267.5
										315.8	—
11	Perforated TI-6AL-4V 48 hour clogging test 0.008 hole	3,048	9.0	17.9	35.2	124.1	159.3	195.1	266.1	301.3	372.3
		11,125	7.0	13.8	41.4	118.6	160.0	195.1	244.1	192.3	368.9
		13,564	7.0	9.6	34.5	100.7	138.6	166.9	200.6	238.6	277.2
12	0.0073 slot assy as received	3,048	—	—	248.2	336.5	443.3	549.5	637.8	762.6	—
		11,125	6.9	28.7	90.3	257.7	341.3	431.6	529.5	—	—
										—	—
12	0.0073 slot assy 48 hour clogging test	3,048	14.5	26.2	124.1	319.2	443.3	501.6	673.6	779.8	921.1
		11,125	6.9	20.7	104.8	320.6	431.6	550.2	—	—	—
										—	—
12	0.0073 slot assy 48 hour clogging test surfaced washed	3,048	—	—	—	319.2	407.5	513.6	628.8	743.9	886.0
		11,125	6.98	20.7	104.8	306.1	424.7	536.4	—	—	—
										—	—
13	0.005 perforated TI strip assy as received	3,048	88.3	248.2	1417.6	—	—	—	—	—	—
		11,125	104.8	257.9	—	—	—	—	—	—	—
										—	—

Table B-7.—(Concluded)

Coupon number	Material configuration, or condition	Equivalent altitude meters	Airflow (kg/s m^2) $\times 10^{-4}$										
			39	78	244	469	547	625	703	781	859	937	1016
14	Brunscoustic strip assy as received	11,125 13,564	20.7 19.3	38.6 37.9	118.6 110.3	229.6 219.9	278.6 267.5	320.6 310.3	362.0 353.7	404.0 —	445.4 —	487.5 —	—
15	Brunscoustic on aluminum core panel assy	11,125	6.9	13.8	35.2	62.7	76.5	90.3	97.2	111.7	125.5	132.4	146.2
16	Perforated Ti-6Al-4V 0.005 hole on aluminum core panel assy	3,048 11,125	26.2 27.6	71.0 55.8	266.1 251.0	743.9 >557.1	974.9 —	1311.4 —	—	—	—	—	

Table B-8.—Reduced Data (Ray Test) (SI Units)

Coupon number	Material configuration, or condition	Equivalent altitude meters	Airflow (kg/s m^2) $\times 10^{-4}$				
			3637	6053	8641	12,107	18,209
17	Polyimide (7-Ply) as received	0	89.6	220.6	393	723	1496
17	48 hour clogging test	0	96.5	234	420	765	1606
17	144 hour clogging test	0	124	275	496	951	1840

APPENDIX C

AERODYNAMIC REQUIREMENTS

The recommended surface smoothness criteria and surface porosity characteristics are representative of the NASA specified airplane mission objectives; range = 10,186 km (5500 nautical miles, 200 passenger commercial transport, $M = 0.8$).

Wing smoothness criteria have an important influence on the manufacturing and maintenance requirements for an LFC wing. Precise aerodynamic smoothness criteria are not generally available. Ultimately, promising materials will have to be wind tunnel (and flight) tested to establish suitability for application on an LFC airplane. The aerodynamic smoothness data and surface porosity requirements that will be used in this study, were derived primarily from Norair data and work by Dr. Pfenninger, (References 1 through 4).

A continuously porous surface is theoretically considered to be the ideal LFC surface for stabilizing the laminar boundary layer. Theory and experiment have both shown that a laminar boundary layer may be kept stable by applying suction at suitable discrete levels. The nearest approximation to the ideal surface although not necessarily the most practical, is a material whose pores and pore spacing are small compared with the boundary layer thickness. The majority of LFC experiments, however, have used suction through a series of narrow slots as on the Northrop X-21 flight test airplane.

Previous experiments have shown that suction through perforated surfaces will in certain circumstances preserve laminar flow as effectively as pores or slotted surfaces. Both the size of the holes and the suction flow through a perforated surface must be small or else transition may be induced rather than postponed. Additionally, the flow conditions at the ends of finite rows of perforations or at the ends of slots of finite length must be carefully controlled to avoid weakening the stability of the boundary layer. Hence the suitability of a material for LFC applications is quite dependent both on the surface smoothness and on the surface suction requirements.

SUCTION REQUIREMENTS AND FLOW RATES NORMAL TO THE SURFACE

The pressure loss associated with the porosity of a material, must provide a compromise between conflicting demands. Minimizing the pressure loss across an LFC surface reduces the suction system design power requirements. However, the inflow distribution of a low resistance surface is quite sensitive to changes in the external pressure distribution such as occurs, for example, as the angle of attack is altered. Excessive variations could lead to outflow through the surface or surging of the flow into the internal ducts.

The porosity of a material for an LFC suction surface should provide balanced flow control with low suction system power requirements and also prohibit local flow disturbances that could feed back into the boundary layer causing transition. The minimum pressure loss must also take into account installation considerations. For example, the use of strips with higher local flow would permit the use of a porous material not suitable for a completely porous surface installation.

The surface flow rate tests of the candidate LFC materials will be generally limited to those considered representative of the design mission requirements. Figure C-1 shows the flow rate envelope for a typical LFC airplane with a slotted surface. This envelope corresponds to a cruise Mach number = 0.8, cruise altitude from 7,620 to 11,582 m (25,000 to 38,000 feet) and a local chord of 7.62 m (25 feet). The losses through the slots and through the bleed holes to the tributary ducts are shown. The wing chord locations used to develop this envelope include 10%, 50% and 95% of chord for the upper and lower surfaces.

This envelope was determined using the calculation procedures established by Norair (Reference 1).

WAVINESS AND SMOOTHNESS REQUIREMENTS TO MAINTAIN LAMINAR FLOW

Criteria specifying wing surface smoothness for avoiding boundary layer transition have been experimentally determined primarily from flat-plate wind tunnel tests without boundary layer suction effects. The limited experimental studies that have investigated the effects of suction on surface smoothness requirements necessary to maintain laminar flow indicate that boundary layer suction can in some instances relax the stringent design tolerances. Comparison of the surface waviness criteria for a laminar flow wing with suction (Reference 2), and without suction (Reference 5), indicate that the allowable surface waviness with suction can be significantly greater than without suction. Reference 6 indicates that the allowable height of a downstep can be doubled with appropriate boundary layer suction.

Boundary layer suction has both favorable and unfavorable effects on disturbances introduced by surface roughness. Suction "thins" and makes the boundary layer more sensitive to the surface condition. The boundary layer profiles on a suction surface are more stable and therefore are more effective in "damping out" disturbances introduced in the boundary layer. Coordinated wind tunnel testing and theoretical analyses are necessary to obtain a more fundamental understanding of these somewhat compensating effects.

The surface waviness design criteria are shown in Figure C-2. These requirements are based on the data of Reference 2. For multiple surface waves, the allowable wave amplitude is given by

$$\frac{h}{\lambda} = 80 \sqrt{\frac{c}{\lambda \cos \Lambda_s}} \text{ Rec}^{-3/4}$$

where h = wave amplitude, m

λ = wave length measured normal to the structural axis, m

c = local chord length, m

Λ_s = sweep of structural axis, radians

Rec = Reynolds number based on the local chord

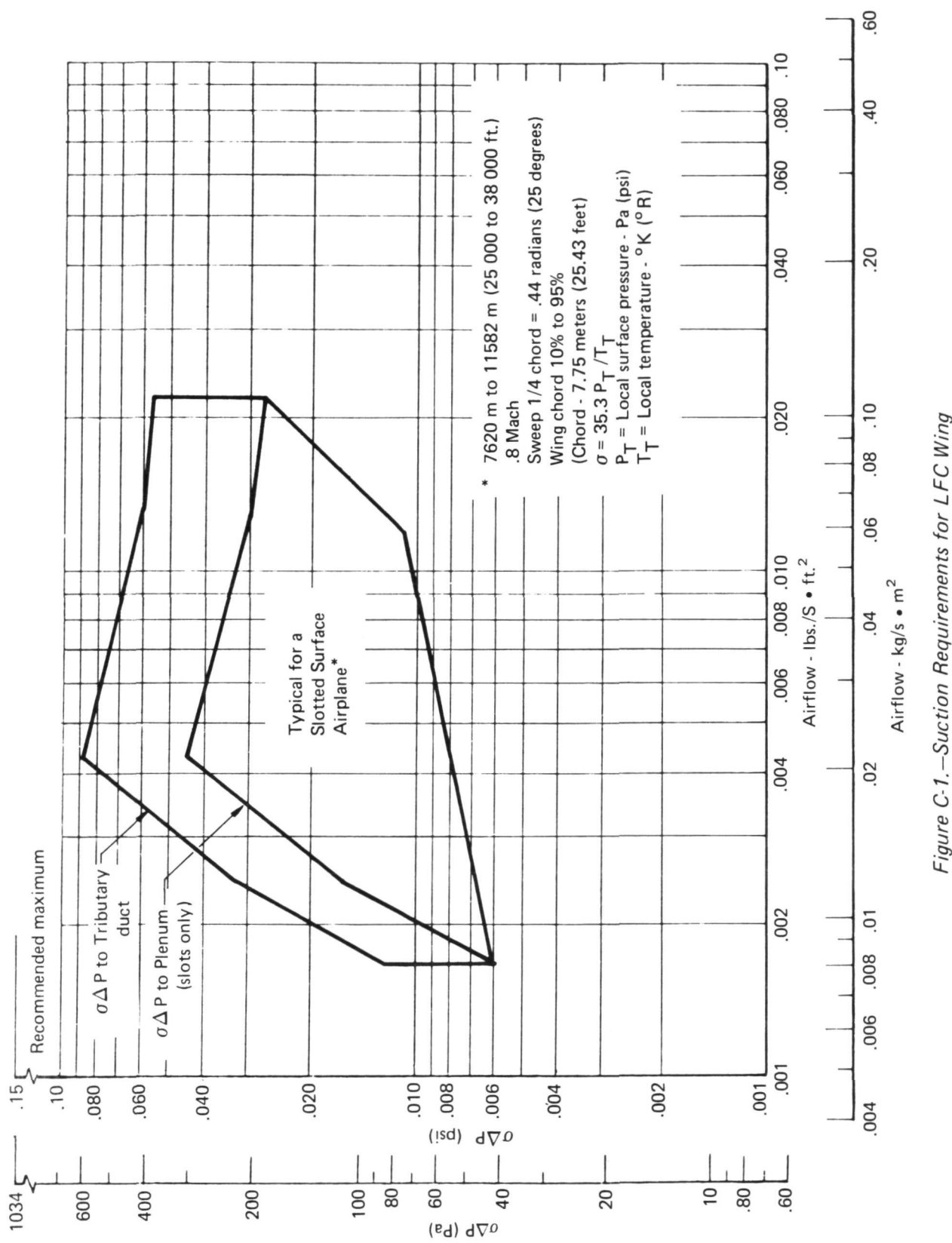
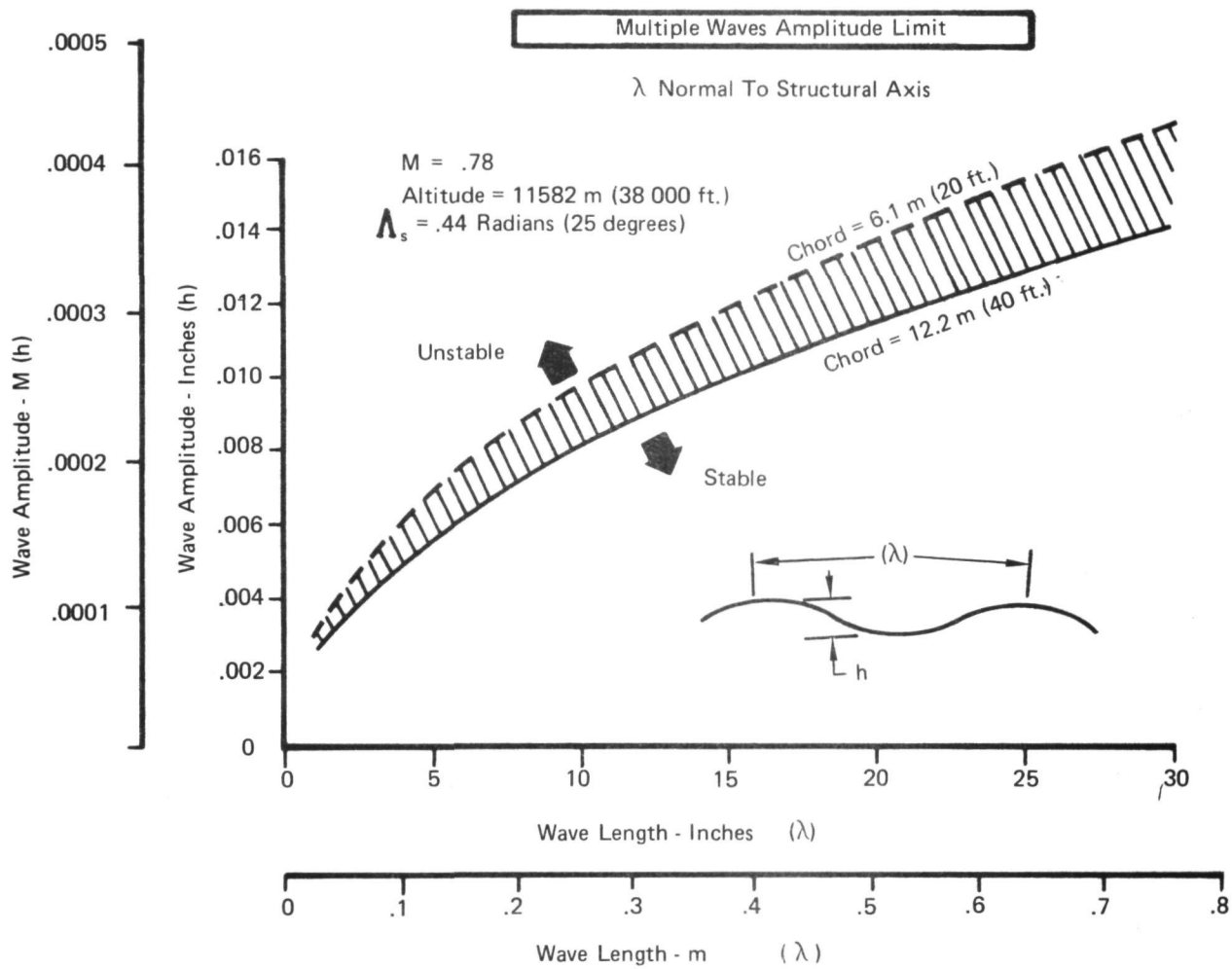


Figure C-1.—Suction Requirements for LFC Wing



NOTES: (1) For waves with λ parallel to structural axis
— Double amplitude

(2) For single wave with λ normal or parallel to
structural axis — Triple amplitude

Figure C-2. —Surface Waviness Criteria For LFC Surface

For single waves normal to the structural axis, three times this value should be used. Twice the value given by the equation should be used for multiple waves with the wave lengths measured along the structural axis.

The data of Reference 2 indicated no detectable influence of chordwise location on the critical wave amplitude ratio. These were obtained from experiments at low to moderate local Mach numbers. Surface waves induce negative pressure peaks that depend on the amplitude ratio (h/λ) and are amplified by increases in local Mach number. The wave-induced pressure peaks introduce two problems to a high subsonic LFC airplane:

- The pressure difference between the surface and the suction chamber could be reduced to a point where outflow from the suction surface may occur.
- At a sufficiently high local Mach number, shocks may form on the waves.

Either of these conditions could lead to transition to turbulent flow. Hence, for high subsonic speeds, there may exist a strong relation between the airfoil design and critical wave length limits at various chordwise locations on the airfoil. More experimental work is necessary to define these relationships.

The wing surface smoothness design criteria for upsteps, downsteps, gaps, etc., are given in figure C-3 which shows the effect of design altitude on the wing smoothness criteria. These criteria were obtained from References 1 and 7.

The previously mentioned surface smoothness and waviness criteria are to be used as the maximum allowable surface irregularities. A smoother surface will result, however, in reduced boundary layer stability concerns. It is therefore recommended to keep the surface as smooth as practical. The maximum recommended surface finish roughness is 125 micro-inches, (per Reference 8).

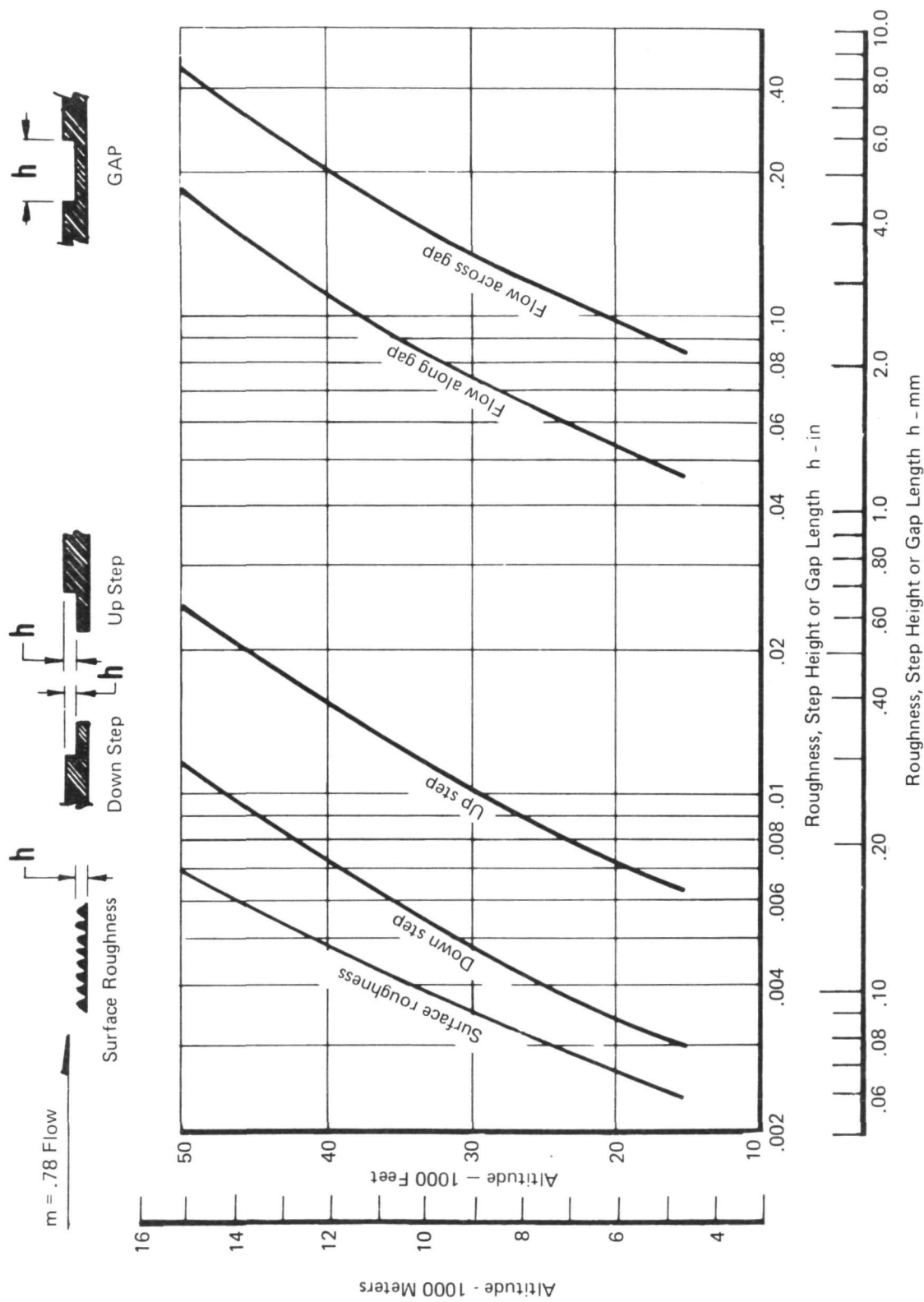


Figure C-3.—Roughness, Step Height or Gap Length

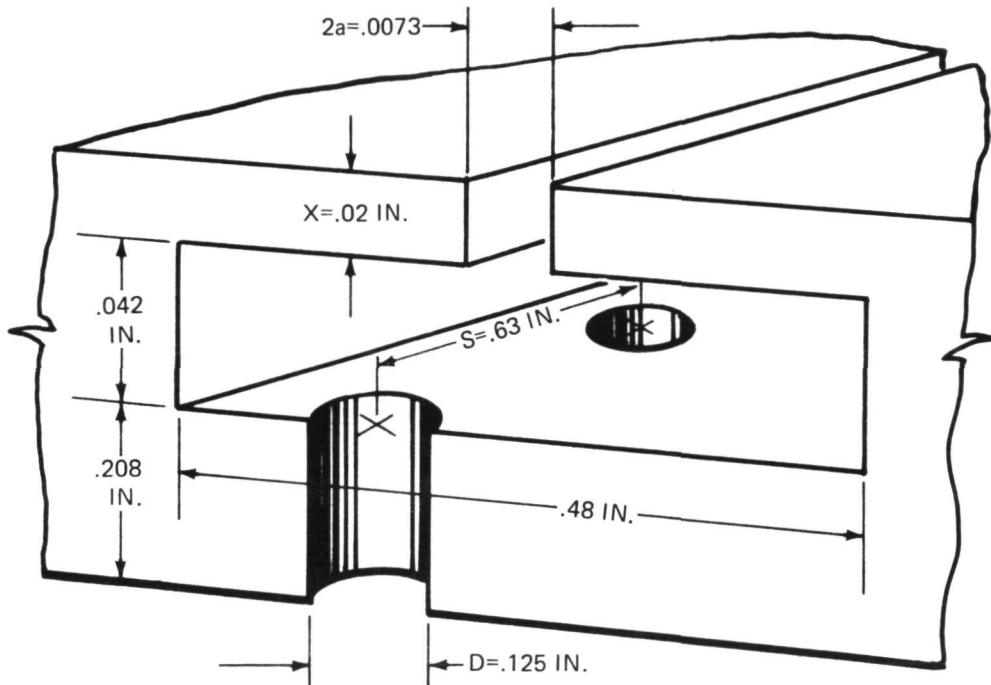
APPENDIX D

SPECIMEN PRESSURE LOSS CORRELATION

I SLOTTED SPECIMEN PRESSURE LOSS CORRELATION

The 0.0073 inch slotted specimen, associated plenum and bleed air hole pressure losses correlate quite closely with the losses predicted using the procedures in Reference 1. This is demonstrated in the following sample calculation.

Slot Specimen Dimensions:



The correlation is based on sea level standard conditions for two airflows.

SLOT PRESSURE LOSS

Slot area

$$A_s = 2aL \left(\frac{0.0073}{12} \right) (1) = 6.0833 \times 10^{-4} \text{ ft}^2$$

Slot flow

$$w_s = \frac{0.01}{4.8} = 2.0833 \times 10^{-3}$$

Slot density

$$\rho_s (2.7) \left(\frac{P}{T} \right) = \frac{(2.7)(14.7)}{(520)} = .076327 \text{ lb/ft}^3$$

Slot velocity

$$V_s = \frac{w_s}{\rho_s A_s} = \frac{2.0833 \times 10^{-3}}{(7.6327 \times 10^{-2})(6.0833 \times 10^{-4})} = 44.87 \text{ ft/sec}$$

Slot dynamic pressure

$$q_s = \frac{\rho_s V_s^2}{2g} = \frac{(7.6327 \times 10^{-2})(44.87)^2}{64.4} = 2.3862 \text{ lb/ft}^2$$

$$\tau = \frac{\chi}{a} = \frac{1.667 \times 10^{-3}}{3.042 \times 10^{-4}} = 5.4799$$

From Reference 1

$$\beta = \frac{\mu \chi g}{V a^2} = \frac{(3.7 \times 10^{-7})(1.667 \times 10^{-3})(32.2)}{(7.6327 \times 10^{-2})(44.87)(3.042 \times 10^{-4})^2} = 0.0627$$

From Figure D-1

$$\frac{\Delta P}{q} = 1.93$$

$$\Delta P = (1.93)(2.3862) = 4.6054 \text{ lb/ft}^2$$

$$= 0.03198 \text{ psi}$$

HOLE PRESSURE LOSS

Holes

$$N_h \text{ number of holes per slot} = \frac{L}{s} = \frac{12}{0.63} = 19.048$$

$$\text{Airflow per hole } w_h = \frac{w_s}{N_h} = \frac{2.0833 \times 10^{-3}}{19.048}$$

$$= 1.094 \times 10^{-4} \text{ lb/sec}$$

From Reference 1

Loss parameter

$$\beta_h = \frac{\pi \mu \chi_h}{\dot{m}_h} = \frac{\pi \mu \chi_h g}{w_h} = \frac{(\pi)(3.7 \times 10^{-7})(1.733 \times 10^{-2})(32.2)}{(1.094) \times 10^{-4}}$$

$$= 5.93 \times 10^{-3} \quad \text{where } \dot{m} = \frac{w_h}{g}$$

$$\tau_1 = \frac{\chi_h}{a_h} = \frac{0.01733}{0.005208} = 3.328$$

From Figure D-1

$$\frac{\Delta P}{q} = 1.64$$

Hole areas

$$A_h = \frac{\pi D^2}{4} = \frac{(\pi)(1.042 \times 10^{-2})^2}{4} = 8.52 \times 10^{-5} \text{ ft}^2$$

Hole velocity,

$$V_h = \frac{w_h}{\rho_h A_h} = \frac{1.094 \times 10^{-4}}{7.6327 \times 10^{-2} \times 8.52 \times 10^{-5}}$$

$$V_h = 16.82 \text{ ft/sec}$$

Hole dynamic pressure

$$q_h = \frac{\rho_h V_h^2}{2g} = \frac{(7.6322 \times 10^{-2})(16.82)^2}{(64.4)} = 0.3354 \text{ lb/ft}^2$$

Hole loss

$$\begin{aligned} \Delta P_{Holes} &= \left(\frac{\Delta P}{q} \right) (q) \\ &= (1.64)(0.3354) = 0.5501 \text{ lb/ft}^2 \\ &= 0.003829 \text{ psi} \\ &= 3.829 \times 10^{-3} \text{ lb/in}^2 \end{aligned}$$

Table D-1.—Pressure Loss Correlation Summary—0.0073 Slotted Specimen

Symbol	Item	Condition	
		1	2
w	Airflow, lb/sec ft ²	0.01	0.001
T	Temperature, °R	520	520
P	Pressure, psia	14.7	14.7
μ	Viscosity, lb/sec ft ²	3.7×10^{-7}	3.7×10^{-7}
N	Number of slots per ft	4.8	4.8
L	Slot length, ft	1	1
A_s	Slot area, ft ²	6.0833×10^{-4}	6.0833×10^{-4}
w_s	Slot airflow, lb/sec ft ²	2.0833×10^{-3}	2.0833×10^{-4}
$\rho_{s,h}$	Density, lbs/ft ³	7.6327×10^{-2}	7.6327×10^{-2}
a	Half slot height, ft	3.042×10^{-4}	3.042×10^{-4}
X	Slot depth, ft	1.667×10^{-3}	1.667×10^{-3}
V_s	Slot velocity, ft/sec	44.87	4.487
q_s	Slot dynamic pressure, lbs/ft ²	2.3862	2.3862×10^{-2}
τ	Slot depth/half height	5.4799	5.4799
β_s	Loss parameter, slot	0.0627	0.627
N_h	Number of holes/slot	19.05	19.05
w_h	Airflow per hole, lb/sec	1.094×10^{-4}	1.094×10^{-5}
X_h	Hole depth, ft	1.733×10^{-2}	1.733×10^{-2}
β_h	Loss parameter, hole	5.93×10^{-3}	5.93×10^{-2}
a_h	Hole radius, ft	5.2083×10^{-3}	5.2083×10^{-3}
τ_1	Hole depth to hole radius	3.328	3.328
A_h	Hole area, ft ²	8.52×10^{-5}	8.52×10^{-5}
V_h	Hole velocity, ft/sec	16.82	1.682
q_h	Hole dynamic pressure, lbs/ft ²	0.3354	3.354×10^{-3}

ΔP Slot	Slot pressure loss, lbs/in. ²	0.032	0.00089
ΔP Holes	Hole pressure loss, lbs/in. ²	0.00383	0.000068
Total ΔP	ΔP slot + ΔP holes, lbs/in. ²	0.03583	0.000958
Test ΔP	(for σ = 1) Figure 25	0.040	0.00140

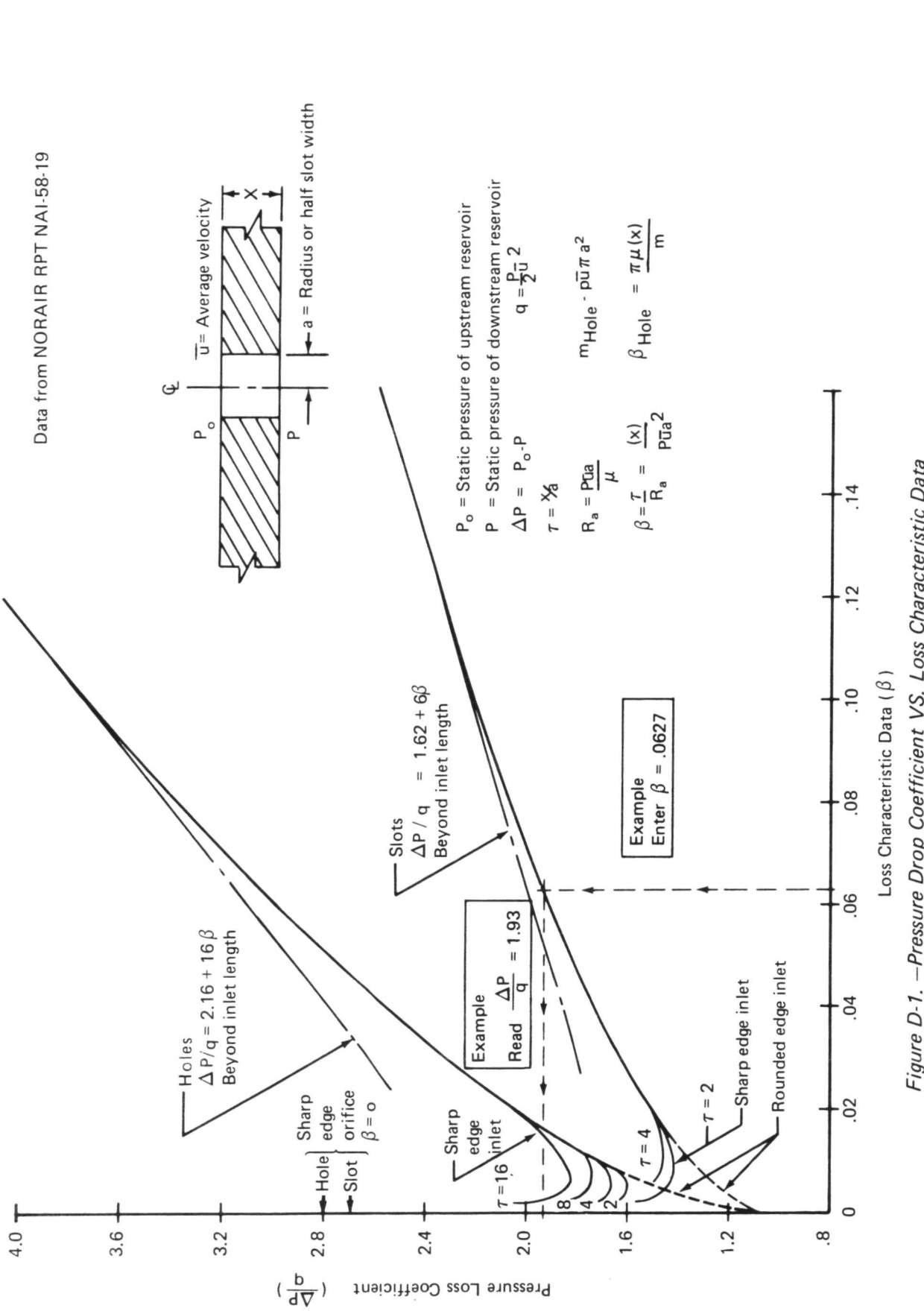


Figure D-1. —Pressure Drop Coefficient VS. Loss Characteristic Data

II PREDICTION METHODS FOR STRIP ASSEMBLIES

The data obtained from the sheet materials coupons No. 3 and 10 can be used to predict the flow resistance of the strip assemblies. To predict the flow resistance of the assemblies the increased local flow is corrected due to the reduced surface area. Then the $\sigma\Delta P$ is read from the curve developed for the sheet material. To this the pressure drop due to the supporting structure, such as bleed holes, is added. The result is the predicted $\sigma\Delta P$ for the strip assembly. Sample calculations for the strip assemblies (coupons No. 13 and 14) are shown below.

Perforated titanium strip assembly coupon No. 13

$$\text{Sheet } \sigma\Delta P = 0.034 \text{ psi at } 0.010 \text{ lb/s}\cdot\text{ft}^2 \text{ (Figure 23)}$$

$$\text{Pressure loss thru backup structure} = 0.0038 \text{ psi}$$

Computed using techniques described in Reference and illustrated in Table D-1.

Correction for flow area

$$\text{Area correction} = \frac{\text{Area Coupon 10}}{\text{Groove Area Coupon 13}} = \frac{9.0 \times 2.5}{9.0 \times 0.48} = 5.21$$

$$\text{Equivalent flow} = \frac{0.010}{5.21} = 0.00192 \text{ lb/s}\cdot\text{ft}^2$$

$$\text{Predicted } \sigma\Delta P = 0.034 + 0.0038 = 0.0378 \text{ psi at } 0.00192 \text{ lb/s}\cdot\text{ft}^2$$

$$\text{Actual } \sigma\Delta P = 0.045 \text{ at } 0.00192 \text{ lb/s}\cdot\text{ft}^2 \text{ (Figure 27)}$$

$$\% \text{ accuracy} = \frac{0.045 - 0.0378}{0.045} = 16\%$$

Brunscoustic strip assembly coupon No. 14

$$\text{Sheet } \sigma\Delta P = 0.0035 \text{ psi at } 0.010 \text{ lb/s}\cdot\text{ft}^2 \text{ (Figure 11)}$$

$$\text{Pressure loss thru backup structure} = 0.0038 \text{ psi (Table D-1)}$$

$$\text{Area Correction} = 5.21$$

$$\text{Predicted } \sigma\Delta P = 0.0035 + 0.0038 = 0.0073 \text{ psi at } 0.00192 \text{ lb/s}\cdot\text{ft}^2$$

$$\text{Actual } \sigma\Delta P = 0.0066 \text{ at } 0.00192 \text{ lb/s}\cdot\text{ft}^2 \text{ (Figure 28)}$$

$$\% \text{ accuracy} = \frac{0.0073 - 0.0066}{0.0066} = 11\%$$

REFERENCES

1. X-21 Engineering Section; "Final Report on LFC Aircraft Design Data – Laminar Flow Control Demonstration Program", NOR 67-136, Norair Division of Northrop Corp., June, 1967.
2. Carmichael, R. H.; and Pfenninger, W.: "Surface Waviness Criteria for Swept and Unswept Laminar Suction Wings", Report NOR-59-438 (BLC 123), August 1959.
3. Nenni, J. P. and Gluyas, G. L.: "Aerodynamic Design of an LFC Surface", Astrodynamics & Aeronautics, July, 1966.
4. Wieder, J.; and Pfenninger, W.: "Structural Aspects of Low Drag Suction Airfoils", IAS/ARS paper 61-150-1844, June, 1961.
5. "Limit of Surface Waviness for Laminar Flow over Wings"; Royal Aeronautical Society Data Sheets, Wings 02.04.11, August, 1957.
6. Hahn, M.; and Pfenninger, W.: "Prevention of Transition over a Backward Step by Suction"; Journal of Aircraft, Vol. 10, No. 10, October, 1973.
7. "Limit of Grain Size for Laminar Flow Over Wings or Bodies," Royal Aeronautical Society Data Sheets, Wings 02.04.09, July, 1955.
8. ANSI B46.1 – 1962 (R1971) Surface Texture (Surface Roughness, Waviness and Lay).
9. BAC 5532 Boeing Process Specification "Manufacture of Polyimide Structural Laminates and Honeycomb Sandwich", November, 1975.

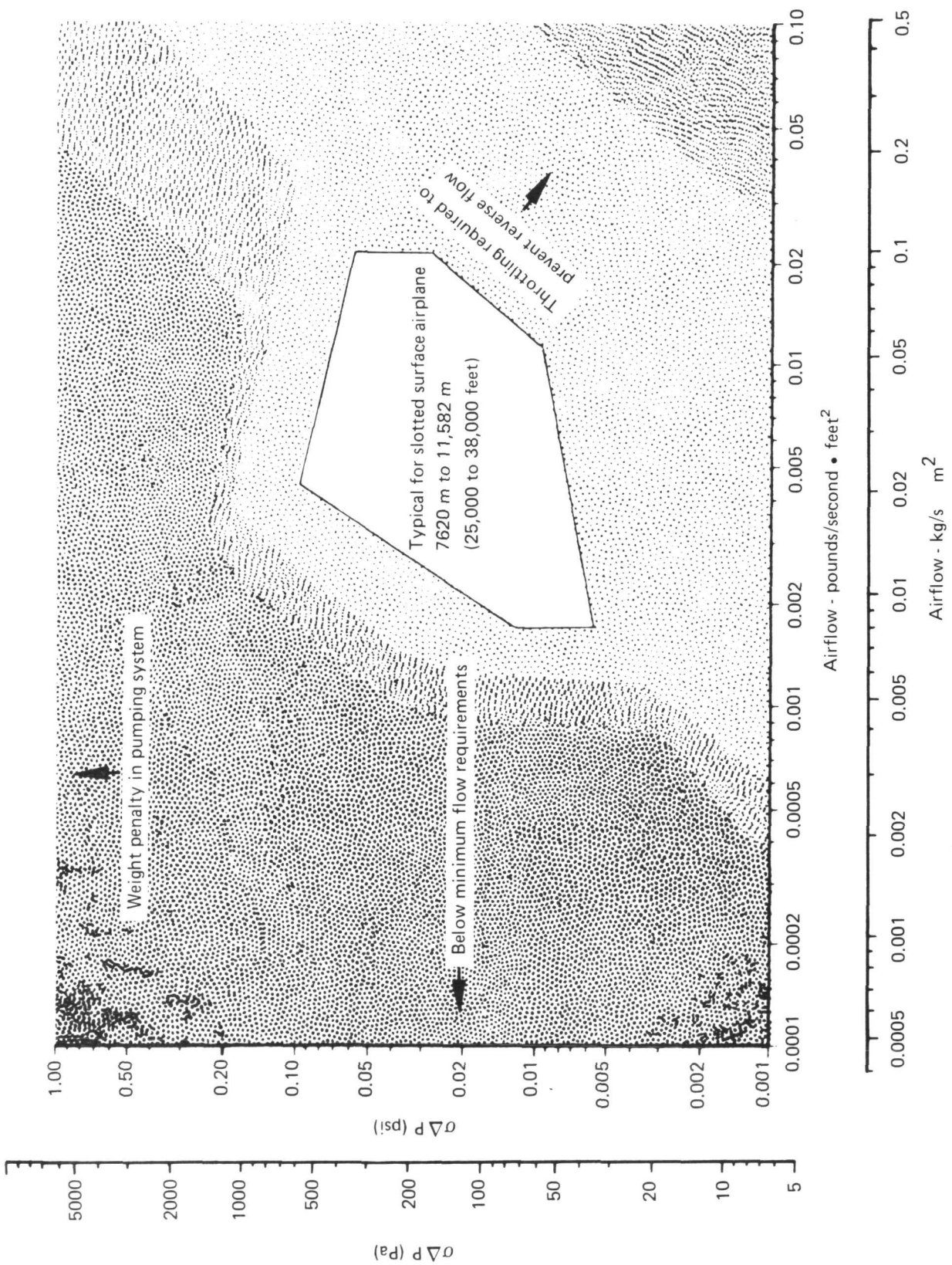


Figure 1.—Suction Requirements for LFC Wing

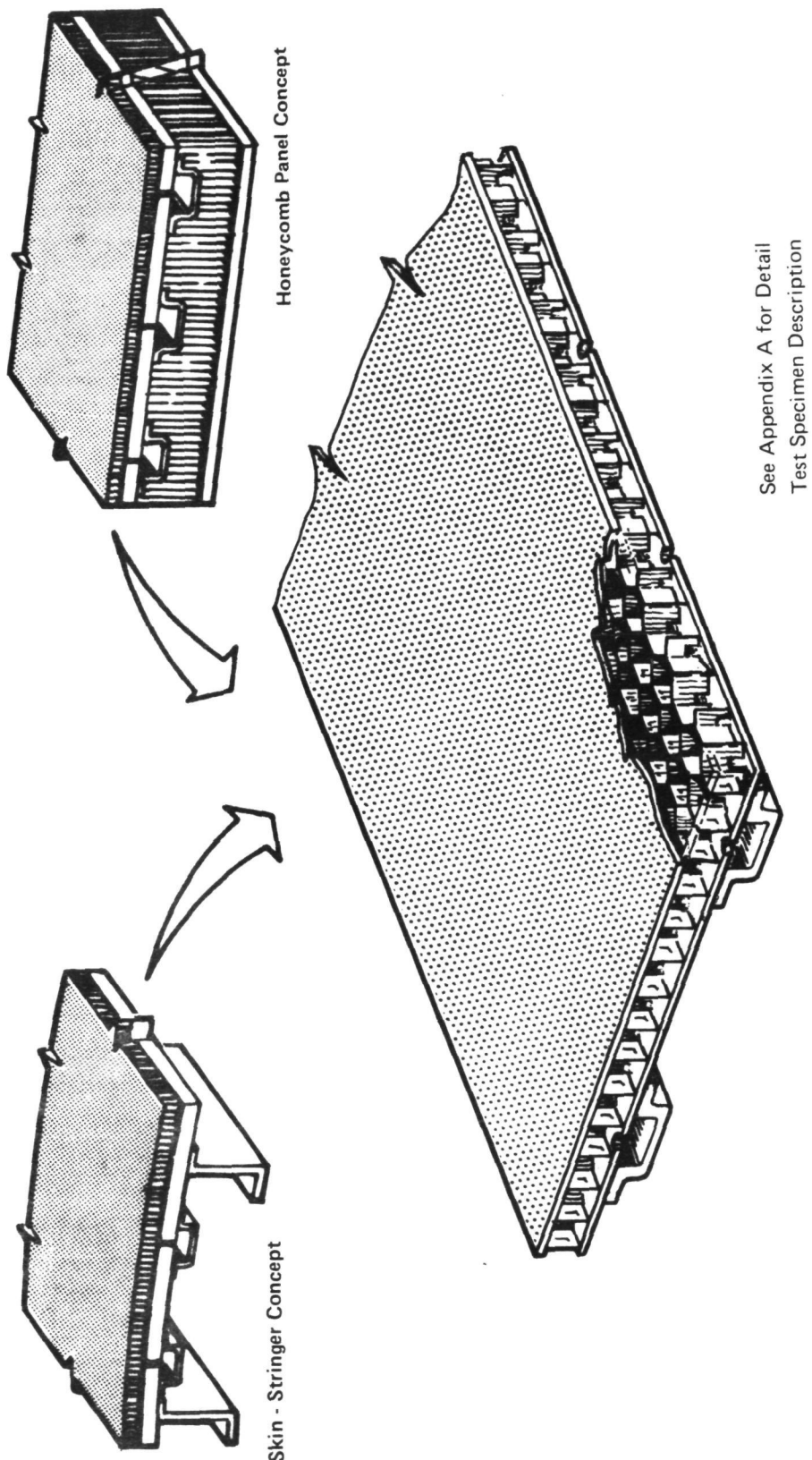


Figure 2.—Continuously Porous or Perforated Skin Concept

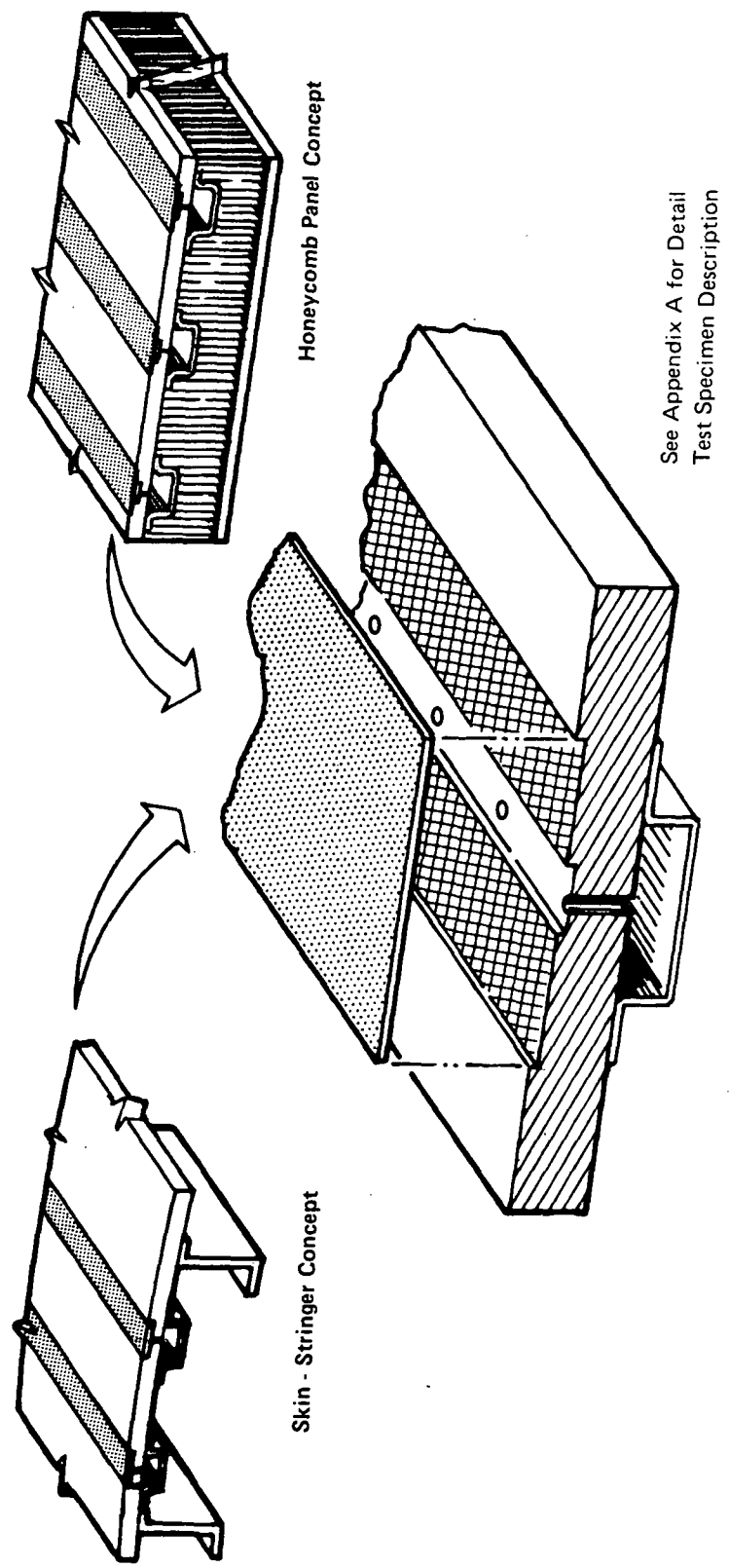


Figure 3.—Porous or Perforated Strip Concept

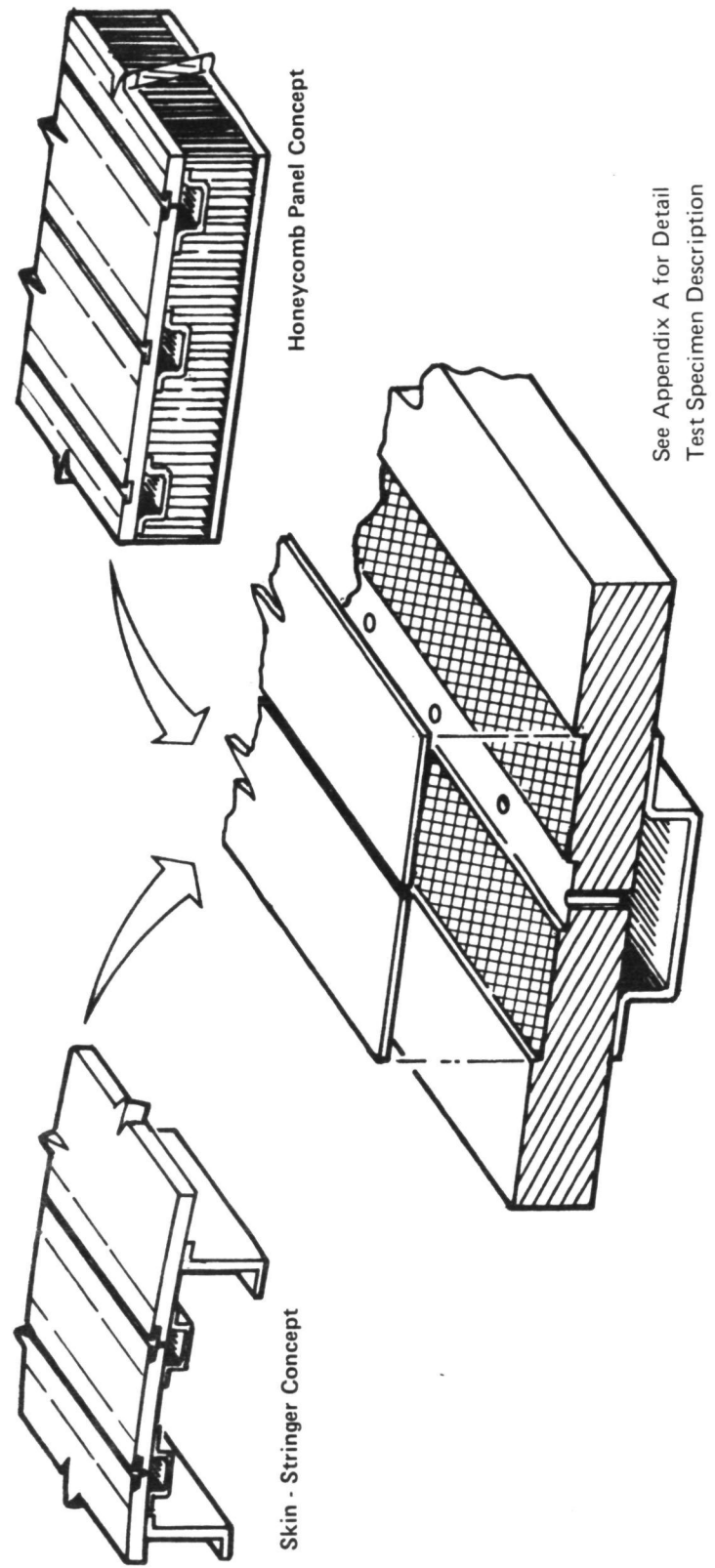


Figure 4.—Slot Metal Overlay Strip Concept

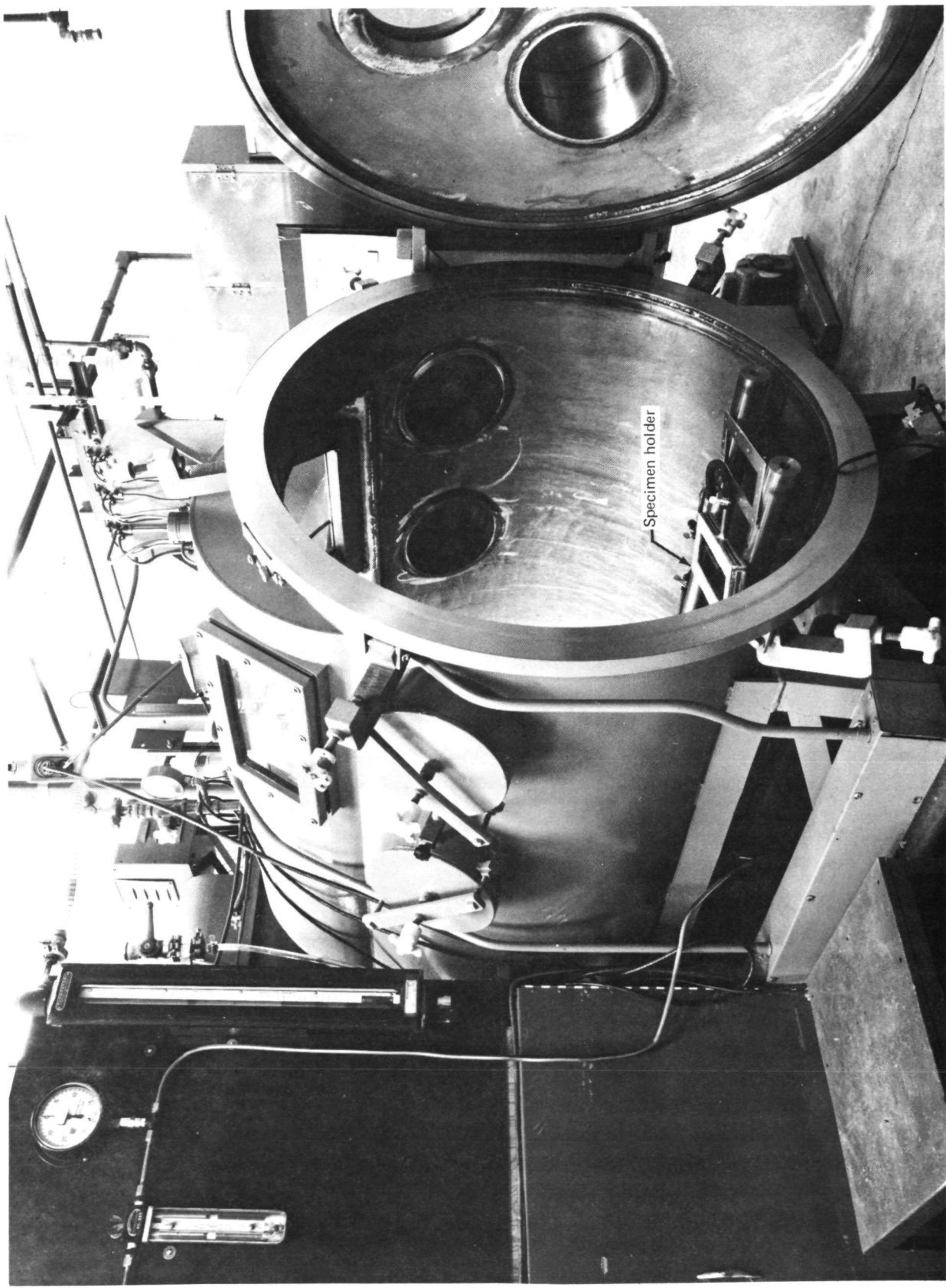


Figure 5.—Photograph of Flow Test Set-Up

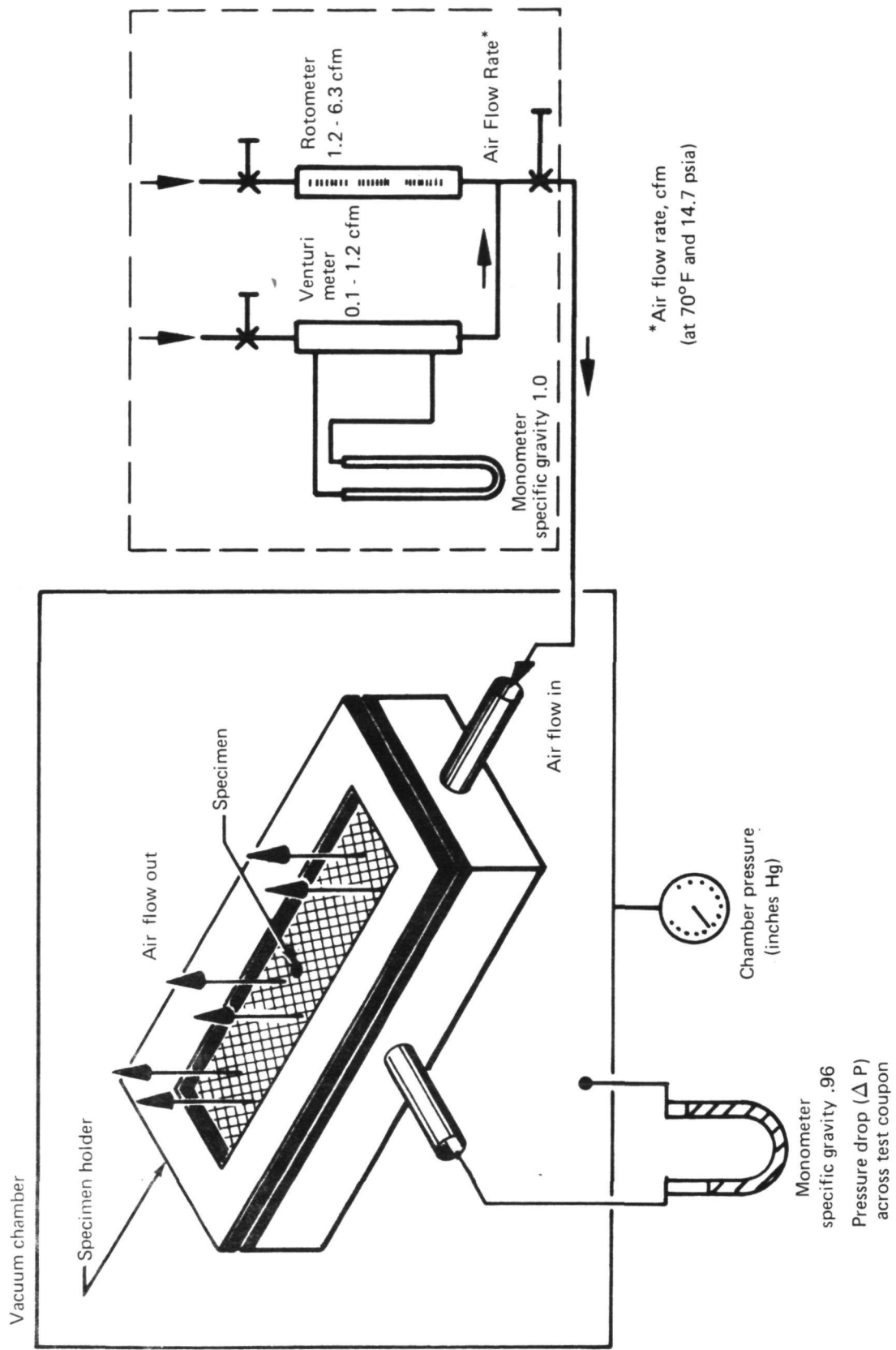


Figure 6.—Schematic of Flow Test Set-Up

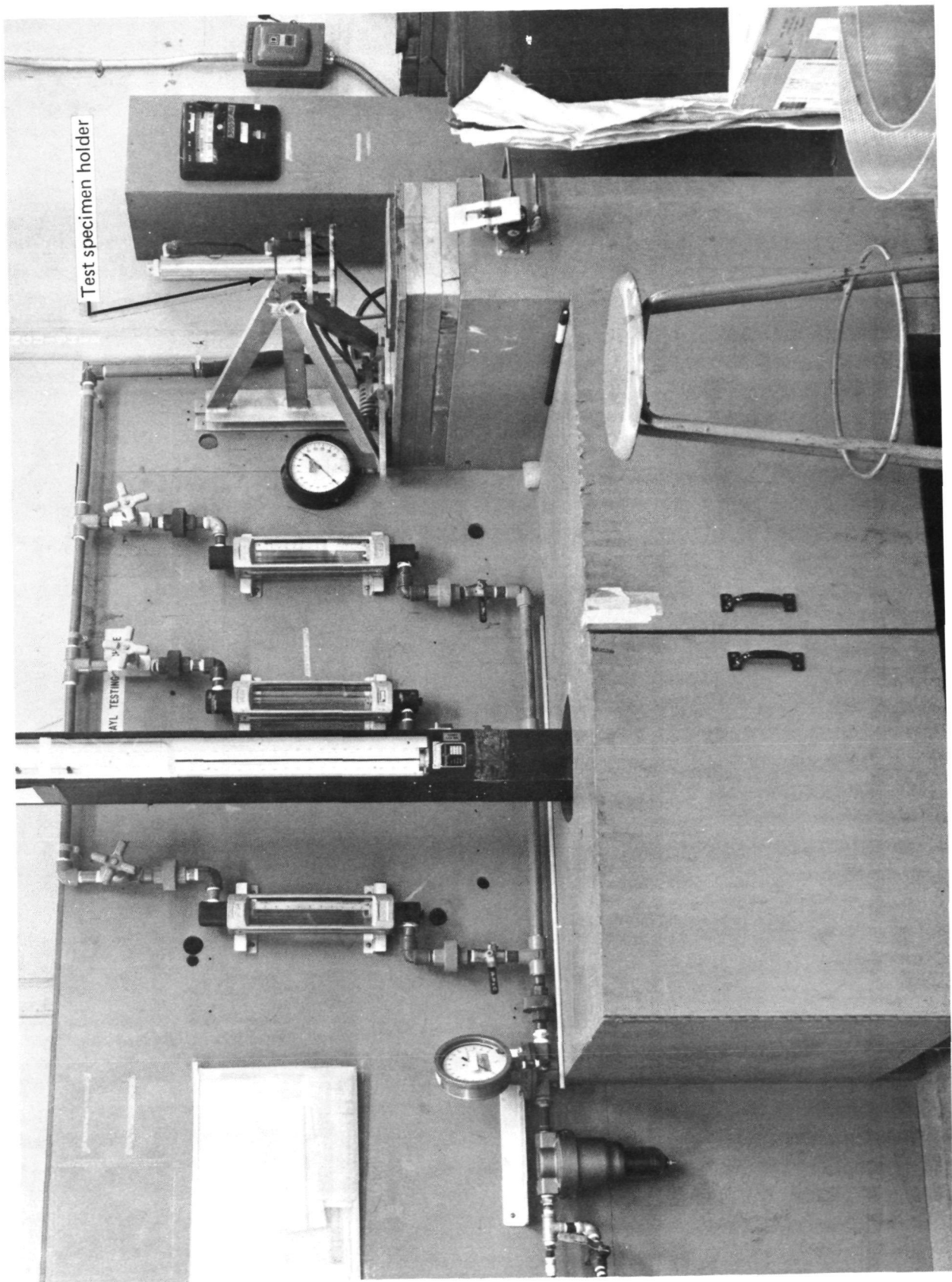
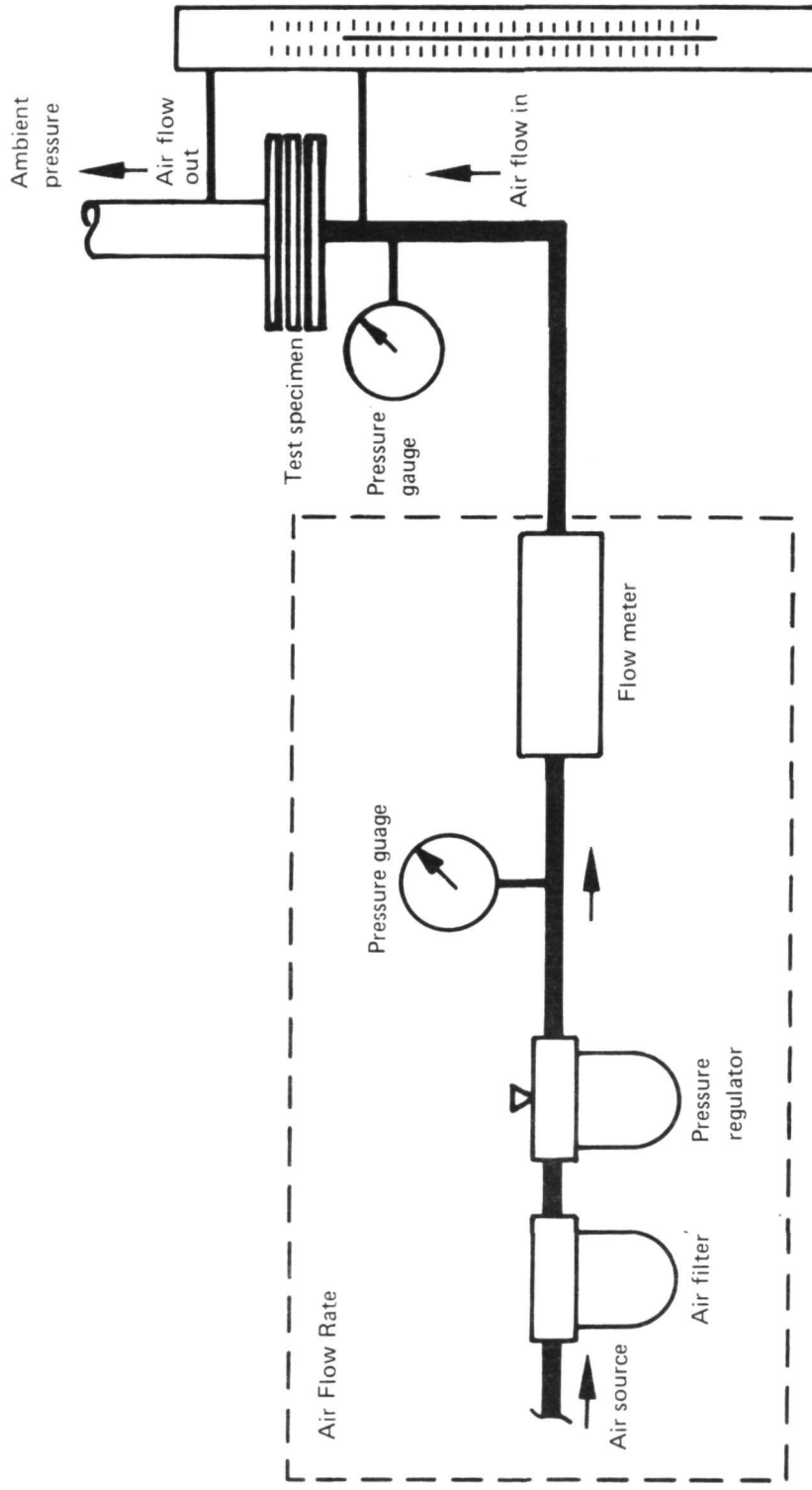


Figure 7.—Photograph of RAYL Test Machine



Meriam instrument company
model 34FB2 monometer
Pressure drop (ΔP) across
test specimen

Figure 8.—Schematic of RAYL Test Set-Up

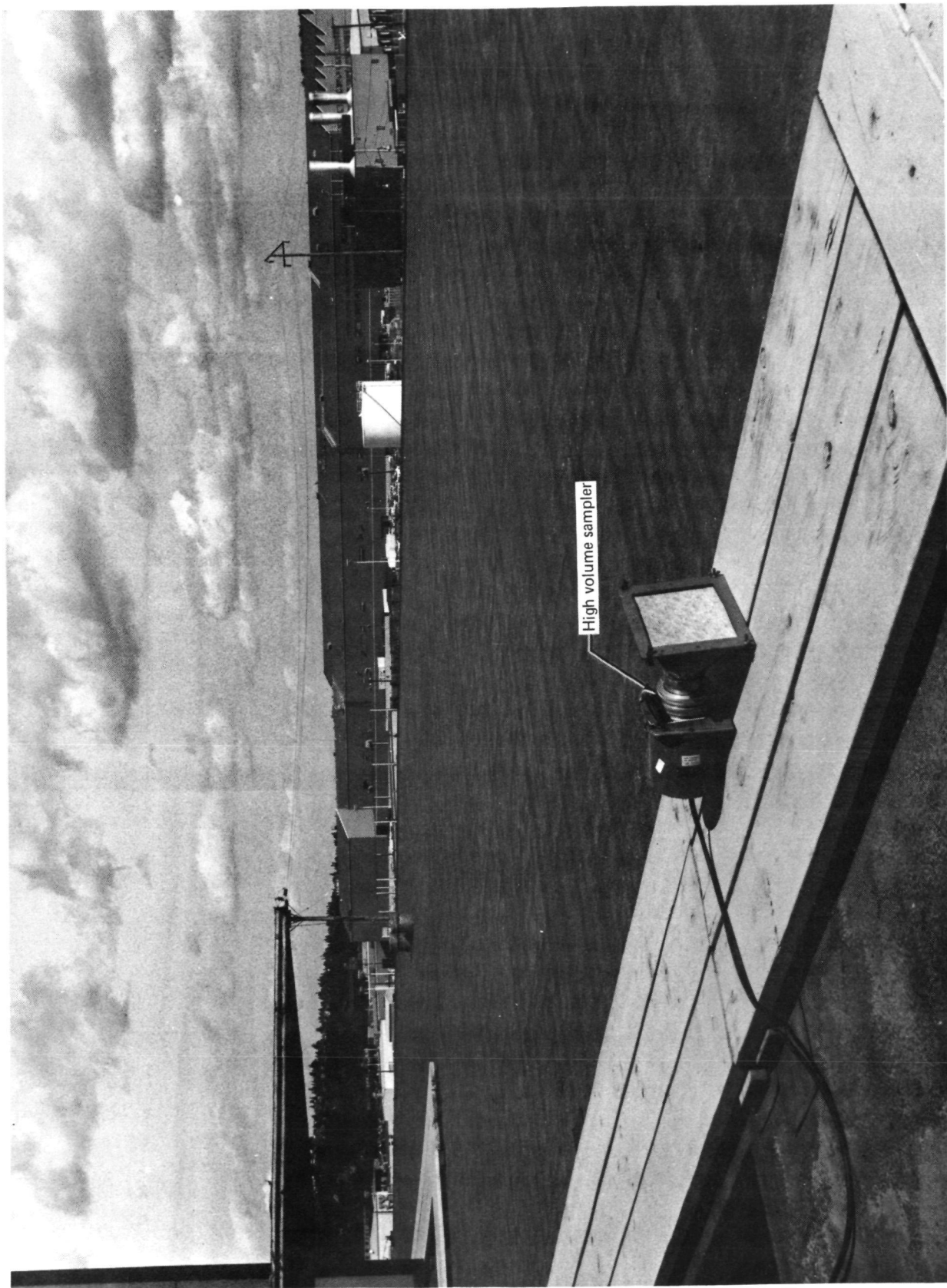


Figure 9.—Photograph of Clogging Test Set-Up and Location

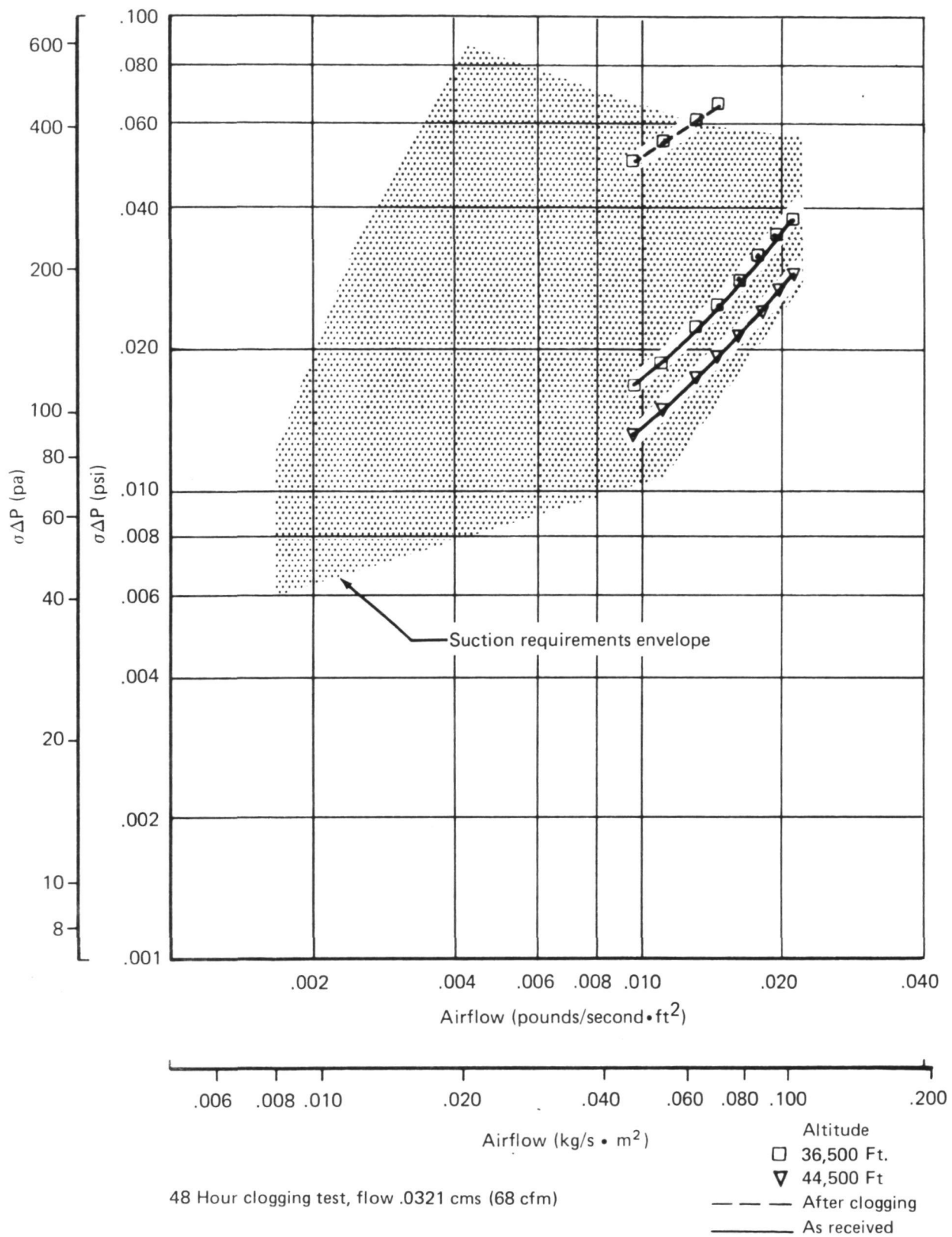


Figure 10.—Flow Test Results, Test Coupon No. 1, Gore-Tex

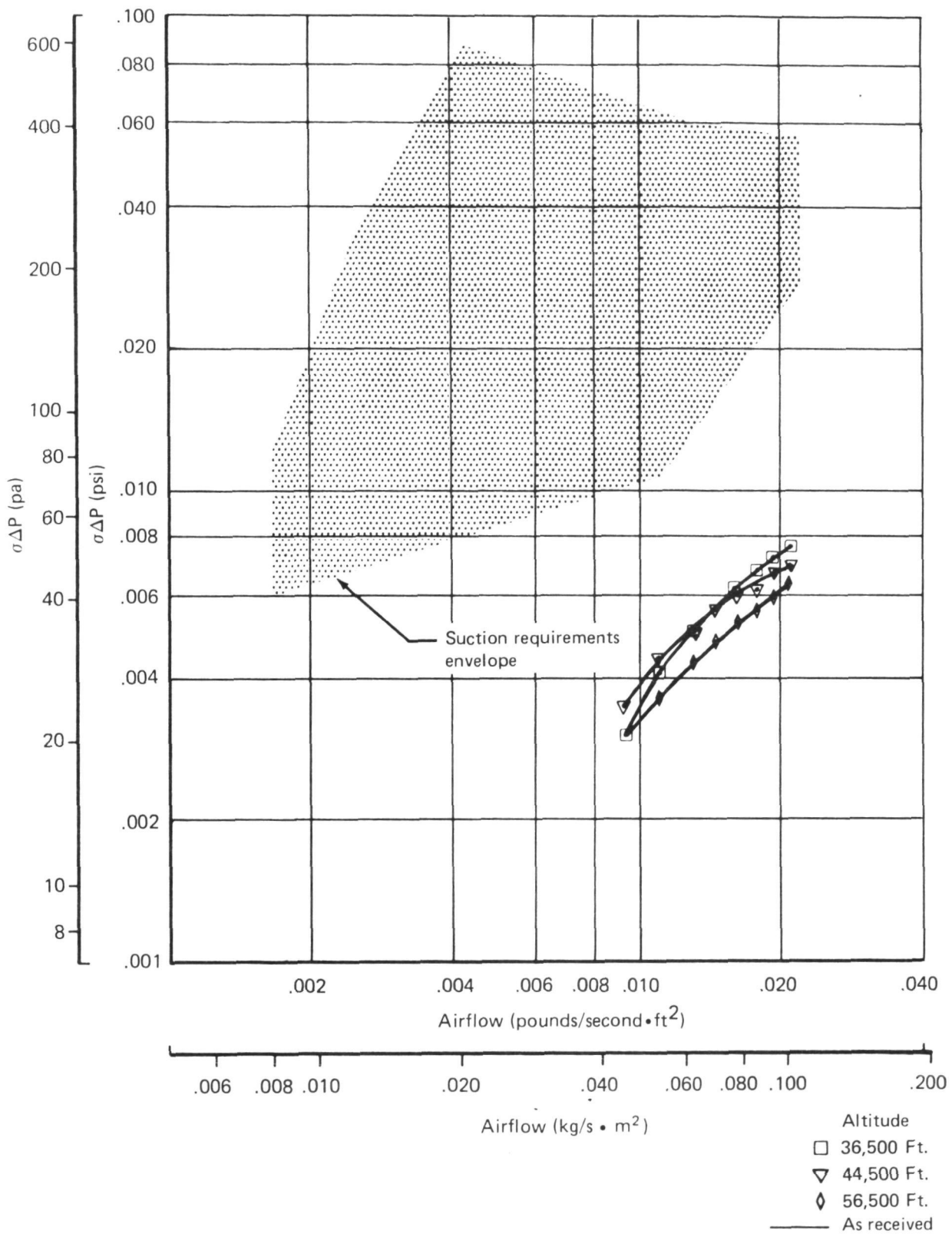


Figure 11.—Flow Test Results, Test Coupon No. 3, Brunscoustic #1, as Received . . .

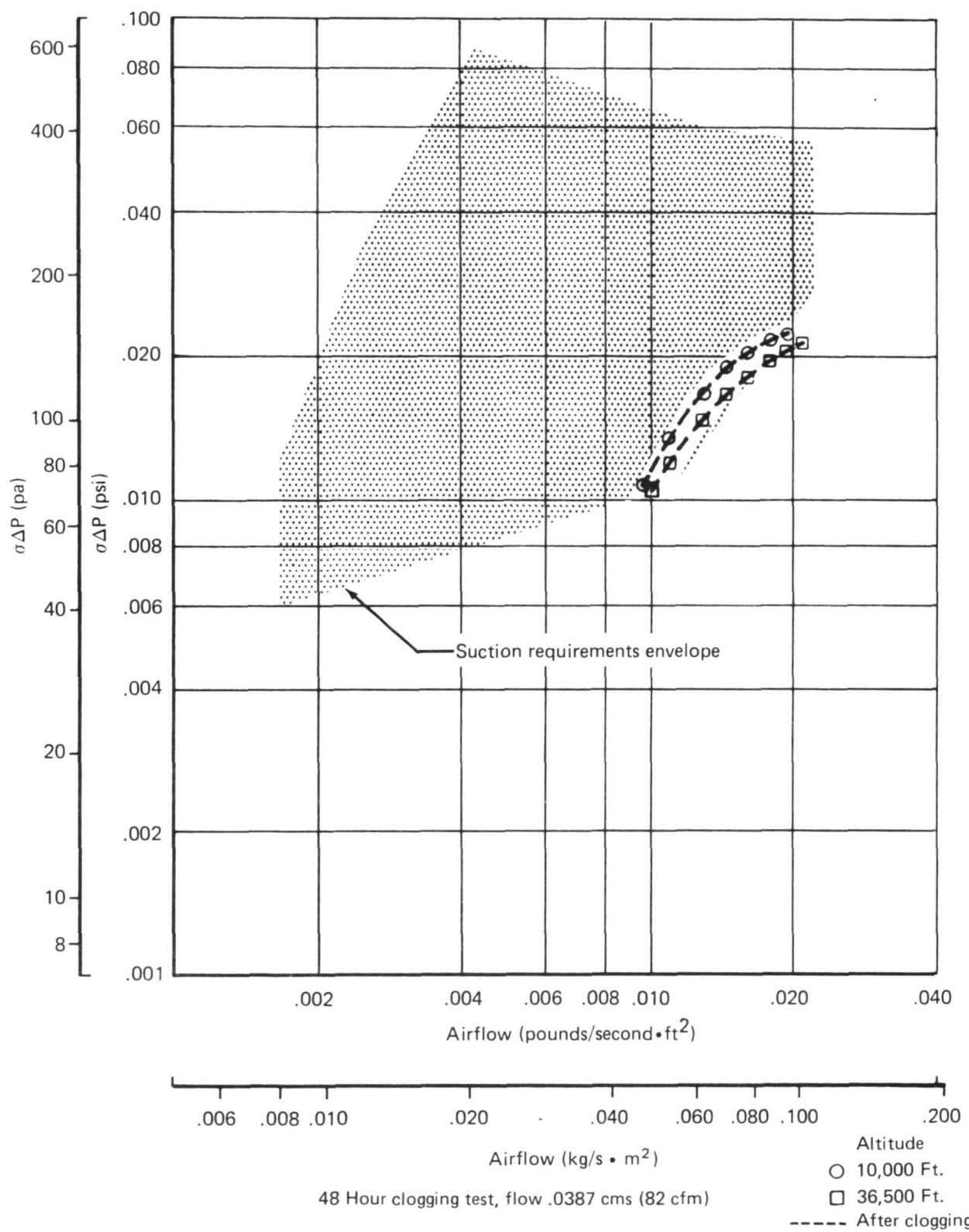


Figure 12.—Flow Test Results, Test Coupon No. 3, Brunscoustic #1,
48 Hour Clogging

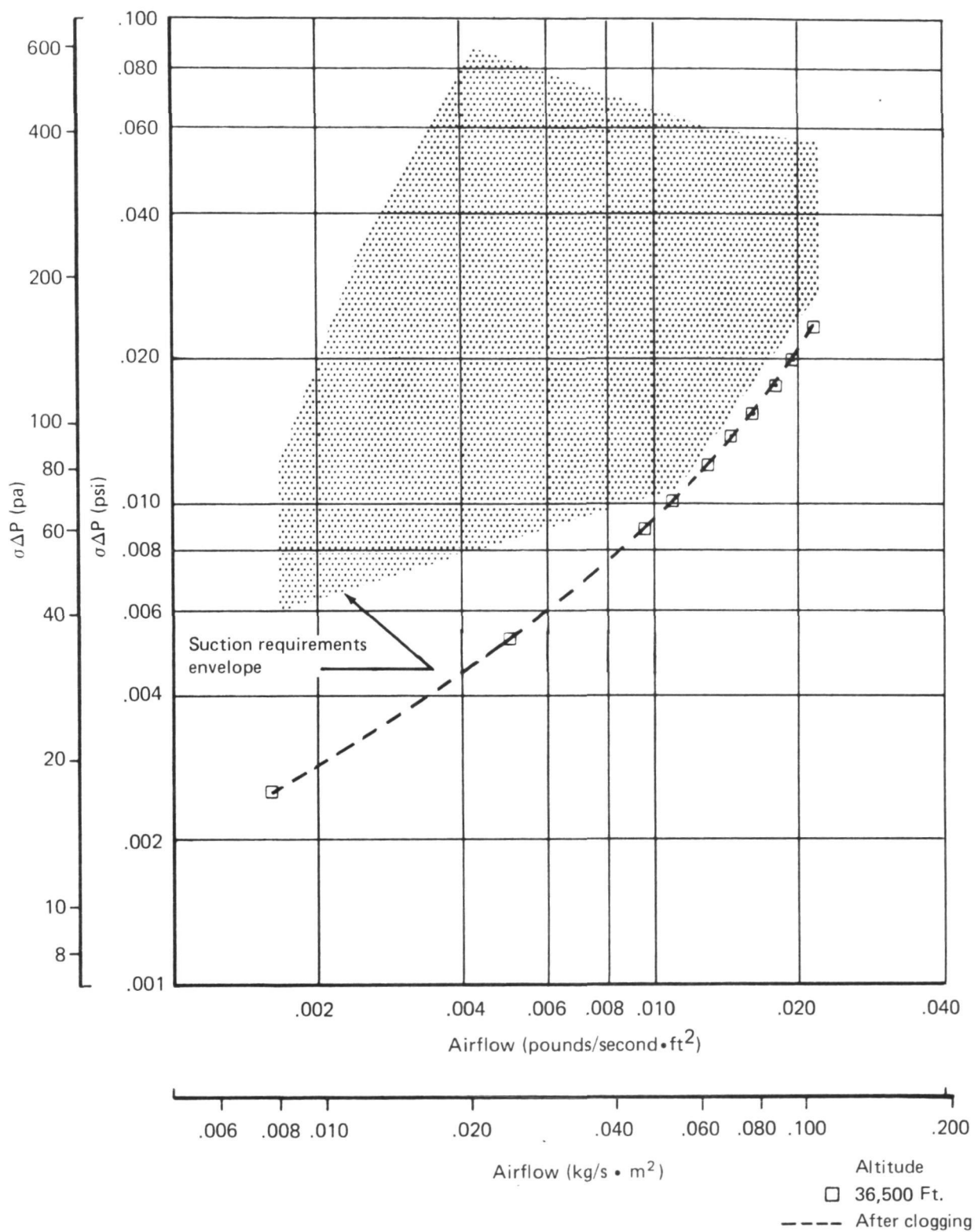


Figure 13.—Flow Test Results, Test Coupon No. 3, Brunscoustic #1, Reverse Flow

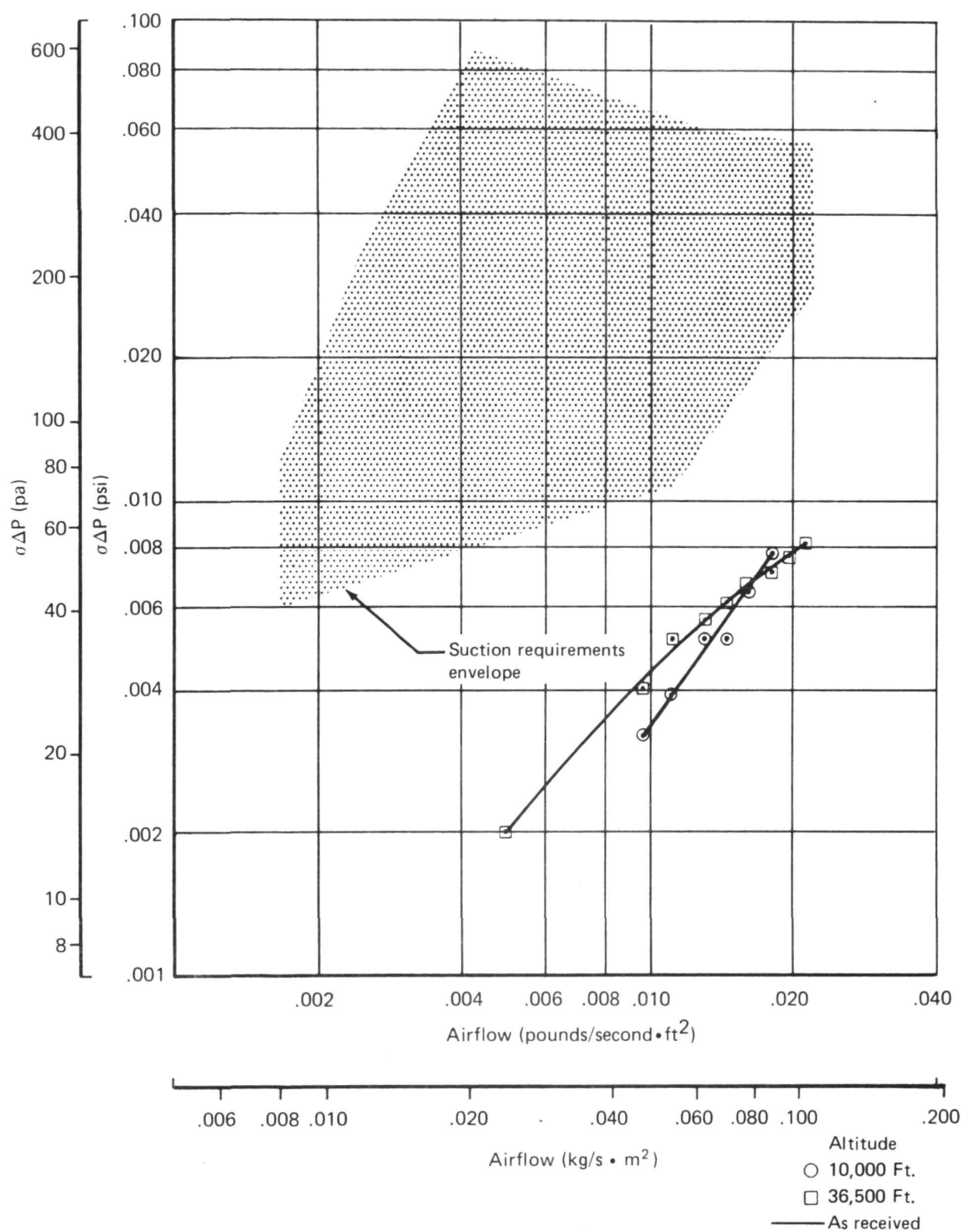


Figure 14.—Flow Test Results, Test Coupon No. 4, Brunscoustic #2, as Received

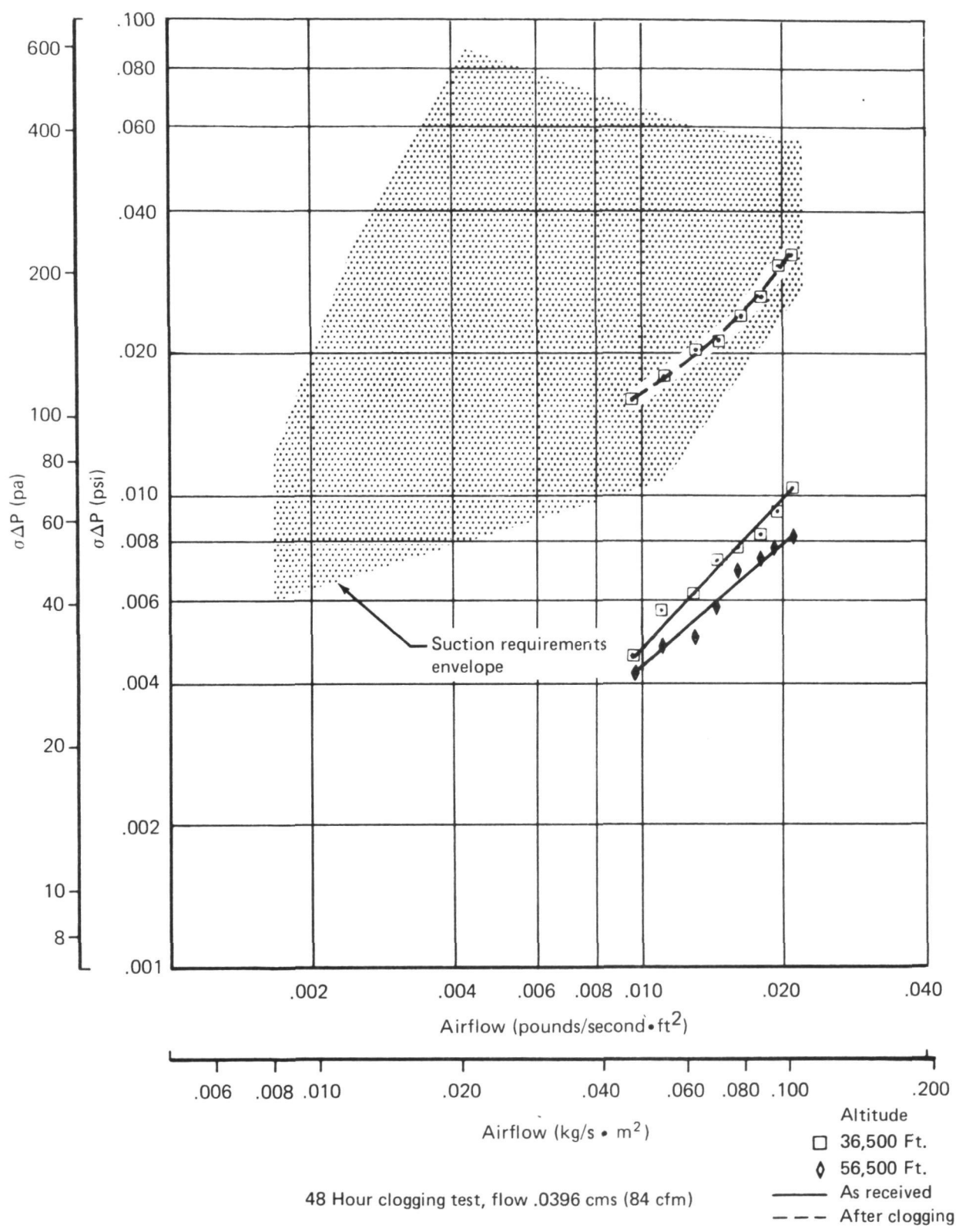


Figure 15.—Flow Test Results, Test Coupon No. 5, Aircraft Porous Media

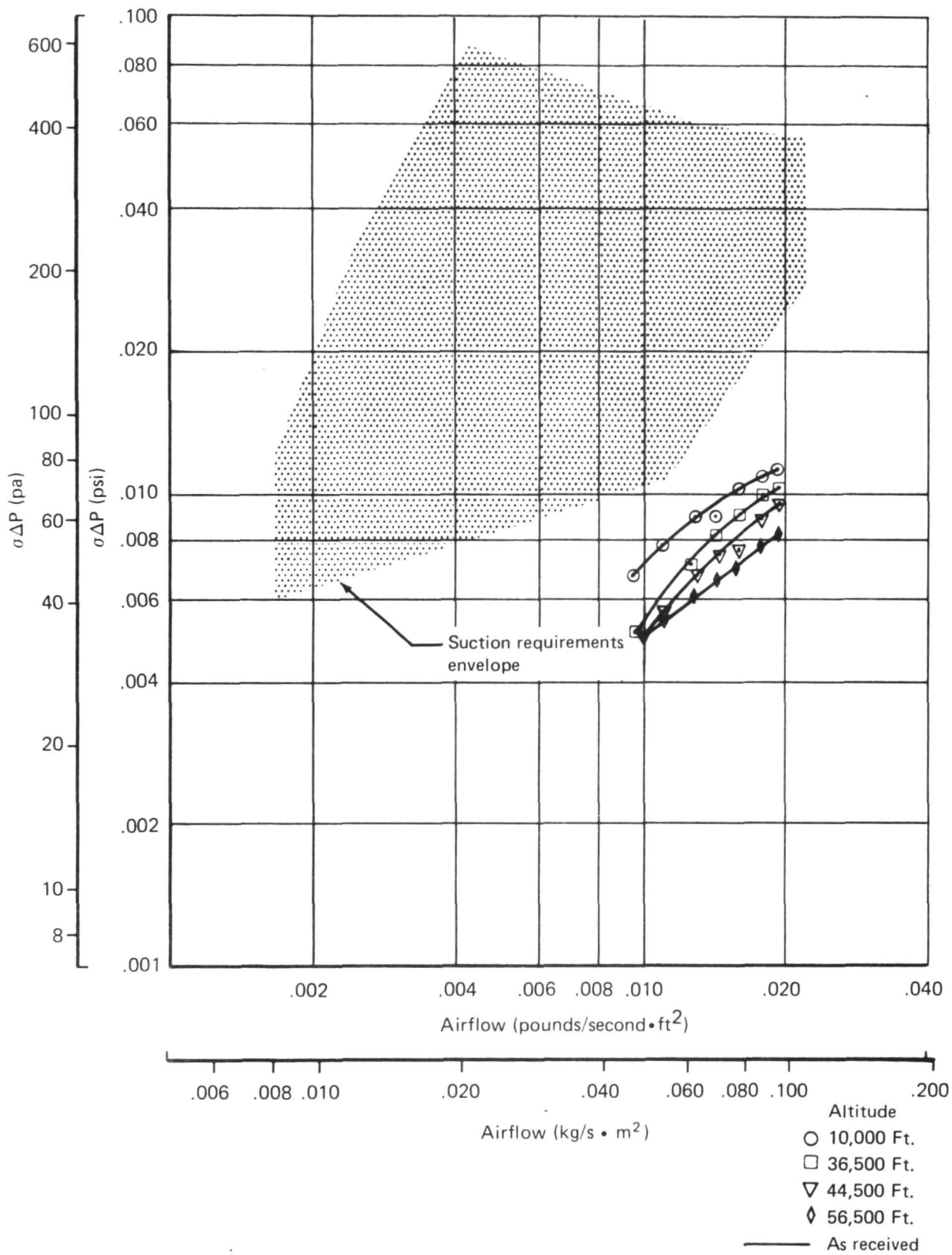


Figure 16.—Flow Test Results, Test Coupon No. 6, Michigan Dynamics, as Received

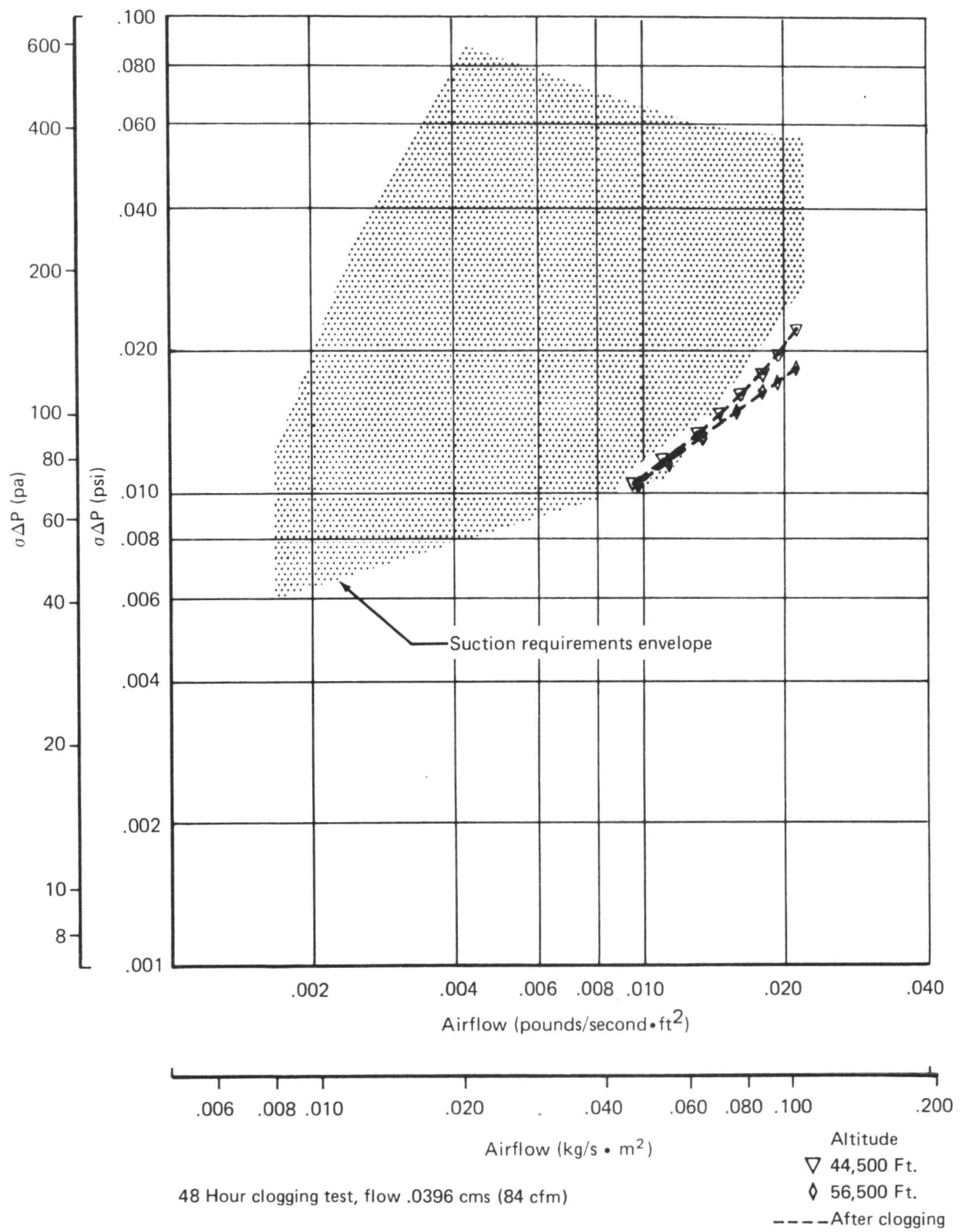


Figure 17.—Flow Test Results, Test Coupon No. 6, Michigan Dynamics, 48 Hour Clogging

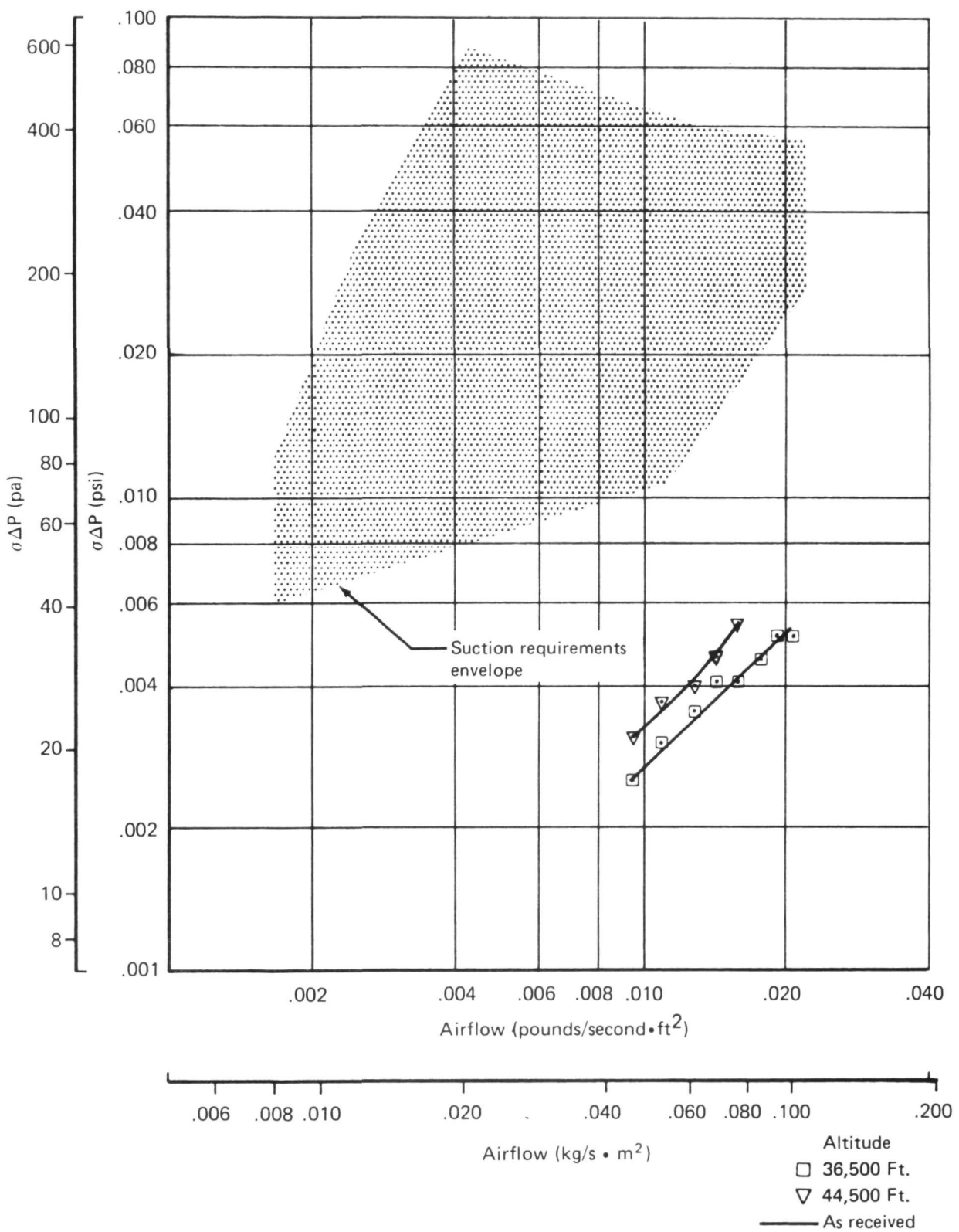


Figure 18.—Flow Test Results, Test Coupon No. 7, Polyimide (16 Ply), as Received

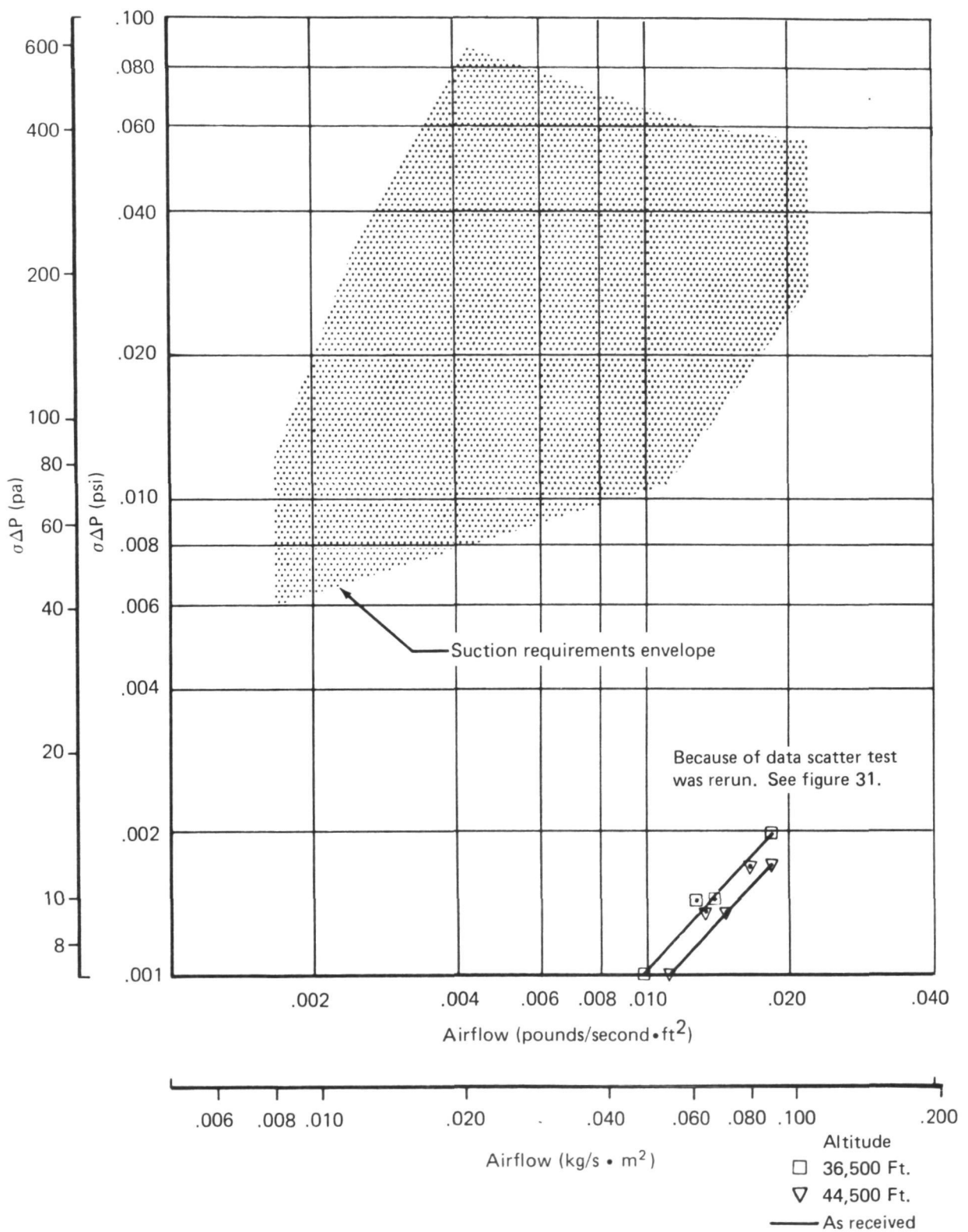


Figure 19.—Flow Test Results, Test Coupon No. 8, Polyimide (7 Ply), as Received

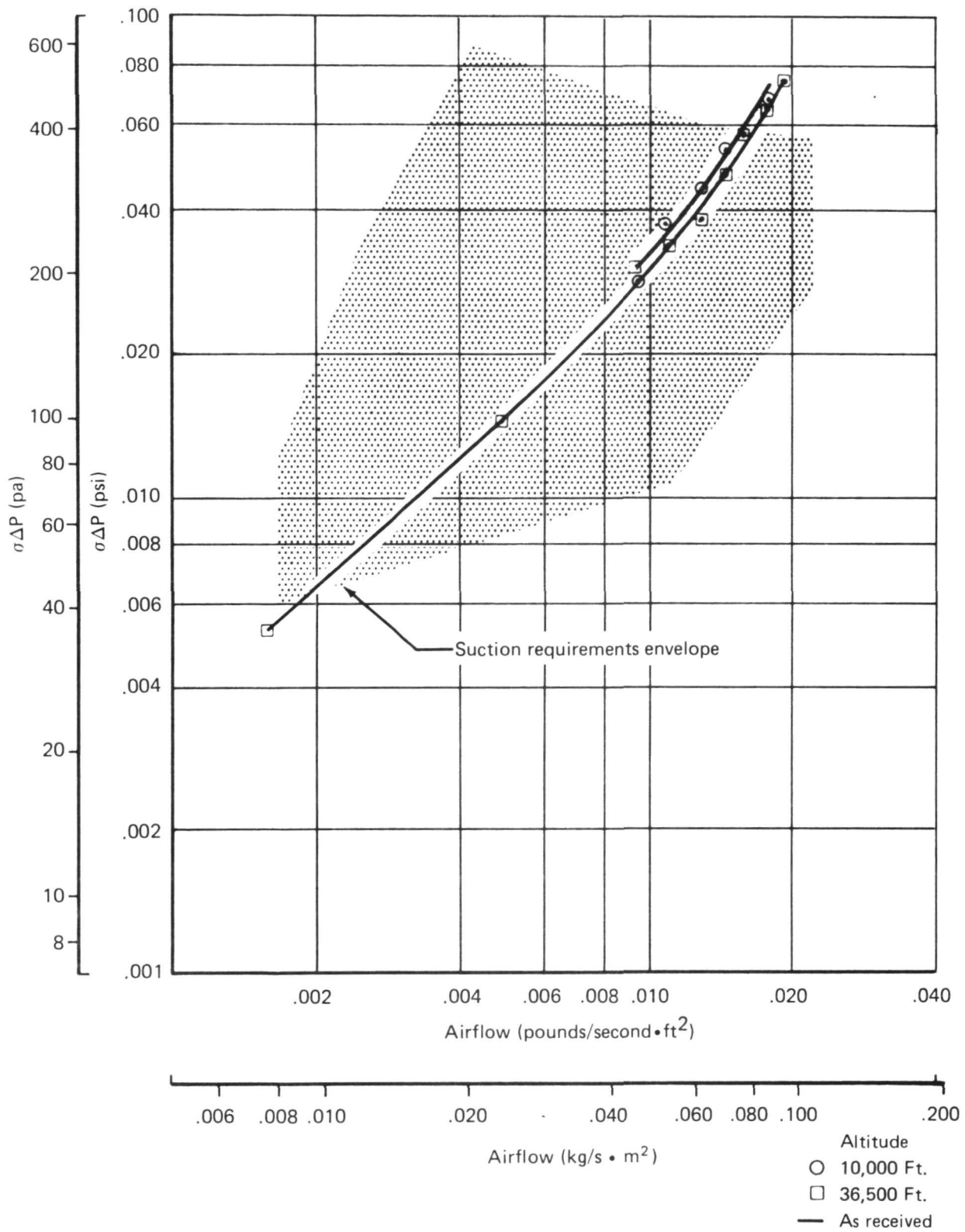


Figure 20. —Flow Test Results, Test Coupon No. 9, Perforated Titanium, .003 Hole, as Received

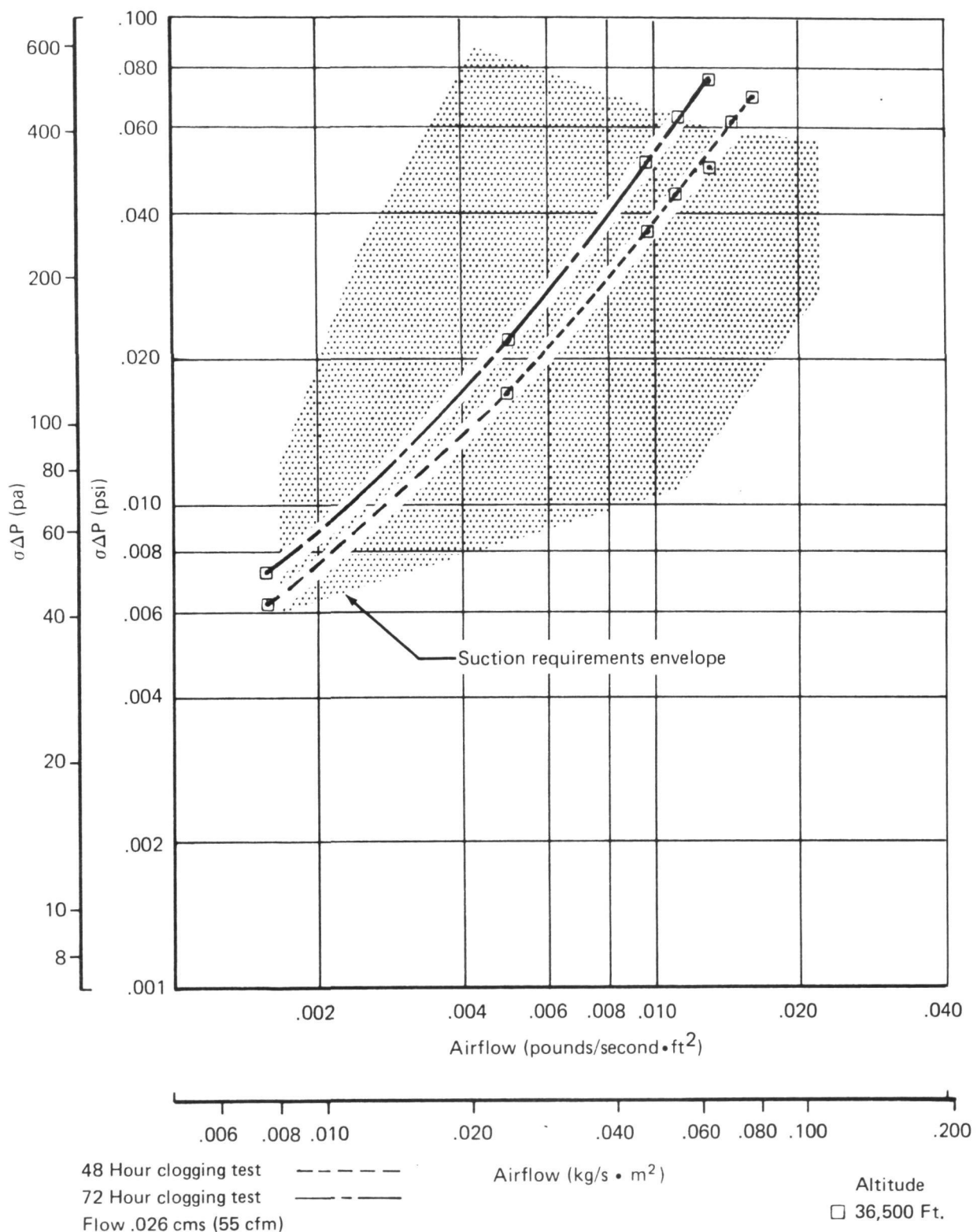


Figure 21.—Flow Test Results, Test Coupon No. 9, Perforated Titanium, .003 Hole, 48 and 72 Hour Clogging

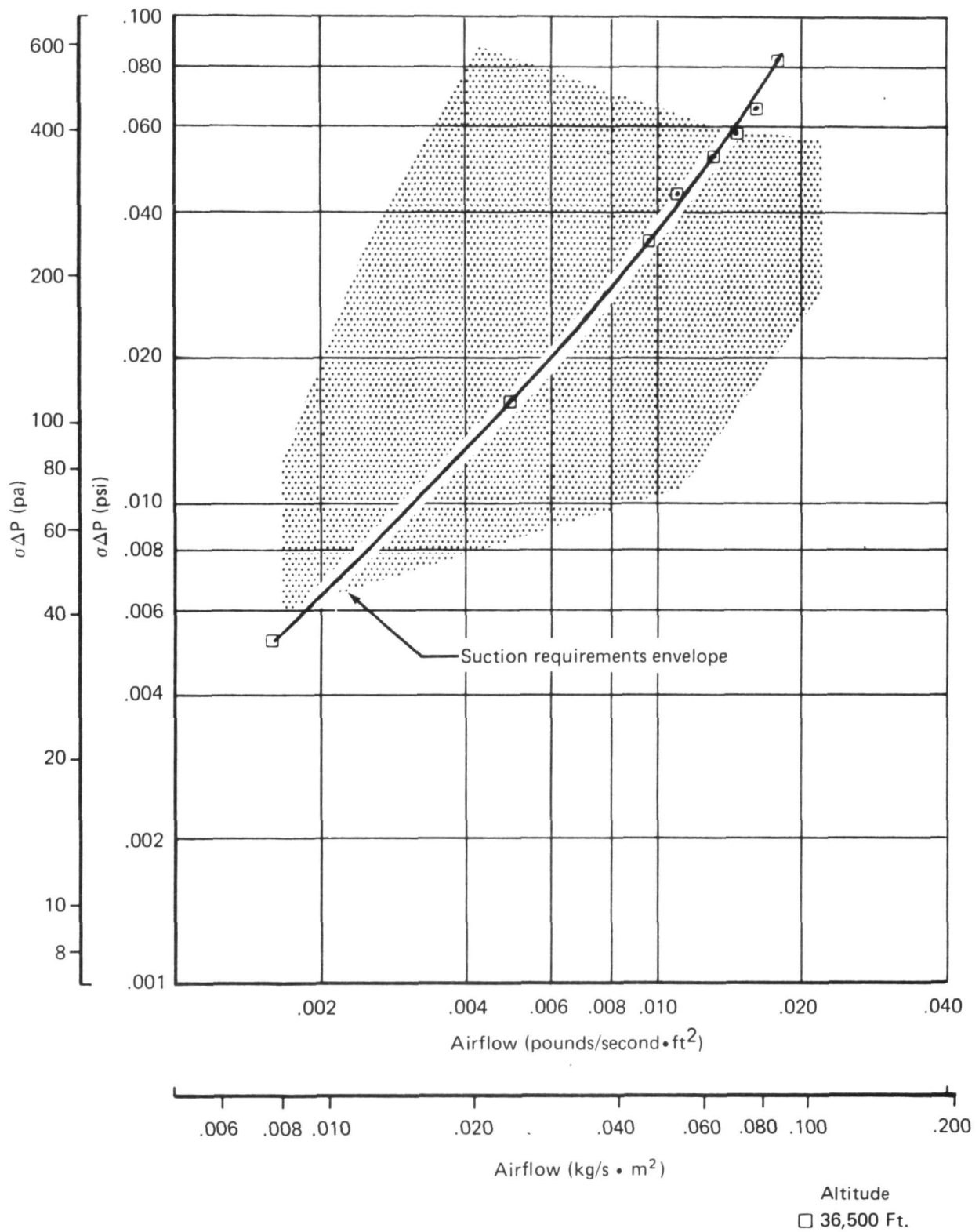
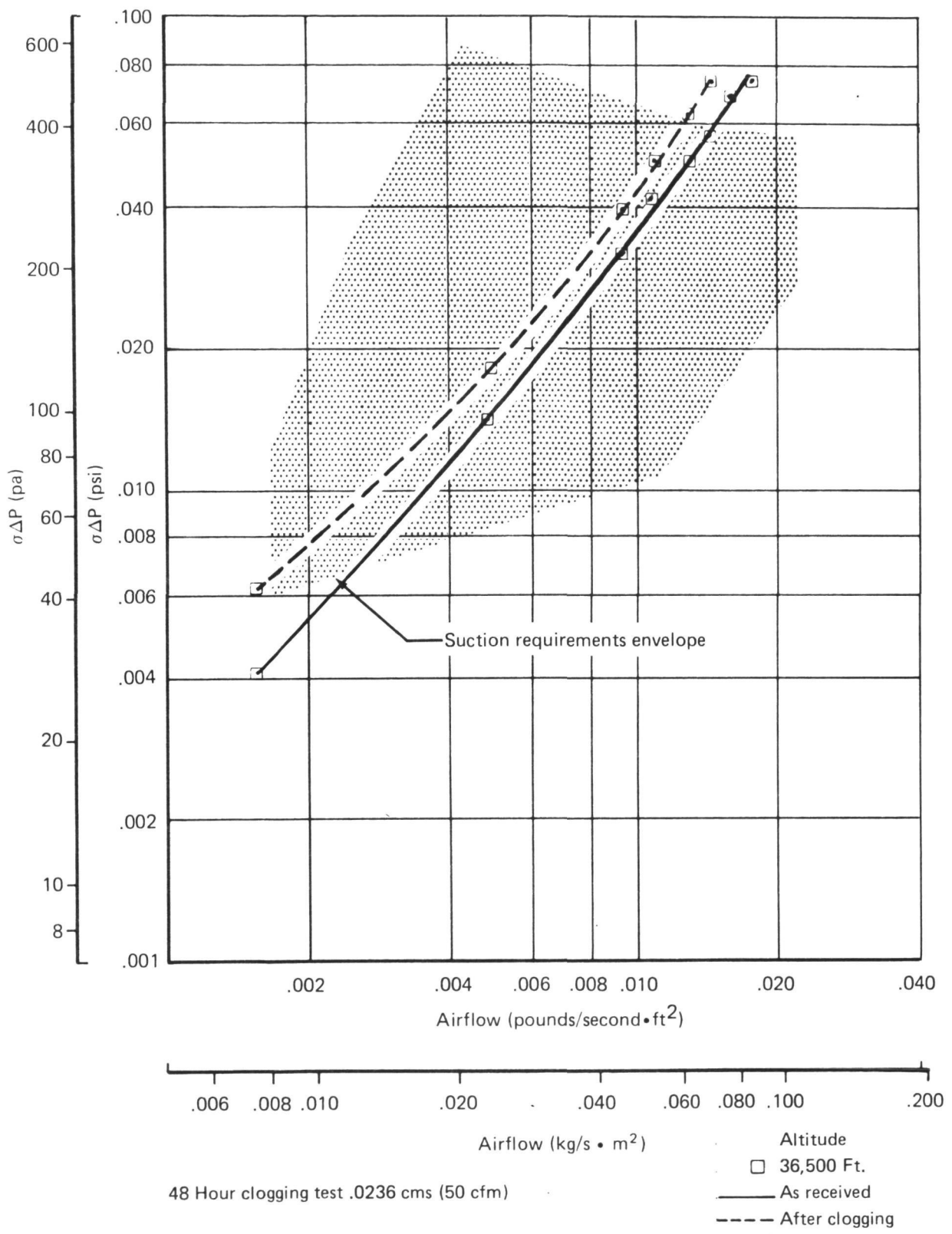


Figure 22.—Flow Test Results, Test Coupon No. 9, Perforated Titanium, .003 Hole, Surface Washed



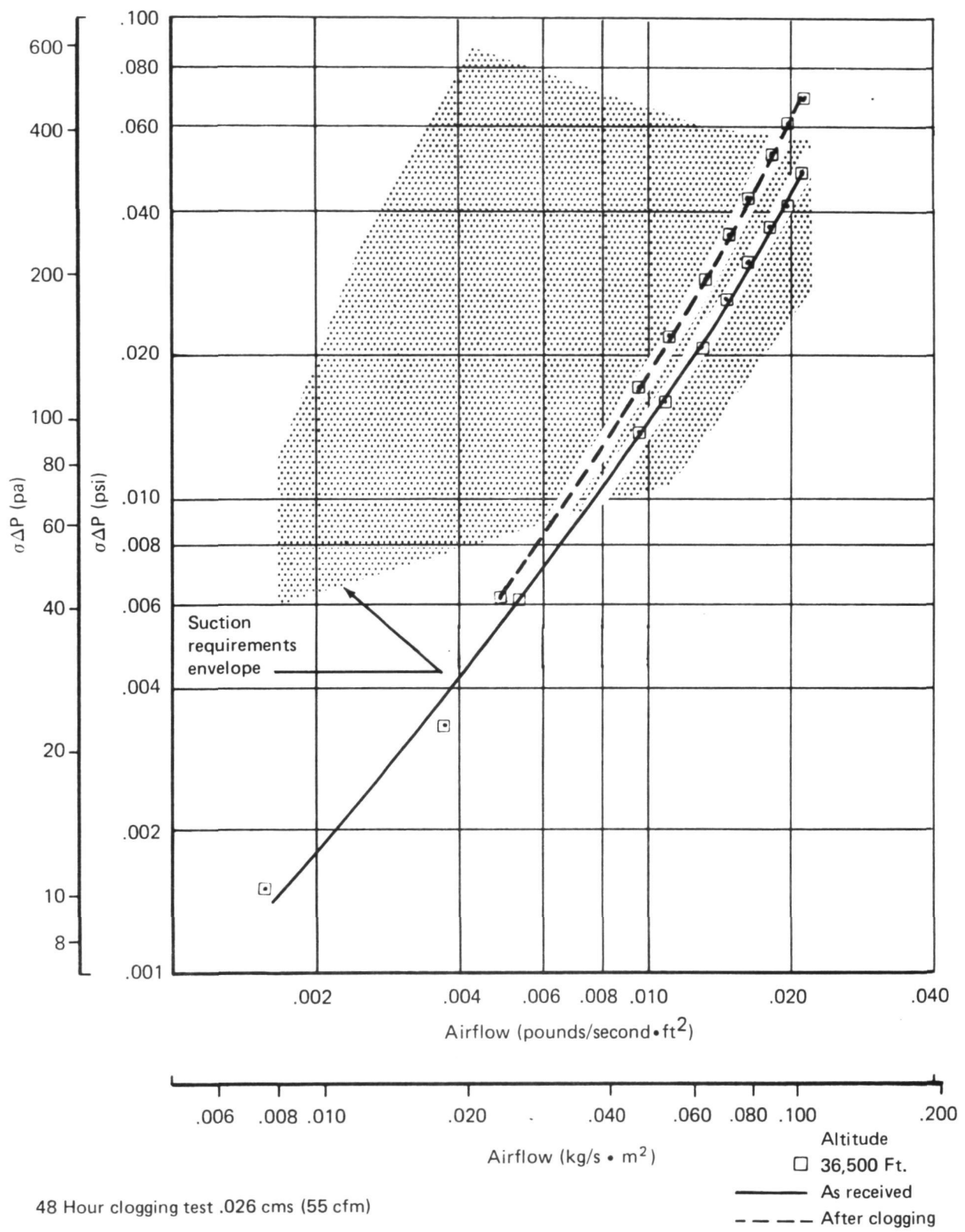


Figure 24.—Flow Test Results, Test Coupon No. 11, Perforated Titanium, .008 Hole

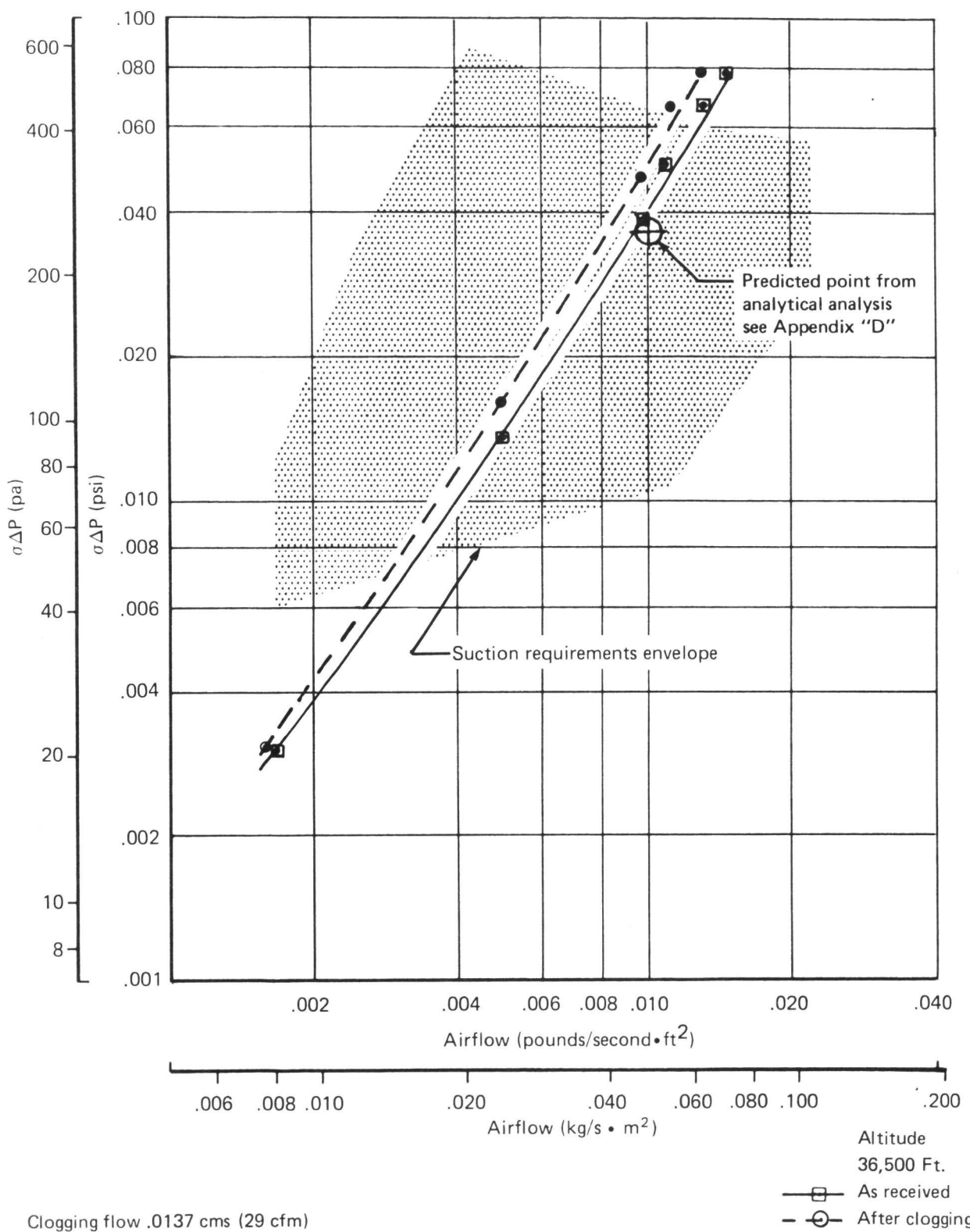


Figure 25.—Flow Test Results, Test Coupon No. 12, .0073 Slot Assembly, as Received, and 48 Hour Clogging

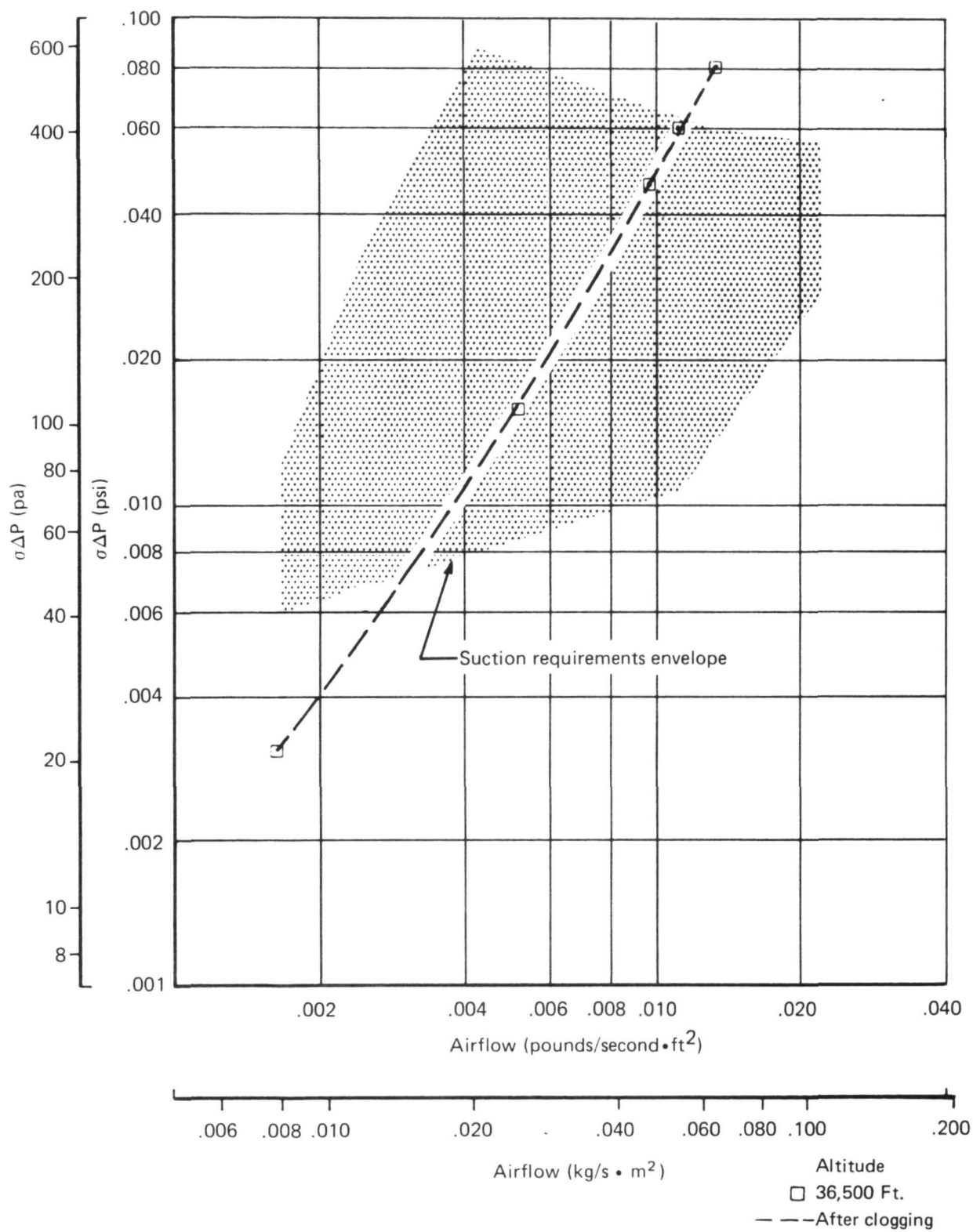


Figure 26.—Flow Test Results, Test Coupon No. 12, .0073 Slot Assembly, Surface Washed

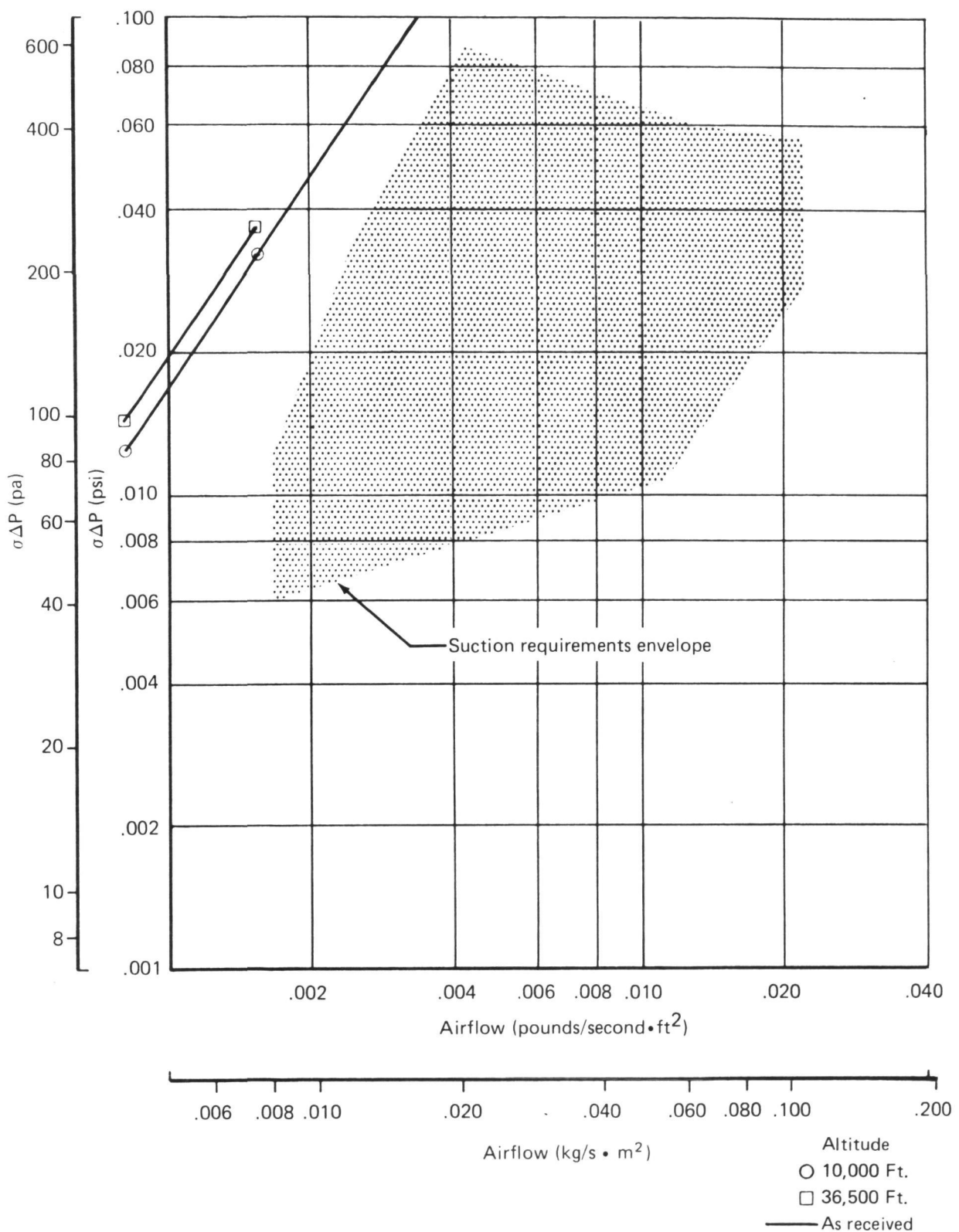


Figure 27.—Flow Test Results, Test Coupon No. 13, Perforated Titanium Strip Assembly

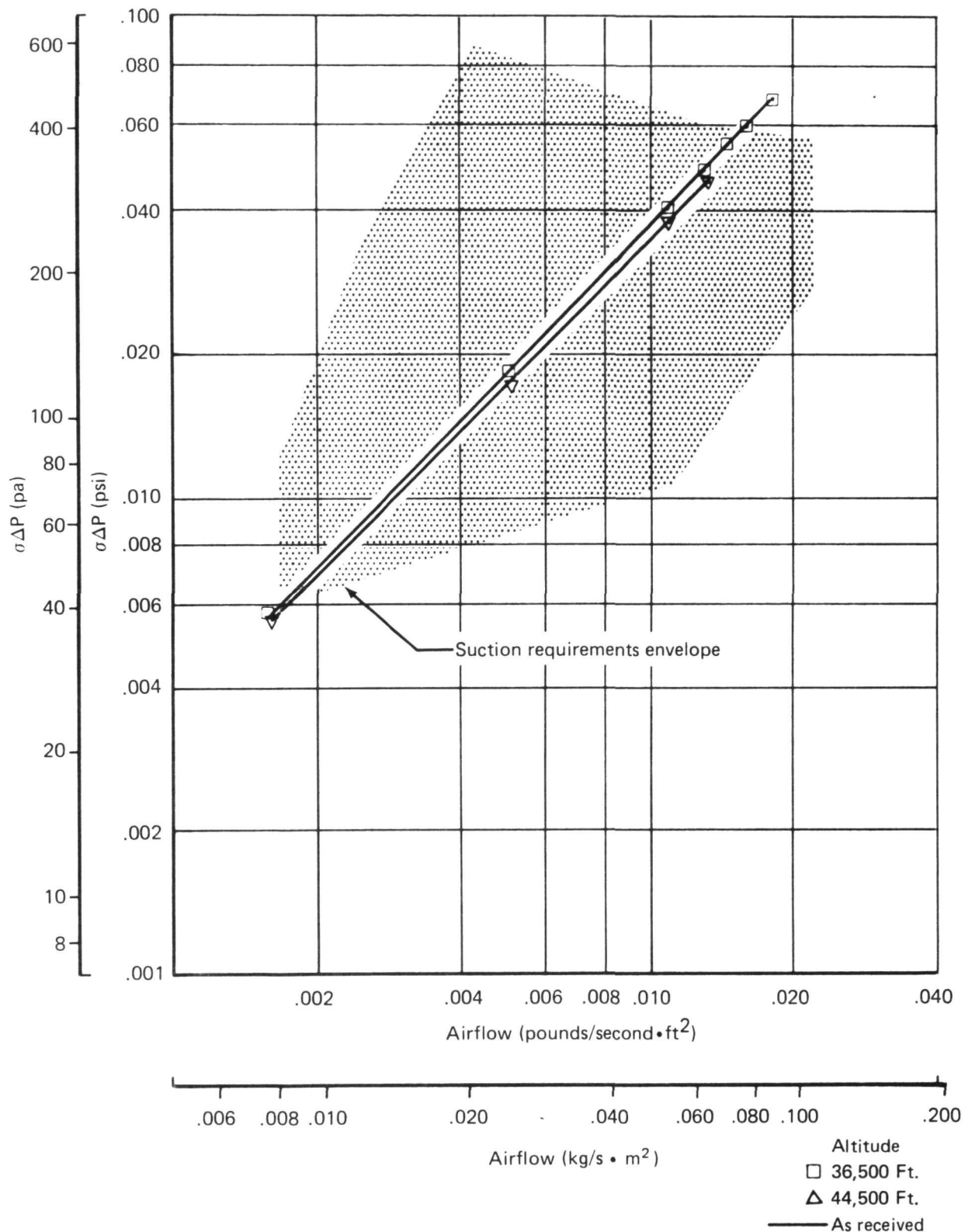


Figure 28.—Flow Test Results, Test Coupon No. 14, Brunscoustic Strip Assembly